THERMODYNAMIC MODELING OF THE INCIPIENT CONDITIONS FOR SINGLE AND MIXED GAS HYDRATE SYSTEMS

BY

MUHAMMAD SAAD WASEEM

A Thesis Presented to the

DEANSHIP OF GRADUATE STUDIES

KING FAHD UNIVERSITY OF PETROLEUM & MINERALS

DHAHRAN, SAUDI ARABIA

In Partial Fulfillment of the
Requirements for the Degree of

MASTER OF SCIENCE

In

CHEMICAL ENGINEERING

MARCH 2017

KING FAHD UNIVERSITY OF PETROLEUM & MINERALS

DHAHRAN- 31261, SAUDI ARABIA

DEANSHIP OF GRADUATE STUDIES

This thesis, written by **MUHAMMAD SAAD WASEEM** under the direction of his thesis advisor and approved by his thesis committee, has been presented and accepted by the Dean of Graduate Studies, in partial fulfillment of the requirements for the degree of **MASTER OF SCIENCE IN CHEMICAL ENGINEERING.**

Dr. Nayef M. Al-Saifi
(Advisor)

Dr. Mohammed Ba-Shammakh
Department Chairman

Dr. Nadhir A.H. Al-Baghli
(Co-Advisor)

Dr. Salam A. Zummo
Dean of Graduate Studies

Dr. Mohammed Mozahar Hossain
(Member)

2/5/17
Date

Dr. Nabeel Salim M. Abo-Ghander
(Member)

Dr. Housam Binous
(Member)

DEDICATION

To my parents
and
my siblings

ACKNOWLEDGEMENTS

First of all, I am grateful to Almighty Allah, the beneficial and merciful, who gave me best of health, knowledge and resilience to accomplish my thesis work. May the salutations and blessings be upon Prophet Muhammad (ﷺ).

I would like to seek this opportunity to express my deepest gratitude to my thesis advisor Dr. Nayef M. Al-Saifi, it was a privilege to work with a mentor like him. He trained me, motivated me and extended his utmost support, both morally and technically, throughout the research work. Furthermore, I would like to thank my co-advisor Dr. Nadhir A. H. Al-Baghli and thesis committee members Dr. Mohammed Mozahar Hossain, Dr. Nabeel Salim M. Abo-Ghander and Dr. Housam Binous for their time, effort in evaluation of my research work and extending their kind remarks for the improvement of same.

Besides, I am grateful to the chairman of chemical engineering department and other faculty members for providing their help and guidance during my masters. I am also obliged to King Fahd University of Petroleum and Minerals for awarding me full time (FT) scholarship to pursue graduate studies. Remarkable research facilities and computational resources provided by KFUPM, contributed to hassle free completion of my research work.

Moreover, I would like to thank my family for supporting and motivating me through every thick and thin of my life. Finally, I want to extend my sincere thanks to my friends, Najm us Saqib, Zeeshan Tariq, Aneeq Nasir, Taha Nasir, Ahmed Sadeed,

Mutsaied Shirazi, Adil Ahmed, Hassan Sheikh, Abdul Asad, Owais Ahmed and Abdullah Khaleel for their generous support and making my tenure at KFUPM a memorable one.

TABLE OF CONTENTS

LIST OF TABLES

LIST OF FIGURES

LIST OF ABBREVIATIONS

SAFT-VR	:	Statistical Associative Fluid Theory-Variable Range
SW	:	Square Well
PC-SAFT	:	Perturbed Chain-Statistical Associative Fluid Theory
PR	:	Peng Robinson
LJ	:	Lenard-Jones
vdWP	:	van der Waals & Platteeuw
EOS	:	Equation of State
TPT1	:	Thermodynamic Perturbation Theory-1
STP	:	Standard Temperature & Pressure
VLE	:	Vapor-Liquid Equilibrium
PVT	:	Pressure-Volume & Temperature
H-V-L	:	Hydrate-Vapor-Liquid
AADP	:	Average Absolute Deviation in Pressure
AADY	:	Average Absolute Deviation in Vapor mole fraction
AADX	:	Average Absolute Deviation in Liquid mole fraction

AADL	:	Average Absolute Deviation in Liquid density
CK-SAFT	:	Chen-Kreglewski -Statistical Associative Fluid Theory
RDF	:	Radial Distribution Function
L_w-H-V	:	Liquid water-Hydrate-Vapor

ABSTRACT (ENGLISH)

Full Name : Muhammad Saad Waseem

Thesis Title : Thermodynamic Modeling of the Incipient Conditions for Single and Mixed Gas Hydrate Systems

Major Field : Chemical Engineering

Date of Degree : March, 2017

This work uses a modeling approach to predict the incipient conditions of vapor–liquid–hydrate equilibrium systems using van der Waals-Platteeuw Model. The vapor-liquid mixtures are modeled by the SAFT-VR Mie with the combination of the Novel LJ association scheme. In this thesis, single and mixed gas hydrate systems are considered and the results are compared with experimental data. The Langmuir constants, which are used in the gas hydrate model, are determined by the simplex optimization technique. The selection of the reference energy parameters is made after comparing different available sets from the literature.

Excellent prediction of VLE of gas hydrate mixtures is obtained including nonpolar systems as well as water-nonpolar systems. It is found that the van der Waals-Platteeuw model with the combination of the SAFT-VR Mie gives excellent prediction of the dissociation pressures of single and mixed gas hydrate mixtures. For eleven single gas hydrate systems, the average absolute deviation (AADP) was less than 4 %. In addition, the dissociation pressure of ten binary mixed hydrate systems is studied with the proposed model and the AADP (%) is found less than 5%. The selected gas hydrate

model is further extended to seven multicomponent hydrate systems as well. The results obtained in this work are compared with those of other studies based on Peng-Robinson (PR) and Perturbed-Chain Statistical Association Fluid Theory (PC-SAFT). The comparison concludes that the SAFT-VR Mie-Novel LJ EOS based gas hydrate model is more accurate than PR and PC-SAFT EOS based gas hydrate models. Finally, the stability test is carried out and it is found that the proposed model is capable to capture the variation of gas hydrate structures in nitrogen system and other gas hydrate systems due to the change of state variables.

ABSTRACT (ARABIC)

ملخص الرسالة

الاسم: محمد سعد وسيم

عنوان الرسالة: نمذجة ديناميكيا حرارية للظروف الأولية لأنظمة هيدارت الغاز الأحادية والمختلطة

التخصص: هندسة كيميائية

التاريخ: مارس 2017م

في هذه العمل تم استخدام نهج النمذجة للتنبؤ بالظروف الأولية لنظام الاتزان لهيدرات البخار- السائل باستخدام نموذج van der Waals-Platteeuw. فقد تم نمذجة خليط بخار- سائل باستخدام SAFT-VR Mie ومخط Novel LJ. في هذه الرسالة، أنظمة هيدرات الغاز الأحادية والمختلطة تم أخذها بعين الاعتبار، وتم مقارنة النتائج التي تم الحصول عليها بالبيانات التجريبية. ثوابت Langmuir(الذي تم استخدامها في نموذج هيدرات الغاز) تم قياسها باستخدام تقنية التحسين البسيط. كما تم اختيار متغيرات الطاقة المرجعية بعد المقارنة بما هو موجود في البحوث العلمية السابقة.

تم الحصول على تنبؤ ممتاز لنظام الاتزان البخاري/ السائل لخليط هيدرات الغاز بما في ذلك الأنظمة اللاقطبية وأنظمة ماء-لا قطبية. وتم الوصول إلى أن نموذج van der Waals-Platteeuw مع SAFT-VR Mie أعطى تنبؤ ممتاز لضغوط التفكك لخليط هيدرات الغاز الأحاية والمختلطة. كما أن متوسط الانحراف المطلق كان أقل من 4 % لأحد عشر نظام من أنظمة هيدرات أحاي الغاز. بالإضافة إلى ذلك، تم دراسة ضغوط التفكك لعشرة أنظمة هيدارت الغازات المختلطة (نظام ثنائي) باستخدام نفس النموذج، وكان متوسط الانحراف المطلق أقل من 5%. أيضاً تم استخدام هذا النموذج في سبعة أنظمة أخرى لهيدارت الغاز متعددة المكونات. وفي الأخير تم مقارنة النتائج التي تم الحصول بالدراسات الأخرى بناء على نظرية Peng-Robinson (PR) و Perturbed-Chain Statistical Association Fluid Theory (PC-SAFT).

CHAPTER 1

INTRODUCTION

1.1 Motivation

Gas hydrates are non-stoichiometric clathrates compounds that contain water and light gases. The water molecules arrange themselves in crystal lattice cavities through hydrogen bonding interactions. The lattice cavities are stabilized by encapsulating light gases such as methane, ethane, propane, nitrogen, carbon dioxide and hydrogen sulfide. The stability of gas hydrates is favored at low temperature and high-pressure conditions. The gas hydrates have become a subject of interest in different areas such as energy resources, separation technologies, gas storage and oil and gas industry (Herzog, 1998; Hunt, 1996; Rouher & Barduhn, 1969; Sloan & Koh, 2008).

The discovery of the gas hydrate in nature was first reported in the Soviet Union in late 1960's (Vasil'ev, Makogon, Trebin, Trofimuk, & Cherskiy, 1970). Since then, about 23 locations have been discovered in different countries, where gas hydrate samples have been recovered. Figure 1.1 illustrates the locations of inferred, recovered and potential gas hydrates reserves present on earth (Sloan & Koh, 2008).These reserves mainly contain methane based gas hydrates. This gives evidence that enormous naturally occurring gas hydrates reserves are available under oceans across the world (Kvenvolden & Claypool, 1988; Kvenvolden & Lorenson, 2001; Sloan & Koh, 2008). The amount of methane gas entrapped in these hydrates' reserves is uncertain and different estimates have been reported in the literature ranging from 10^{15} to 10^{18} m^3 (STP) (Sloan & Koh,

2008). The most conservative estimate indicates that the amount of gas hydrates is higher than that of the conventional gas reserves with two to third orders. This makes gas hydrates a popular subject of study.

Another key area where the gas hydrates have been given special interest is in the oil and gas industry. The attention is paid to resolve the flow assurance problems associated with the formation of the gas hydrates. Hammerschmidt (1934) determined that the formation of the gas hydrates is the major cause of plugging pipelines in the transportation of natural gas. Every year, more than one hundred million dollars are spent worldwide to control and prevent the gas hydrates formation (Carroll, 2009; Sivaraman, 2002; Sloan, 1994). This makes gas hydrates as one of the major problems encountered in the oil and gas industries. This is why it is not surprising to find extensive research interest about gas hydrates.

The research interest of gas hydrates is noticeable in the growing number of experimental and modeling studies. Experimental measurements for the determination of gas hydrates formation and dissociation conditions have been reported since last decade (Breland & Englezos, 1996; Holder, Corbin, & Papadopoulos, 1980; D. R. Marshall, Saito, & Kobayashi, 1964; Servio, Lagers, Peters, & Englezos, 1999; Ward et al., 2014). Researchers have developed many empirical correlations and charts for the prediction of gas hydrates phase equilibrium based on these experimental measurements (Baillie & Wichert, 1987; Carroll & Duan, 2002; Carson & Katz, 1942; Sloan & Koh, 2008; W. I. Wilcox, Carson, & Katz, 1941). Table 1-1 gives examples of gas hydrate equilibrium data found in the literature for various gas hydrates formers.

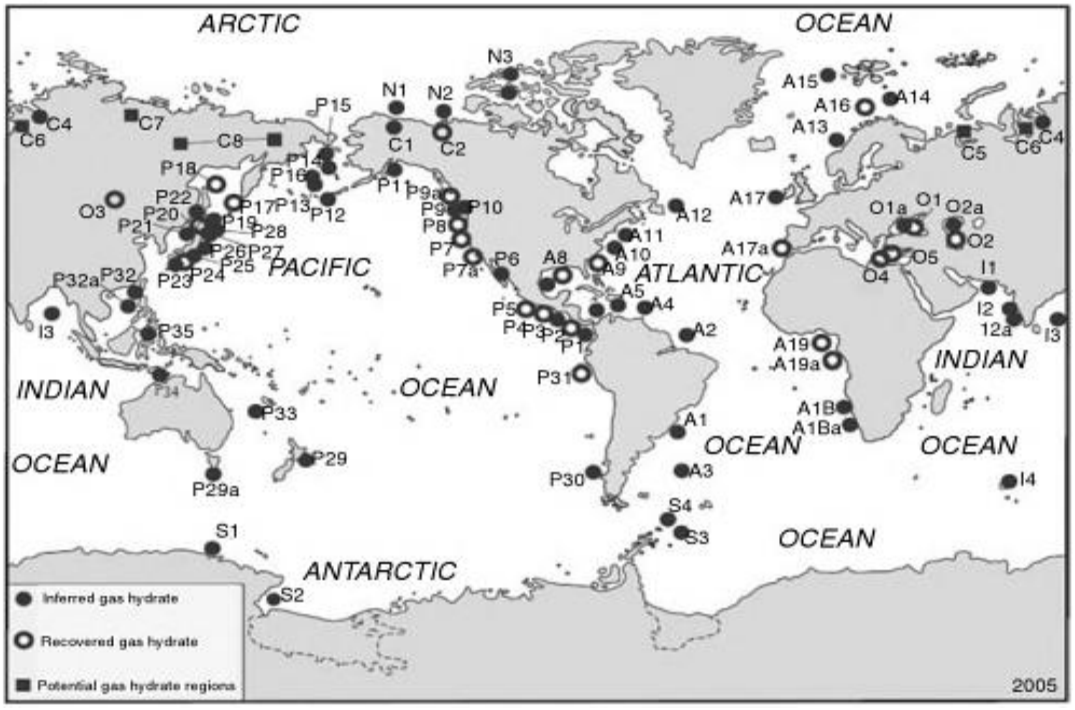

Figure 1.1: Locations of inferred, recovered and potential gas hydrates reserves present on earth (Sloan & Koh, 2008)

Although experimental measurements are crucial and available in the literature, it is unlikely that one could find the desired operating conditions. Gas hydrate equilibrium experiments are conducted at high pressures, which may pose safety concerns in the lab. Moreover, one of the important hydrate former in the natural gas industry is the H_2S gas, which is poisonous by nature and its handling at lab scale can be hazardous. Excessive time consumption and high costs, in conducting gas hydrate equilibrium experiments for different proportions of inhibitors at varying conditions, are two more major factors that add difficulty in experimental measurements. This is why it is important to approach the problem theoretically.

Hence, the above-indicated issues and the need for reliable models to carry out accurate gas hydrates calculations drive the motivation for this thesis.

Before introducing the research objectives, it is necessary to give a brief overview about the theoretical models associated with gas hydrates calculations. A detailed discussion will be given in subsequent chapters.

Table 1-1: Examples of experimental data and their data sources for various gas hydrates formers

Hydrate Formers	**Data Sources**
Single Hydrate Formers	
Methane	(Nakamura, Makino, Sugahara, & Ohgaki, 2003)
Ethane	(D. Avlonitis, 1988)
Propane	(B. Miller & Strong, 1946)
Isobutane	(Schneider & Farrar, 1968)
Carbon Dioxide	(Adisasmito, Frank, & Sloan, 1991)
Nitrogen	(van Cleeff & Diepen, 1960)
Ethene	(Tumba, Hashemi, Naidoo, Mohammadi, & Ramjugernath, 2013)
Ethyne	(Tumba et al., 2013)
Argon	(D. R. Marshall et al., 1964)
Oxygen	(van Cleeff & Diepen, 1965)
Hydrogen Sulfide	(Selleck, Carmichael, & Sage, 1952)
Binary Hydrate Formers	
Methane-Ethane	(McLeod Jr. & Campbell, 1961)
Methane-Propane	(Deaton & Frost, 1946)
Methane-CO_2	(Adisasmito et al., 1991)
Propane-Nitrogen	(Ng, Petrunia, & Robinson, 1977)
Methane-Nitrogen	(Mei, Liao, Yang, & Guo, 1996)
Ethane-Propane	(Holder & Hand, 1982)
Methane-Isobutane	(Wu, Robinson, & Ng, 1976)
Methane-Ethylene	(Ma, Chen, Wang, Sun, & Guo, 2001)
Nitrogen-Oxygen	(Mohammadi, Tohidi, & Burgass, 2003)

Methane-H_2S	(Noaker & Katz, 1954)
CO_2-N_2	(Kang, Lee, & Ryu, 2001)
Multicomponent Hydrate Formers	
Methane-CO_2-N_2	(Nixdorf & Oellrich, 1997)
Methane-Ethane-N_2	(Nixdorf & Oellrich, 1997)
Methane-Ethane-Propane	(Nixdorf & Oellrich, 1997)
Methane-Ethane-CO_2-N_2	(Nixdorf & Oellrich, 1997)
Methane-Propane-CO_2-N_2	(Nixdorf & Oellrich, 1997)
Natural Gas Mixtures	(Deaton & Frost, 1946; W. I. Wilcox et al., 1941)

1.2 Gas Hydrate Equilibrium Calculations

The first model proposed for the determination of gas hydrate formation and dissociation conditions was that of van der Waals and Platteeuw (vdWP) in 1959. Although there were quite some limitations of vdWP model, its concept related to prediction of gas hydrate equilibrium was sound and clear (Bakker, 1998). Its advent became an important milestone in gas hydrate research (Klauda & Sandler, 2003) and became the basis for all other gas hydrate models (Ballard & Sloan, 2002; Klauda & Sandler, 2000). A significant increase in number of gas hydrate publications with the arrival of vdWP model can be noticed in Figure 1.2.

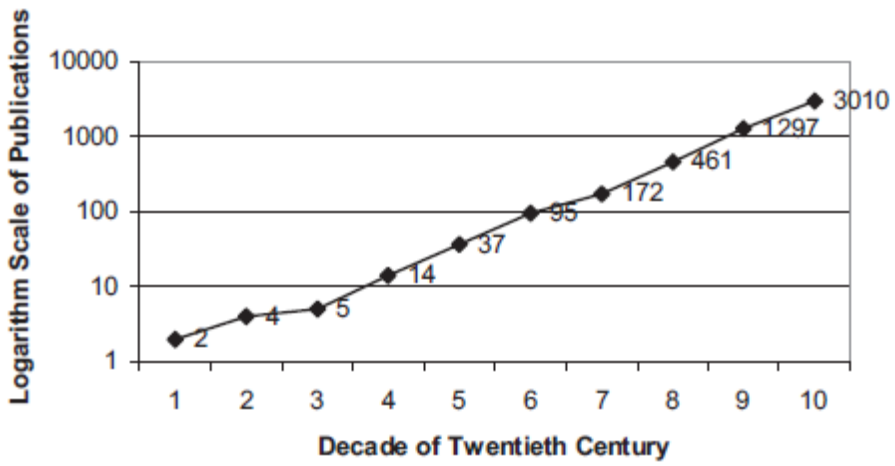

Figure 1.2: Number of gas hydrate based publications per decade of twentieth century (Sloan, 2004)

Over the years, vdWP model has been improved by many studies either by modification to assumptions or by considering different approach for phase equilibrium calculations. The most notable modification was made by Parish and Prausnitz (1972) who extended the vdWP model for multiple guest molecules in hydrate cavities. Other modifications to vdWP model included the consideration of multiple cavity shells (John & Holder, 1982), introduction of correction factor for asymmetric and non-spherical guest molecule interactions (V. T. John, Papadopoulos, & Holder, 1985) and consideration of variable reference chemical potential based on different guests (Zele, Lee, & Holder, 1999). Although these modifications contributed to refinement of the vdWP model, they did not bring dramatic improvement in incipient conditions prediction (Englezos, 1993). In fact, Avlionitis et al. (1991a, 1991b) reported that these modifications caused overestimation in the prediction of incipient conditions. For this reason, these modifications are not taken into account in this thesis. The thesis's work is based on vdWP model with Parish and Prausnitz extension.

To conduct multiphase equilibrium calculations in the presence of gas hydrate, proper selection of accurate models for gas and liquid phases are crucial since the calculations are based on the equality of chemical potentials for the co-existing phases. The previous studies are mainly based on fugacity based models for the gas phase and activity coefficient models for liquid phases (Barkan & Sheinin, 1993; Klauda & Sandler, 2000, 2003). To avoid inconsistency, this thesis uses the same model, which is based on the first-order of Wertheim perturbation theory (TPT1), for both phases. To account for the effect of association interactions between water particles, several association theories have been tested and implemented with TPT1. In particular, the thesis combines a variable range statistical association fluid theory based on Mie potential (SAFT-VR Mie, 2013) with vdWP model. The details of gas hydrates and vdWP gas hydrate model are found in Chapter 2 while Chapter 3 is dedicated to the TPT1 based model including SAFT-VR Mie.

1.3 Thesis Objectives

The main objectives of this thesis are:

- To predict the incipient conditions (dissociation pressure) for single and mixed gas hydrate systems using vdWP and SAFT-VR Mie equation of state by conducting multiphase calculations between gas-liquid-hydrate systems and to compare the results with experimental data from the literature.
- To study the SAFT-VR Mie in predicting vapor-liquid equilibrium for water-non-polar mixtures and compare with experimental data.

- To evaluate the effect of the association theories with employing different pairwise potential references; namely Square-well, Lennard-Jones and Mie potentials.
- To study the capability of the above objectives to capture the possibility of the variations of gas hydrates structures on the same system with the change of temperatures and pressures.
- To optimize the interaction parameters between the guest and host particles in the gas hydrate systems in order to get quantitative results and to compare with the original Kihara potentials proposed by Parish and Prausnitz.

1.4 Systems of Interest

The systems of interest in this thesis are selected based on gases involved in natural gas environment, which are the main systems that cause gas hydrate problems in oil and gas industries. Systems of interest considered in this study are summarized in Table 1-1.

1.5 Thesis Organization

Chapter 2 deals with the detail explanation of gas hydrate structures, types, its guest molecules and its properties. It is followed by analysis on gas hydrate models present in the literature. At the end, a detail summary of vdWP model and its parameters are presented. In Chapter 3, an overview about SAFT EOS models is given with a detailed elaboration on SAFT-VR Mie EOS. Chapter 4 deals with the evaluation of SAFT-VR Mie EOS in VLE calculations for non-associative mixtures in this thesis.

Chapter 5 reports the VLE calculation results of water-nonpolar systems using SAFT-VR Mie EOS. Chapter 6 sheds light on the results obtained from vdWP Model for single and mixed gas hydrate systems along with discussion. Chapter 7 concludes the results that have been obtained in this research work followed by future recommendations.

CHAPTER 2

GAS HYDRATES

2.1 Introduction

As indicated in Chapter 1, gas hydrates are crystalline cavities that encapsulate light gas molecules at high pressures and low temperatures. The need for a detailed understanding of gas hydrate crystalline structures, their properties and theoretical models is required to predict their incipient conditions. For this purpose, the subsequent sections will elaborate a great deal on gas hydrate structures and their properties, followed by comprehensive information on the theoretical models for the determination of gas hydrate equilibria.

2.2 Gas Hydrate Structures and Properties

Gas hydrate structures, based on the shape and size of cavities and hydrate formers, are categorized into three categories: Structure-I, Structure-II and Structure-H. These structures consist of cavities called cages, formed due to hydrogen bonding interactions among the water molecules. Each structure consists of different types of cages, classified as small, medium and large cages according to their cavity radii. There are different adjusted values of cavity radii reported by Sloan (2008) and John et al (1985). More realistic values are usually obtained from the crystallographic measurements (Klauda & Sandler, 2000) . In this thesis, we adopt the values obtained from crystallographic measurements. The properties including size, shape, hydrate former

types and other properties of each hydrate structure are explained in the following three sections.

2.2.1 Structure I

Structure I consist of two kinds of cages: small and large cages. The small cage is a twelve pentagonal sided polyhedron called dodecahedron (5^{12}) with a cavity radius of 3.906 °A. The large cage, known as tetrakaidecahedron ($5^{12}6^2$), is a fourteen-sided polyhedron with twelve pentagonal and two hexagonal sides. It has a cavity radius of 4.326 °A. These two cages are shown in Figure 2.1.

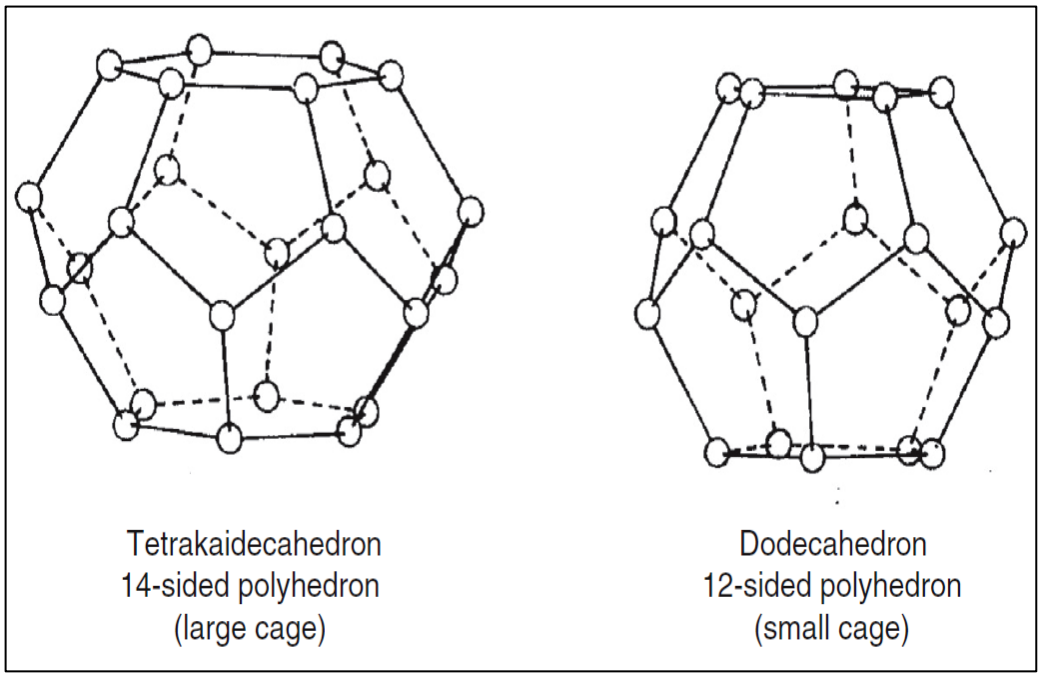

Figure 2.1: Structure I cavity types (Carroll, 2009)

There are two small cages and six large cages with a total of 46 water molecules per unit cell. The number of water molecules per cavity, known also as coordination number, is 20 for the small cage while it is 24 for the large cage. Examples for Structure-I

hydrate formers are methane, ethane, carbon dioxide and hydrogen sulfide that occupy small and large cages depending on their molecular size.

2.2.2 Structure II

Structure II also contains two types of cages, a small cage and a large cage. The small cage of structure II is similar in shape to the one that is found in structure I but with a slightly smaller cavity radius of 3.902 °A. Its large cage consists of twelve pentagonal sides and four hexagonal sides. This makes it a polyhedron and commonly known as hexakaidecahedron ($5^{12}6^4$). Hexakaidecahedron has a cavity radius of 4.682°A. The two cages are illustrated in Figure 2.2.

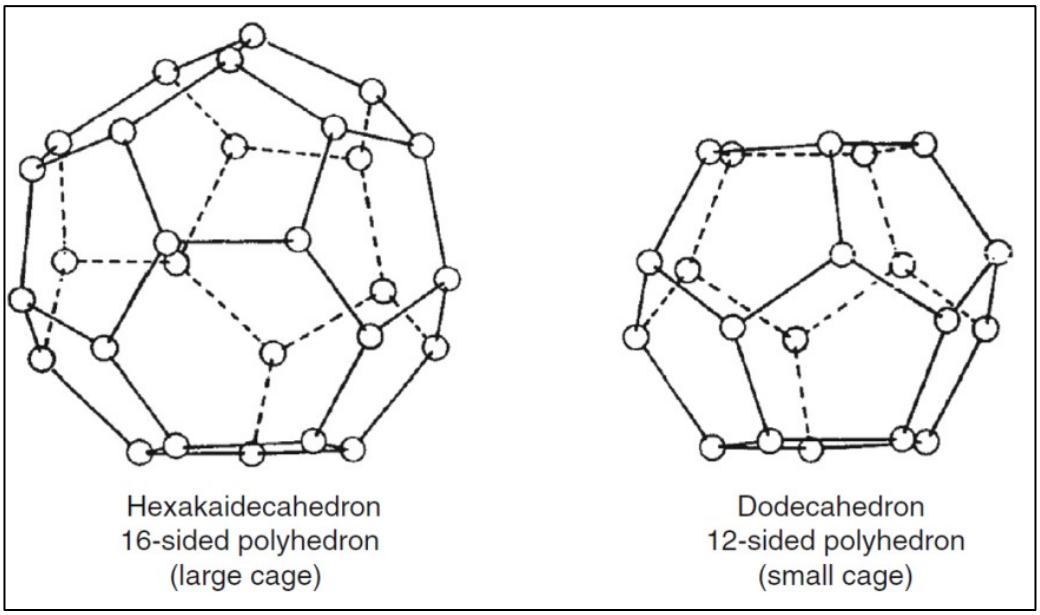

Figure 2.2: Structure II cavity types (Carroll, 2009)

There are sixteen small cages and eight large cages that contain a total of 136 water molecules per unit cell. Coordination number of the small cage is 20, while that of large cage is 28. Nitrogen, propane and isobutane are some of the examples of formers for structure II.

2.2.3 Structure H

Structure H hydrates are the complex of the three hydrate structures. They contain three types of cages, generally classified as small, medium and large cages. The small cage is a typical dodecahedron shaped cage as found in other structures as well. The medium cage is a dodecahedron ($4^3 5^6 6^3$), but irregular one. It contains three square, six pentagonal and three hexagonal sides. The large cage is an irregular twenty-sided polyhedron ($5^{12} 6^8$), also called icosahedron, with twelve pentagonal and eight hexagonal faces. A unit cell of structure H consists of three small cages, two medium and one large cage made up of 34 water molecules. Structure H hydrate formation requires two hydrate former molecules to exist. One molecule must be small such as methane or hydrogen sulfide that will fill the small and medium cages, whereas the other molecule must be a larger one such as cyclohexane, cycloheptane, 2-methylbutane or neo hexane.

Figure 2.3 summarizes the cavity types, shapes, numbers and guest molecules combination that results in aforementioned hydrate structures.

Since this work deals with the gas hydrates found in natural gas industry, structure H hydrate will not be considered since it doesn't form in natural gas processing environments. Therefore, prediction of incipient conditions of structures I and II is the subject of interest in the present work. Table 2-1 summarizes the important properties of structures I and II, which help in understanding and predicting the gas hydrate incipient conditions through theoretical models that will be explained in Section 2.3.

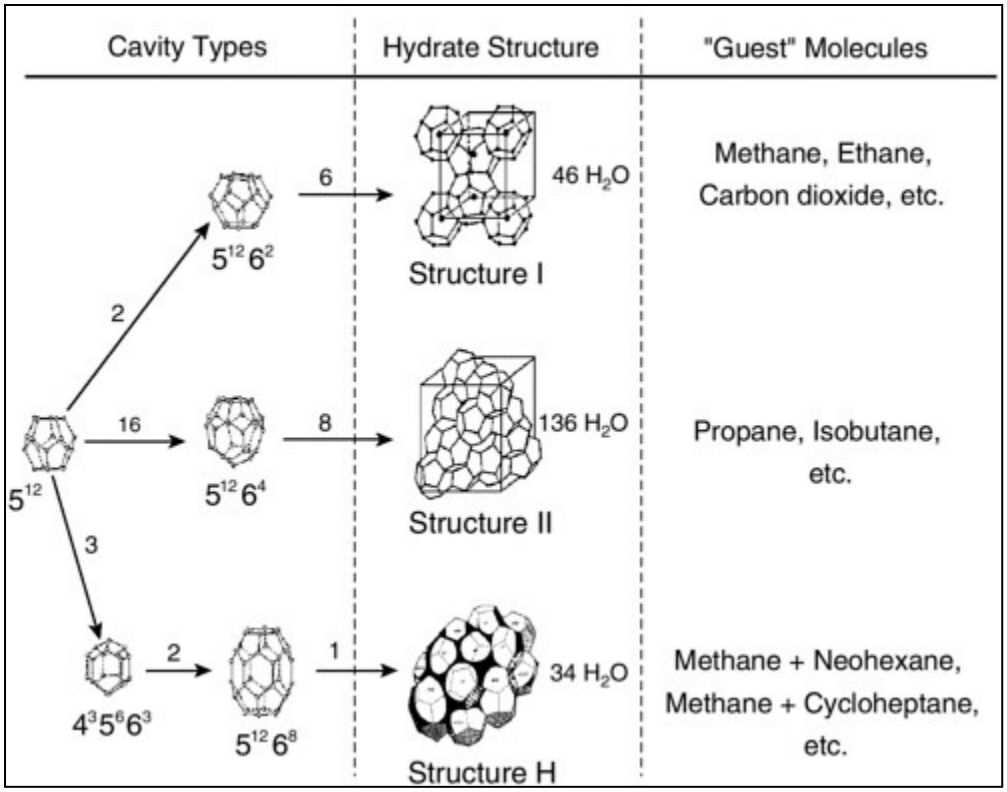

Figure 2.3: Schematic view of types of gas hydrate structure which summarizes information related to cavity types, hydrate structures and their probable guest molecules (Sloan, 2000)

Table 2-1: Physical properties of Structure I and Structure II

Properties	**Structure-I**		**Structure-II**	
Cage Type	Small	Large	Small	Large
Cage Description	5^{12}	$5^{12}6^2$	5^{12}	$5^{12}6^4$
Number of Cages per unit Cell	2	6	16	8
Cavity Radius (°A)	3.906	4.326	3.902	4.682
Coordination Number	20	24	20	28
Number of Water Molecules per unit Cell	46		136	

2.3 Gas hydrate Theoretical Modelling

Interest in gas hydrates research started in 1934, when Hammerschmidt reported that the natural gas pipeline plugging at high pressures and low temperatures was due to the formation of ice like substance called gas hydrates. In the early times of gas hydrate research, the gas hydrates equilibrium measurements were limited to macroscopic level such as studies of Wilcox et al (1941), Carson et al (1942), Deaton & Frost (1946). Macroscopic experimental techniques are time consuming and quite expensive, even a simple agitated smaller apparatus cost more than $50,000 (Sloan, 2004). On the other hand, little notable work was available at microscopic level such as XRD data by Von Stackhelberg (1952) that led to the establishment of gas hydrate structures I and II (Pauling & Marsh, 1952). Moreover, there was absence of modelling techniques that can predict the incipient conditions based on theory. Hence, an efficient and cost-effective modelling technique was required. A modelling technique that utilizes the information from both macroscopic and microscopic domains to predict accurate gas hydrate equilibrium conditions.

The bridging of aforementioned domains was fulfilled by the principles of statistical thermodynamics, which brought evolution in gas hydrate research with the development of a theoretical model for the prediction of gas hydrate incipient conditions. Van der Waals and Platteeuw (1959) proposed this model for a single guest molecule, considering the parameters such as cage occupancy, cage dimensions, pressure, temperature and mole fraction that can have significant impact on determination of gas hydrate equilibrium.

Van der Waals and Platteeuw (vdWP) model became an important milestone in the gas hydrate research area. It made a significant impact on boosting research publications (Sloan, 2004). The model became a basis for the modern gas hydrate models. The next section is dedicated to the theoretical background of van der Waals and Platteeuw model, and its assumptions and mathematical formulation.

2.3.1 Van der Waals and Platteeuw (vdWP) Model

2.3.1.1 Theory

For the prediction of gas hydrate incipient conditions, vdWP Model adopts the concept of equality of change in chemical potential of hydrate phase (H) and other coexisting phases (π) such as ice and liquid water with respect to a reference phase. The reference phase was selected as the empty hydrate phase (β). The empty hydrate phase is a thermodynamically unstable state and is stabilized by encaging the guest molecule (s). Mathematically, the equilibrium condition was given by:

$$\Delta\mu_w^H = \mu_w^\beta - \mu_w^H = \mu_w^\beta - \mu_w^\pi = \Delta\mu_w^\pi \qquad (2.1)$$

It is the change in chemical potential term of hydrate phase, which was derived using the statistical thermodynamics principles. Van der Waals and Platteeuw used the Langmuir type adsorption theory to determine the chemical potential of the hydrate phase. Each cavity was considered as an adsorption site, which can act as an active or inactive site. The active one occupies the guest molecule(s) whereas inactive sites are empty (V. T. John et al., 1985). Apart from above theory, the following assumptions were considered in the establishment of vdWP model (van der Waals & Platteeuw, 1958):

1) The mode of occupation of guest molecule does not affect the hydrate crystal lattice size and thus the reference chemical potential of a specific hydrate structure remains constant. A cavity can at most encage a single guest molecule.
2) Mutual interactions between the guest molecules are neglected and guest molecules are free to rotate in their cavities. This is because all internal partition functions of solute molecules are assumed similar as found in ideal gas.
3) The potential energy of a solute molecule at a distance 'r' from the center of its cage is given by the spherically symmetrical potential w(r) proposed by Lennard- Jones and Devonshire(Lennard-Jones & Devonshire, 1937, 1938).

Although these assumptions have some limitations, vdWP model was able to give a clear concept of connection between dissociation pressure, composition and chemical potential of water in hydrate (Bakker, 1998). The limitations of assumptions of vdWP model were later studied and amended (V. John & Holder, 1982; McKoy & Sinanoğlu, 1963; Parrish & Prausnitz, 1972; Zele et al., 1999) to ensure the physical integrity at molecular level along with better prediction of gas hydrate equilibrium. Of these amendments, notable improvements to prediction of incipient conditions of gas hydrates were accomplished by Mckoy and Sinonglu (1963) and extended by Parish and Praunitz (1972). Therefore, the Parrish and Prausnitz extension is adopted in this thesis.

For a better understanding, next section deals in detail with the mathematical representation of vdWP model along with Parish and Prausnitz extension.

2.3.1.2 Mathematical Model

The mathematical model for gas hydrate equilibrium, given by eq. (2.1), which accounts for both hydrate and interacting phase (ice, liquid water). The left hand side of eq. (2.1) needs the determination of change in chemical potential of water in hydrate phase, $\Delta\mu_w^H$. On the other hand, the right hand side requires chemical potential difference for interacting phases (ice, liquid water), $\Delta\mu_w^\pi$, with reference to empty hydrate phase.

2.3.1.2.1 Hydrate (H) Phase

The former quantity was determined by the masterpiece equation developed by Van der waal and Platteeuw (1959), using the statistical and molecular thermodynamics principles. The equation is presented as follows:

$$\Delta\mu_w^H(T,P) = -RT\sum_m v_m \ln\left(1-\sum_j \Theta_{mj}\right) \tag{2.2}$$

where, v_m is the number of cages of type 'm' per water molecule and Θ_{mj} is the fraction of cages occupied by guests. The summation in eq. (2.2) is applicable not only for a single guest but also for multiple guests. Parish and Prausnitz (1972) improved the vdWP model by modifying it for multiple guest molecules. This modification made it practically possible for the determination of incipient conditions of natural gas mixtures (Henley, Thomas, & Lucia, 2014). The summation encages the cage occupancy fraction term, Θ_{mj}, calculated by eq. (2.3). It is based on the Langmuir isotherm relation that treats each hydrate cavity as an active site for the hydrate formers(van der Waals & Platteeuw, 1958).

$$\Theta_{ml}(T,P) = \frac{C_{ml}(T) f_l(T,P)}{1 + \sum_j C_{mj}(T) f_j(T,P)} \tag{2.3}$$

The fugacity, $f_l(T,P)$, of hydrate formers can be calculated by any equation of state. The Langmuir constant,$C_{ml}(T)$, signifies the interaction between the hydrate former and the water cavity molecules and is generally given by

$$C_{ml}(T) = \frac{4\pi}{kT} \int_0^{R(cell)-a} \exp\left(\frac{W(r)}{kT}\right) r^2 \, dr \tag{2.4}$$

where $W(r)$ is the spherically symmetric cell potential for the entire hydrate cavity. An interaction pair potential is used to determine interaction forces between each guest and host molecule. Once the interaction forces for each binary guest-host interaction are determined, Lenard-Jones-Devonshire cell theory is then applied. Lenard-Jones-Devonshire cell theory sum up guest-host pair potentials of the entire cavity to produce a spherically symmetric cell potential, $W(r)$, for entire cavity. This spherically symmetric cell potential is inserted in eq. (2.4) to calculate Langmuir constants for a particular cage.

Originally, vdWP model used Lenard-Jones 12-6 cell potential to demonstrate guest and host molecular interactions. By that time, van der Waals and Platteeuw (1959) pointed out the limitation of Lenard-Jones 12-6 cell potential. The Lenard-Jones 12-6 cell potential's applicability was valid for monoatomic gases such as Ar, Kr, Xe, etc. and spherical guest molecules like CH_4, but not for rod-like molecules such as C_2H_6, C_3H_8, N_2, O_2, CO_2 and H_2S.

Later, Mckoy and Sinonglu (1963) came up with an important comparison between LJ 12-6, LJ 28-7 and Kihara pair potentials, for accurate prediction of incipient conditions of different gas hydrate formers. These formers included monoatomic, spherical and rod like molecules. They confirmed that Lenard-Jones 12-6 cell potential predicts satisfactorily for monoatomic and spherical guest molecules. Whereas for rod-like molecules, Kihara spherical or line core potential gave better results as compared to other pair potentials. It was due to the consideration of shape and size parameters of guest molecules that provided satisfactory prediction of dissociation pressures of hydrates of rod-like molecules. These conclusions reported by Mckoy and Sinonglu (1963) improved the accuracy of incipient conditions of various hydrate formers significantly. Most recent work in the literature (Haghighi, Chapoy, Burgess, & Tohidi, 2009; Klauda & Sandler, 2000; Le Quang et al., 2016; Tumba et al., 2013) employs the spherical or line core Kihara cell potential to determine the interactions between the hydrate former and the water cavity molecules:

$$\Gamma(r) = \infty, r \leq 2a \tag{2.5}$$

$$\Gamma(r) = 4\epsilon\left[\left(\frac{\sigma}{r-2a}\right)^{12} - \left(\frac{\sigma}{r-2a}\right)^{6}\right], r > 2a \tag{2.6}$$

As indicated above, a spherically symmetrical pair potential, $W(r)$, for entire cavityis produced by employing the Lenard-Jones-Devonshire cell theory on guest-host interaction potentials. For Kihara potential function, spherically symmetrical pair potential, $W(r)$, for entire cavity is represented as:

$$W(r) = 2z\epsilon\left[\frac{\sigma^{12}}{R(cell)^{11}r}\left(\delta^{10} + \frac{a}{R(cell)}\delta^{11}\right) - \frac{\sigma^{6}}{R(cell)^{5}r}\left(\delta^{4} + \frac{a}{R(cell)}\delta^{5}\right)\right] \tag{2.7}$$

With,

$$\delta^N = \frac{\left[\left(1 - \frac{r}{R(cell)} - \frac{a}{R(cell)}\right)^{-N} - \left(1 + \frac{r}{R(cell)} - \frac{a}{R(cell)}\right)^{-N}\right]}{N} \tag{2.8}$$

where σ is the core distance at zero potential, $a$is the core radius,ϵ is the characteristic energy, z is the coordination number, r is the radial distance and R (cell) is the radius of the cavity or shell. σ, ϵ and a are the Kihara molecular parameters. The selection and determination of Kihara parameters must be obtained with care because the dissociation pressures prediction are highly sensitive to these parameters (McKoy & Sinanoğlu, 1963).

Different methodologies are present in the literature for the determination of Kihara potential parameters (Dimitrios Avlonitis, 1994; Parrish & Prausnitz, 1972; Saito, Marshall, & Kobayashi, 1964). The two noteworthy methods are based on the second virial coefficient and viscosity data and fitting the hydrate dissociation data. The former method uses pure component experimental second virial coefficient and viscosity data to determine the Kihara potential parameters, employing mixing and combining rules to address the effect of guest-water interactions. The later method fits the Kihara potential parameters against the hydrate dissociation data by minimizing the difference between experimental and calculated fugacities or chemical potential of water.

The second virial coefficient and viscosity fitted Kihara parameters have predicted single hydrate equilibrium quite effectively (Klauda & Sandler, 2000). However, these parameters are ineffective in predicting multi-component gas hydrate

equilibrium (Klauda & Sandler, 2003) due to the inadequacy of arbitrary mixing rules for guest-host interactions and inability of fitting water virial coefficients over wide range of data (Dimitrios Avlonitis, 1994). On the other hand, fitting the Kihara parameters with the simple hydrate dissociation data, results in better prediction of both single and multi-component hydrate systems without any additional adjustable parameters. Kihara potential parameters fitted with hydrate dissociation data automatically accounts for water molecules effects, which eliminate the application of arbitrary mixing rules and in turn improve the accuracy of gas hydrate model.

In the present work, Kihara parameters from different literature are used in the gas hydrate calculations. The Kihara potential core parameter is determined using second virial coefficient data, with water spherical core parameter equals to zero (McKoy & Sinanoğlu, 1963). The other two potential parameters, σ and ϵ/k, are fitted to the hydrate dissociation data by minimizing the difference between experimental and calculated values of chemical potential or fugacities of water. Table 2-2 gives the values used in this thesis.

For a temperature range of 260 to 300 K, it is a common practice in the literature to simplify eq. (2.4) by:

$$C_{ml}(T) = \frac{A_{ml}}{T} exp\left(\frac{B_{ml}}{T}\right) \tag{2.9}$$

where, A_{ml} and B_{ml} are the adjustable parameters with units of Kelvin. For many tested gases, the maximum deviation does not exceed 0.2 %. Literature (Parrish & Prausnitz, 1972) values of adjustable parameters for calculation of Langmuir constants for small and large cavities of structures I and II are listed in Table 2-3. The formers whose adjusted

parameters values are not available, their values have been determined by fitting with the experimental data. Moreover, some of these literature values have also been improved in the present work. Adjusted parameter values determined in this work are reported in **Chapter 5**.

Table 2-2: Literature values of Kihara potential parameters for hydrate formers

Guest	a, Å	σ, Å	ϵ/k, K	Data Reference
Argon	0.184	2.9434	170.50	(Parrish & Prausnitz, 1972)
Methane	0.3	3.2398	153.17	
Ethane	0.4	3.3180	174.97	
Propane	0.68	3.3030	200.94	
Isobutane	0.8	3.1244	220.52	
Nitrogen	0.35	3.6142	127.95	
Carbon dioxide	0.31	2.9681	169.09	
Hydrogen Sulfide	0.31	3.1558	205.85	
Oxygen	0.31	2.7673	166.37	
Ethylene	0.47	3.2910	172.87	
Ethyne	0.363	3.255	171.94	(Tumba et al., 2013)

Table 2-3: Literature values (Parrish & Prausnitz, 1972) of Langmuir constant adjustable parameters

Guest	Small	Large	Small	Large
	$A_{ml} \times 10^3$, K	$B_{ml} \times 10^{-3}$, K	$A_{ml} \times 10^2$, K	$B_{ml} \times 10^{-3}$, K
Structure – I hydrates				
Methane	3.7237	2.7088	1.8372	2.7379
Propane	0	0	0	0
Isobutane	0	0	0	0
Nitrogen	3.8087	2.2055	1.8420	2.3013
Ethylene	0.0830	2.3969	0.5448	3.6638
Structure – II hydrates				
Argon	21.8923	2.3151	186.6043	1.5387
Methane	2.9560	2.6951	7.6068	2.2027
Ethane	0	0	4.0818	3.0384
Propane	0	0	1.2353	4.4061
Isobutane	0	0	1.3136	4.6534
Nitrogen	3.0284	2.1750	7.5149	1.8606
Ethylene	0.0641	2.0425	3.4940	3.1071
Carbon dioxide	0.9091	2.6954	4.8262	2.5718
Oxygen	14.4306	2.3826	15.3820	1.5187

2.3.1.2.2 Aqueous Liquid (L_w) Phase

Other than hydrate phase, hydrate formation process comes across with interacting phases such as ice, aqueous liquid, condensed hydrocarbon liquid. The

formation of hydrate occurs due to the interaction of gas and hydrate phase. The gas hydrate model addresses the gas phase (V) behavior by taking into account the gas phase fugacities. Therefore, it is not treated as an interacting phase. Aqueous liquid phase is the most common interacting phase, present as free water in natural gas production lines. In cold ambient conditions, interacting phases like ice and condensed hydrocarbon liquids are also present. Moreover, inhibiting liquid that is added to prevent hydrate formation does not take part in hydrate structure (Davidson, Gough, Ripmeester, & Nakayama, 1981) and due to high solubility in water, it is considered as a part of aqueous liquid phase. The interacting phase considered in this work are aqueous liquid phases.

The aim for prediction of L_w-H-V equilibrium has been chosen on multiple grounds. Firstly, availability of large amount L_w-H-V data helps testing theoretical models. Secondly, water is a complex component with strong associative forces, hence this is another challenge addressed in present thesis work. Moreover, free water is found in excess in natural gas production pipelines due to which hydrate formation probability is quite high. Hence, accurate prediction of L_w-H-V equilibrium has significant industrial application as well.

Due to the existence of aqueous liquid phase, its effect in hydrate equilibrium condition equation (eq. (2.1)) is considered by calculating the reduction in chemical potential of water in aqueous liquid with the reference of empty hydrate phase, $\Delta\mu_w^L$. It is determined on the basis of classical thermodynamics principles and is given by (Anderson & Prausnitz, 1986; Englezos, Huang, & Bishnoi, 1991):

$$\frac{\Delta\mu_w^L(T,P)}{RT} = \frac{\Delta\mu_w(T_0,P_0)}{RT_0} - \int_{T_0}^{T} \frac{\Delta h_w^L(T)}{RT^2} dT + \int_{P_0}^{P} \frac{\Delta v_w^L(T)}{RT} dP - lnx_w \qquad (2.9)$$

where $\Delta\mu_w(T_0, P_0)$ is chemical potential difference of liquid water and empty hydrate at reference conditions ($T_0 = 273.15\,K$ at zero absolute pressure). It is an experimentally determined quantity. $\Delta h_w^L(T)$ and $\Delta v_w^L(T)$ represent the molar enthalpy and molar volume differences between the liquid water and reference empty hydrate phase. The second and third terms correct the chemical potential from reference temperature and pressure to incipient hydrate conditions. The molar enthalpy difference is given by:

$$\Delta h_w^L(T) = \Delta h_w^0(T_0) + \int_{T_0}^{T} \Delta Cp_w dT \qquad (2.10)$$

where,

$$\Delta Cp_w = \Delta Cp_w^0(T_0) + \beta(T - T_0) \qquad (2.11)$$

$\Delta h_w^0(T_0)$ and $\Delta Cp_w^0(T_0)$ are molar enthalpy and heat capacity differences between liquid water and reference empty hydrate phase determined at the reference conditions. $\Delta h_w^0(T_0)$, $\Delta Cp_w^0(T_0)$ and β values are fitted against the experimental hydrate dissociation data. Some of the values reported in the literature are found in Table 2-4. The chosen reference energy values in this thesis are reported in **Chapter 5**.

Table 2-4: Literature values of reference thermodynamic properties

Parameters	Structure I	Structure II	Reference
$\Delta\mu_w^o$ (J/mol)	1235±10	-	(Holder et al., 1980)
	1297	937	(Dharmawardhana, Parrish, & Sloan, 1980)
	1264	883	(Parrish & Prausnitz, 1972)
	1299.5±10	-	(Holder, Malekar, & Sloan, 1984)
	1287	1068	(Handa & Tse, 1986)
Δh_w^o (J/mol)	-4327	-	(Ng & Robinson, 1985)
	-4622	-4986	(Dharmawardhana et al., 1980)
	-4860	-5203.5	(Parrish & Prausnitz, 1972)
	-4150	-	(Holder et al., 1984)
	-5080	-5247	(Handa & Tse, 1986)
ΔCp_w^o $(J/mol.K)$	-38.13	-38.13	(Parrish & Prausnitz, 1972)
	-34.583	-36.8607	(V. T. John et al., 1985)
β $(J/mol.K^2)$	0.141	0.141	(Parrish & Prausnitz, 1972)
	0.189	0.1809	(V. T. John et al., 1985)
Δv_w (cm^3/mol)	4.6	5.0	(Parrish & Prausnitz, 1972)

The effect of pressure on molar volume of water in both liquid and solid phases is very small. Therefore, the molar volume difference term is considered as a constant value stated in various research articles. Table 2-4 contains molar volume difference values for both structures I and II. The last term in eq. (2.9) accounts for the effect of solubility of gas in liquid water. However, the term $ln\ x_w$ is only considered at pressures in excess of 10 MPa, at which effect of solubility of gas is found to be considerable (Holder et al., 1980).

2.3.1.3 Computational Methodology

The methodology used for the determination of incipient conditions is based on the equality of fugacities of gas hydrate components in each vapor, liquid and hydrate phase:

$$f_i^V = f_i^L = f_i^H \tag{2.12}$$

Flash calculations are carried out to determine the vapor and liquid fugacities of each gas hydrate component, whereas the vdWP model is used for the calculation of hydrate phase fugacity. In terms of fugacity (van der Waals & Platteeuw, 1958), vdWP model can be represented as:

$$f_w^H = f_w^\beta exp\left(\frac{-\Delta\mu_w^H(T,P)}{RT}\right) \tag{2.13}$$

where, $\Delta\mu_w^H(T,P)$ term is calculated by eq. (2.2) and f_w^β is the fugacity of empty hydrate phase. The empty hydrate fugacity can be determined by:

$$f_w^{\beta} = f_w^{L} exp\left(\frac{\Delta\mu_w^{L}(T,P)}{RT}\right) \tag{2.14}$$

In above equation, $\Delta\mu_w^{L}(T,P)$ term is calculated by eq. (2.9) and f_w^{L} is pure water liquid fugacity, which is obtained from phase equilibrium calculation with the help of equation of state.

The computational methodology of predicting gas hydrate incipient conditions is adopted from Englezos et al. (1991). The clarity of such computer algorithm has convinced its application in present work. There are two major steps of the algorithm, first the calculation of vapor liquid equilibrium between the existing components and phases. The flash calculations are provided with feed composition, temperature and an assumed hydrate pressure. The second major step includes the calculation of fugacity of water in hydrate phase at the assumed hydrate pressure. The fugacities obtained from flash calculations and vdWP model are compared through a tolerance criterion defined in Figure 2.4.

The tolerance used in present work is 10^{-6}. If the fugacity of water in hydrate phase becomes equal to fugacities obtained from flash calculations, then the assumed hydrate pressure is the predicted hydrated pressure. On the other hand, if the fugacities are not equal at assumed pressure, then through secant method, a new pressure value updates the initial assumed hydrate pressure. This process is continued until the achievement of convergence criteria. The computational scheme can be better understood through Figure 2.4.

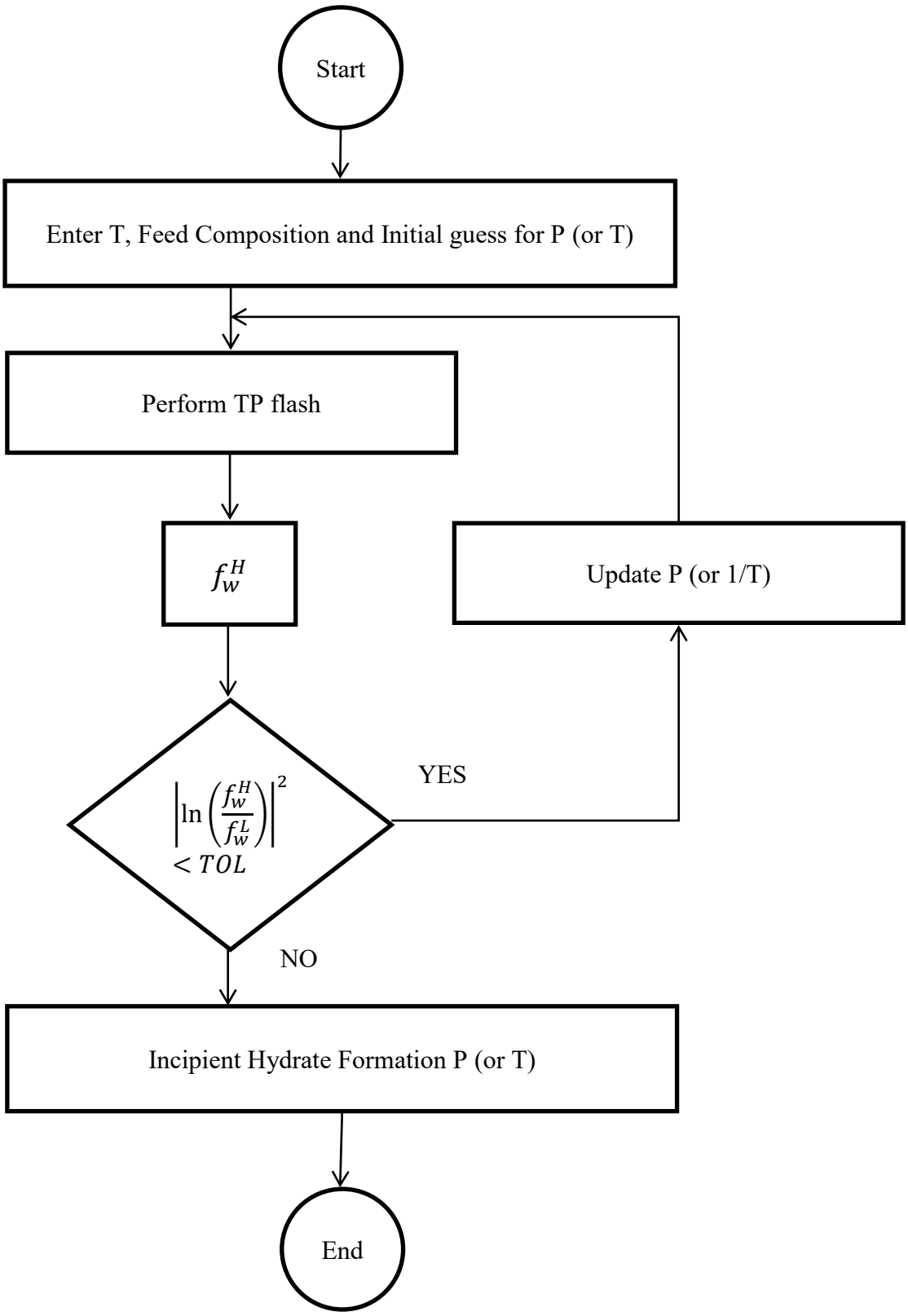

Figure 2.4: Computational methodology for gas hydrate equilibrium calculations

CHAPTER 3

SAFT-VR MIE EOS

3.1 Introduction

For accurate prediction of incipient conditions of gas hydrates, accurate vapor-liquid equilibrium is important. The vapor-liquid equilibrium is conveniently conducted by flash calculations, which require an adequate equation of state that can address the effects of molecular size and shape as well as the involved intermolecular forces. The gas hydrate systems usually involve both associating (alcohols, water etc.) and non-associating molecules (lighter hydrocarbons, light gases etc.). Semi-empirical cubic equations of state, like Soave-Redlich Kwong and Peng Robinson EOSs, are usually limited to non-polar and simple systems. For associating mixtures, the cubic equations of state alone are incapable to give accurate results unless they are combined with activity coefficient models. However, the limited capability of cubic equation of states for associating fluids (Müller & Gubbins, 2001) and inapplicable prediction of activity coefficient models at high-pressure systems (Dadmohammadi, Gebreyohannes, Abudour, Neely, & Gasem, 2016), call for a more comprehensive model. The statistical associative fluid theory (SAFT) is an alternative option since it has not only accounted for intermolecular forces like association, but also taken into account the molecular shape and size of molecules. In this thesis, a variant of the original SAFT EOS known as SAFT-VR Mie (Statistical Associative Fluid Theory-Variable Range Mie, 2013) has been

selected. It has recently gained importance due to its reasonable accuracy for the prediction of thermodynamic properties and VLE (Lafitte et al., 2013).

This chapter has two major parts. The first one deals with the description of SAFT and its development whereas the second one gives a detailed explanation of the SAFT VR Mie EOS. The chapter starts with shedding light on associative theories that led to the development of SAFT (Section 3.2). This follows with the advancement; applicability and physical concept of SAFT (Section 3.3). Finally, Section 3.4 summarizes the SAFT VR Mie EOS and its mathematical representation.

3.2 Associating Fluid Theories

In thermodynamics, the intermolecular forces of fluids are characterized by bond strength among the molecules. Fluids range from simple fluids (van der Waal's intermolecular forces) to strong chemical bonded fluids. The associating fluids are those whose bond strength lies in between the simple and true chemical bonds fluid. Figure 3.1 illustrates the bond strengths ranging from simple to strong chemical bonded fluids (Müller & Gubbins, 2001).

Several theories have been proposed to model the impact of associating forces on the fluid behavior and for the prediction of accurate thermodynamic properties of associating fluids. Such theories have been classified into three major categories chemical, quasi-chemical and physical theories.

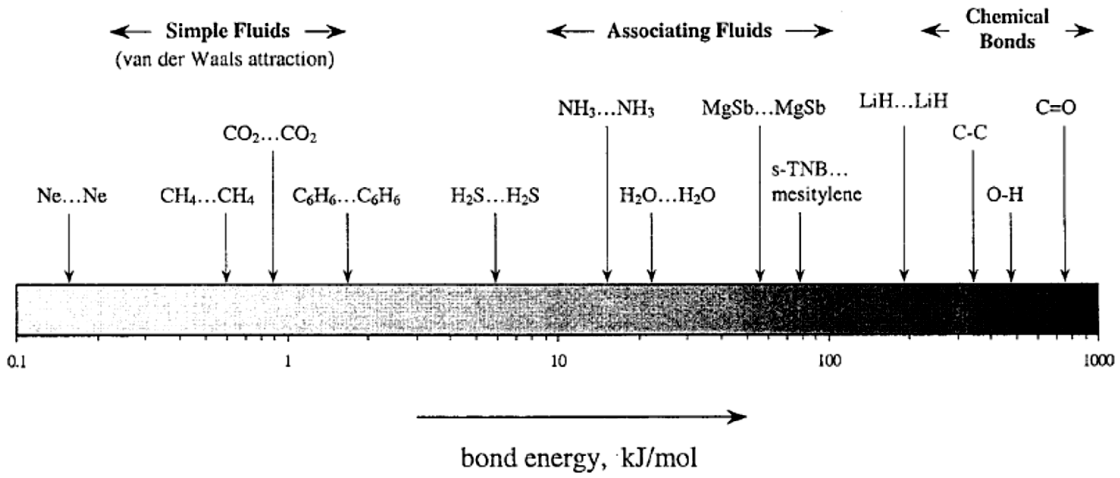

Figure 3.1: Classification of thermodynamic fluids based on bond strength values (Müller & Gubbins, 2001)

The review paper by Muller and Gubbins (2001) comprehensively discusses the pros and cons of these associative theories. A summary of associative theories can be found in Appendix A. It clearly demonstrates that thermodynamic inconsistencies can exist while using chemical and quasi-chemical theories in combination with physical equations of state. On the other hand, physical associating theories being thermodynamically consistent with physical EOS, shows a promising approach in modelling of associating fluids. Andersen's physical theory, which was developed based on geometry and interaction forces, provided a firm basis for further development of accurate physical associating theories. Later, the only limitation related to Andersen's theory was resolved by considering two-density formalism (HØye & Olaussen, 1980; Wertheim, 1984). Two density approach considers the cluster expansion in both monomer and total number density of associating fluid (B. D. Marshall, 2014). This approach helps in predicting correct low density limit of the second virial coefficient as well as provide an accurate representation of the extent of dimerization for liquid-like densities(Wertheim, 1984).

Wertheim was motivated by the Andersen's ideas and the versatility of two-density approach, determined an important expression for residual Helmholtz free energy for associating molecules as a function of monomer density. The Wertheim's approach gave the limit of complete association; it produced expressions for covalently bonded molecular chains (Wertheim, 1986, 1987).These key expressions for association were derived by cluster expansion analysis (Wertheim, 1984, 1986, 1987).

The Wertheim's theory and its extension by Chapman et al (1988) was derived based on thermodynamic perturbation theory (TPT). The general idea of TPT is to expand the Helmholtz free energy of real fluid behavior around the free energy of a known reference such as the hard sphere by Taylor series expansion. It combines the fluid structure and molecular interactions to develop an algebraic expression that can be used to model thermodynamic properties. Figure 3.2 provides the general theoretical framework of TPT.

The idea of perturbation theory was known before Wertheim's work. Examples of thermodynamic perturbation theories are Zwanzig (1954), Barker-Henderson perturbation theory (1967), Weeks-Chandler-Anderson perturbation theory (1971). However, these theories did not account for association effects on fluid behavior. Wertheim's TPT not only captured the association and molecular shape effects, but also provided flexibility in definition of reference fluid. These important contributions of Wertheim's TPT allowed Chapman et al. (1988,1989) to produce a masterpiece theoretical equation of state known as SAFT (Statistical Associative Fluid Theory) EOS.

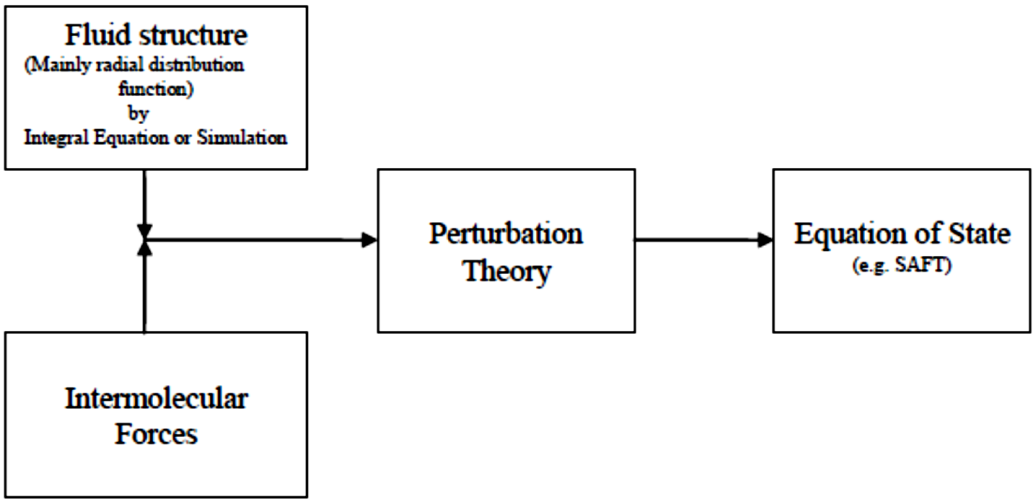

Figure 3.2: General concept of Perturbation Theory

3.3 Statistical Associative Fluid Theory (SAFT):

3.3.1 Advancement and Applicability

SAFT was derived based on Wertheim TPT. Initially, SAFT was proposed for pure component fluids and was later extended to real mixtures (Walter G. Chapman, 1988; Jackson, Chapman, & Gubbins, 1988). A major boost was observed in advancement of SAFT, when parameterization of various fluids such as light gases, organic compounds, water and polymers was carried out (Huang & Radosz, 1990). This allowed the prediction of correct VLE behavior of multi-component mixtures at wide ranges of pressures (Huang & Radosz, 1991). Since then, many modifications of SAFT have been conducted to improve its applicability for wide variety of real mixtures and conditions. Table 3-1 shows some of the SAFT applications to various fluid systems.

In the first decade after the advent of SAFT, more than 200 articles were published related to its improvement and further development (Müller & Gubbins, 2001). This success translated into production of several number of SAFT versions over the

years. Some of well-known versions of SAFT are given in Table 3-2. One of the key aspects of Wertheim TPT is flexibility in selecting the reference fluid. This makes it possible to incorporate other molecular interactions and to improve the accuracy of the association term. This flexibility is a major component for further development. Even at present new versions of SAFT like SAFT VR-Mie (Lafitte et al., 2013) and SAFT-gamma (Papaioannou et al., 2014), have been introduced and being checked for their applicability and adequacy on various systems.

In the next section, a brief overview is given for the major SAFT terms.

3.3.2 SAFT terms

Most of the SAFT variants, like PC-SAFT, CK-SAFT, simplified SAFT, SAFT VR-Mie (Walter G. Chapman, Gubbins, Jackson, & Radosz, 1990; Gross & Sadowski, 2002; Huang & Radosz, 1991; Lafitte et al., 2013), differ from each other based on distinct dispersion perturbation term. Figure 3.3 (b-e) explains the SAFT procedure of formation of a molecule.

At first the molecule consists of repulsive hard sphere segments, then dispersive forces are added. Chain sites are incorporated to each hard sphere and the formation of chain molecules occur due to covalent bonding. At last, the association sites appear through which association complexes are formed (Fu & Sandler, 1995). Each of above-indicated steps contributes for the Helmholtz free energy of the system. The final form of the Helmholtz free energy, a^{RES}, in the SAFT EOS can be algebraically represented as follows:

$$a^{RES} = a^{HS} + a^{DISP} + a^{CHAIN} + a^{ASSOC} \quad (3.1)$$

The dispersive and associative forces are classified as molecular interactions. In order to account for their part in SAFT, adequate spherically symmetrical interaction potentials are required. The association terms are quite computationally intensive (Müller & Gubbins, 2001) and thus many SAFT versions such as PCSAFT, Simplified SAFT, CKSAFT usually adopt a simple interaction potential like square well (SW) potential.

3.3.3 SAFT adjustable parameters

The interaction potentials and molecular geometry in SAFT EOSs introduce several adjustable parameters that differ for each pure component. The interaction potential for dispersion forces, such as Lenard-Jones potential, requires two parameters: well-depth (ϵ) and diameter(σ). Moreover, the chain length of molecules in SAFT is defined by the number of segments (m) of molecules. Wertheim used the square-well (SW) potential for the interaction among association molecules. SW potential is a function of two adjustable parameters: well-depth and well-width. Usually, the well-width is replaced by a bonding volume parameter that describes the volume of association corresponding to well width (K_{ab}). All these SAFT adjustable parameters are determined by minimizing an objective function of experimental and calculated liquid density and vapor pressure.

In this work, SAFT VR Mie is selected for the determination of VLE of gas hydrate systems and will be discussed further from now on.

Table 3-1: Some applications of different SAFT versions for wide variety of fluid systems (Kontogeorgis & Folas, 2010)

SAFT variant	**Applications**	**Reference**
Original SAFT	Methanol–pentane VLE and LLE; CO_2–water–ethanol.	(Jog, Garcia-Cuellar, & Chapman, 1999; Zhang, Yang, & Li, 2000)
SAFT–VR	Water–alkanes	(B. H. Patel, P. Paricaud, A. Galindo, & Maitland‡, 2003; Behzadi, Patel, Galindo, & Ghotbi, 2005)
PC–SAFT	Alcohols, water, amines, acetic acid (VLE and LLE); Amino acids +alcohol/water; SLE with complexes (alcohols, water, phenols, etc.); Polycarbonates; Poly (E-co-methacrylic acid) co-polymers.	(Fuchs, Fischer, Tumakaka, & Sadowski, 2006; Gross & Sadowski, 2002; Kleiner, Tumakaka, Sadowski, Latz, & Buback, 2006; Tumakaka, Prikhodko, & Sadowski, 2007; van Schilt et al., 2005)
CK–SAFT	Acid–hydrocarbon VLE;	(Chen, Banaszak, & Radosz, 1995; Huang & Radosz, 1991;

	CO_2 – alcohol VLE Water, alcohols, acids – emphasis on cross-associating mixtures; Poly(E-co-P) + olefins	Suresh & Beckman, 1994; Wolbach & Sandler, 1997)
Simplified SAFT	Alcohols, acids, water VLE (especially cross-associating mixtures)	(Fu & Sandler, 1995)
Soft-SAFT	Perfluoroalkanes + water; Glycols and PEG mixtures	(Dias, Llovell, Coutinho, Marrucho, & Vega, 2009; Pedrosa, Pàmies, Coutinho, Marrucho, & Vega, 2005)
SAFT-VR Mie	CO_2-Decane Water-Methanol Water-light gases (methane, carbon dioxide and other light gases)	(Dufal, Lafitte, Haslam, et al., 2015; Lafitte et al., 2013)

Table 3-2: Some well-known SAFT variants and their contributions (Kontogeorgis & Folas, 2010)

SAFT variant	Reference	Comments
Original SAFT	(W.G. Chapman, Gubbins, Jackson, & Radosz, 1989; Walter G. Chapman et al., 1990)	Mostly comparisons against simulation data. Parameters for six hydrocarbons and two associating fluids are given.
CK–SAFT	(Huang & Radosz, 1991)	Parameters for 100 different fluids.
Simplified SAFT	(Fu & Sandler, 1995)	Parameters for ten non-associating and eight associating compounds.
LJ–SAFT	(Kraska & Gubbins, 1996)	Alkanes, alkanols, water (pure components) / mixtures of alkanes, alkanols, water.
SAFT–VR	(GilVillegas et al., 1997; McCabe & Jackson, 1999)	Alkanes, perfluoroalkanes (pure components) / comparisons against simulation data.
PC–SAFT	(Gross & Sadowski, 2002)	The Gross and Sadowski article contains parameters for 100 compounds. Similarly, Tihic et al. (2006) contains another 400 parameters.

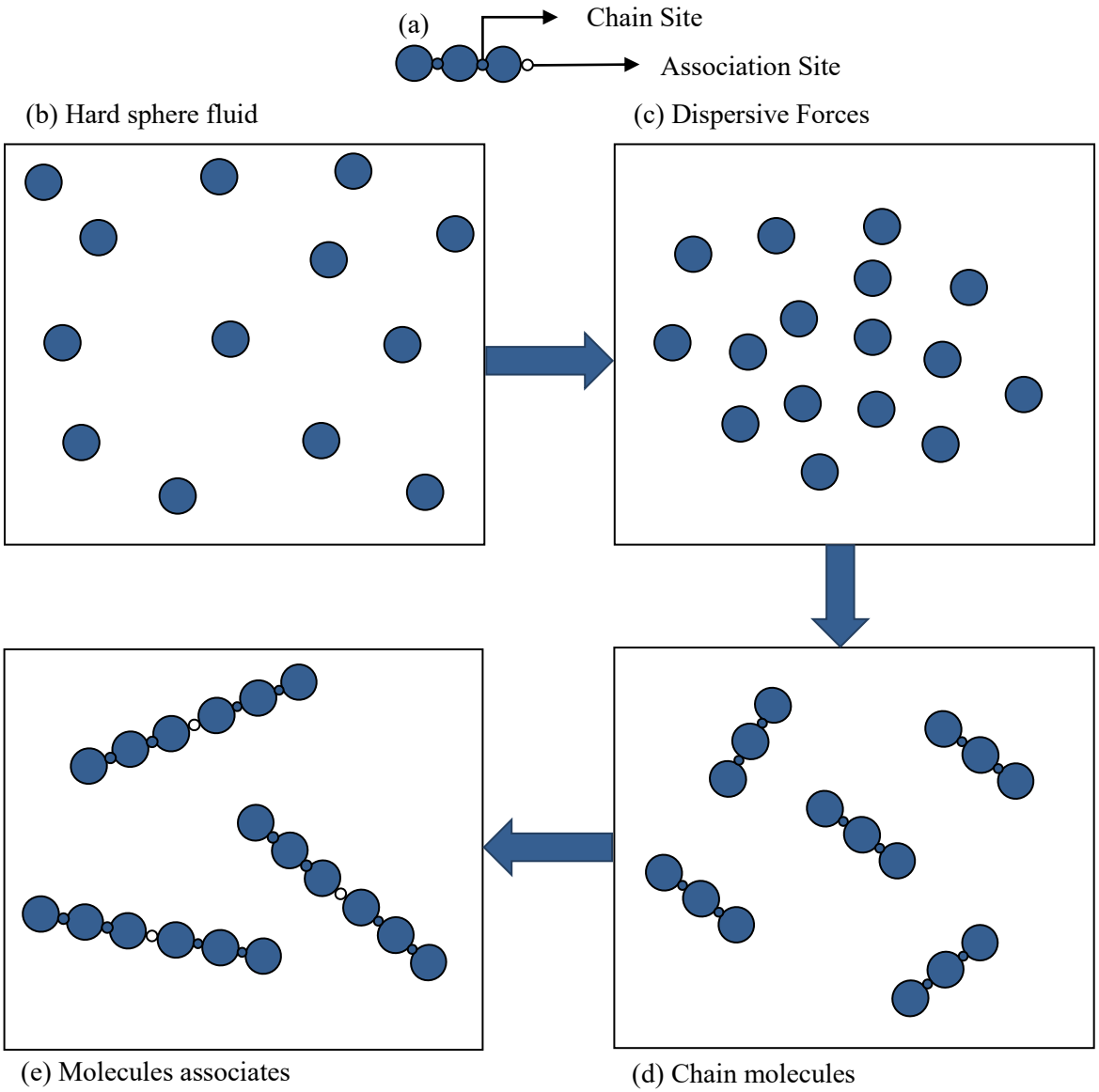

Figure 3.3: (a) Chain and Association sites (b),(c),(d),(e) Illustration of procedure for molecule formation through SAFT (Kontogeorgis & Folas, 2010)

3.4 SAFT VR Mie EOS

The motivation of developing new SAFT versions is to avoid some limitations in the previous SAFT versions and to improve the prediction capability. Most SAFT versions give inadequate representation of thermodynamic second derivative properties (enthalpy of vaporization, single-phase density, speed of sound, isobaric heat capacity,

and Joule–Thomson coefficient) and overestimation of critical properties (Tc, Pc) (GilVillegas et al., 1997; Lafitte et al., 2013) .Recently, a new version of SAFT EOS known as SAFT VR Mie EOS (Lafitte et al., 2013) catered above stated discrepancies, which opened new doors for inspection of its applicability for wide variety of systems. This makes the SAFT-VR Mie a very good candidate to utilize in this thesis.

The repulsive and attractive terms in the SAFT-VR Mie were represented by Mie pair potential. Mie pair potential is a generalized form of Lenard Jones interaction potential, in which variable repulsive 'λ_r' and attractive 'λ_a' exponents are used. These variable exponents address the softness and hardness of repulsive interactions and the range of dispersive interactions (Dufal, Lafitte, Galindo, Jackson, & Haslam, 2015). This ultimately tunes the prediction of thermodynamic properties and VLE. Hence, the hard spheres governed by Mie potentials will be described as Mie segments from now on. The Mie segments through covalent bonding become Mie chains. Finally, the association sites based on Wertheim TPT1 appear on Mie chains to produce associating molecules. Mathematically, Mie pair potential between two Mie spheres separated by a distance 'r' can be represented as:

$$u_{ij}^{Mie} = C_{ij}\epsilon_{ij}\left(\left(\frac{\sigma_{ij}}{r_{ij}}\right)^{\lambda_{r,ij}} - \left(\frac{\sigma_{ij}}{r_{ij}}\right)^{\lambda_{a,ij}}\right) \tag{3.2}$$

with,

$$C_{ij} = \frac{\lambda_{r,ij}}{\lambda_{r,ij} - \lambda_{a,ij}}\left(\frac{\lambda_{r,ij}}{\lambda_{a,ij}}\right)^{\frac{\lambda_{a,ij}}{\lambda_{r,ij}-\lambda_{a,ij}}} \tag{3.3}$$

where C_{ij} is a prefactor that ensures the minimum value of Mie potential be -ϵ, σ is the segment diameter, ϵ is the well-depth of Mie potential. The application of Mie

potential in SAFT EOS introduces two more adjustable parameters as λ_r and λ_a which increase the number of adjustable parameters of pure compound to five for non-associative compounds and seven for associative compounds. The values of adjustable parameters must be carefully determined, keeping in mind the physics of each component. As stated above, these adjustable parameters are determined by fitting against vapor pressures and liquid densities data. Second derivative properties such as speed of sound, heat capacities, were also used to find the adjustable parameters to improve the SAFT VR Mie prediction (Lafitte, Bessieres, Piñeiro, & Daridon, 2006).

3.4.1 Mathematical Representation

The SAFT VR Mie EOS is expressed in terms of residual Helmholtz energy. Each term is added in terms of Helmholtz free energy. Mathematically, the residual Helmholtz energy of an associating fluid using the SAFT VR Mie methodology is given by:

$$a^{RES} = a^{MONO} + a^{CHAIN} + a^{ASSOC} \tag{3.4}$$

where a^{MONO},a^{CHAIN} and a^{ASSOC} are the Helmholtz free energy contribution of Mie segments, Mie chains and association interactions. The purpose of this mathematical representation is to give an idea of the algebraic expressions used in the determination of residual Helmholtz energy of a fluid. The detailed derivations that contributed to the development of these Helmholtz energy can be found in literature (Lafitte et al., 2013).

3.4.1.1 Excluded volume and mean field terms

The monomeric term addresses the contribution of hard spheres and the dispersion interactions among these hard spheres. The SAFT VR Mie, like other versions,

adopts the concept of hard spheres as reference fluid with the attractive interactions being considered as perturbative terms (GilVillegas et al., 1997). Barker and Henderson high temperature perturbation theory is applicable for such hard core systems. This theory expands the perturbative term i.e. dispersion term, in terms of series of inverse temperature $\beta = \frac{1}{kT}$ up to third order. Hence, the SAFT VR Mie monomeric term is mathematically expressed as:

$$a^{MONO} = \left(\sum_{i=1}^{n} x_i m_i\right) a^M \tag{3.5}$$

$$a^M = a^{HS} + \beta a_1 + (\beta)^2 a_2 + (\beta)^3 a_3 \tag{3.6}$$

where x_i is the component 'i' mole fraction,m_i is the number of Mie segments, a^{HS} is the Helmholtz free energy contribution of hard spheres and a_1,a_2, a_3 are the mean free energy contribution of attractive interactions.

The hard sphere contribution to the monomeric Helmholtz energy term is given by the expression determined by Boublík (Boublík, 1986) and Mansoori et al.(Mansoori, Carnahan, Starling, & Leland, 1971). This expression is given by:

$$a^{HS} = \frac{6}{\pi \rho_s}\left[\left(\frac{\xi_2^3}{\xi_3^2} - \xi_0\right)\ln(1-\xi_3) + \frac{3\xi_1\xi_2}{1-\xi_3} + \frac{\xi_2^3}{\xi_3(1-\xi_3)^2}\right] \tag{3.7}$$

where ρ_s is the overall segment number density, ξ_k is expressed as:

$$\xi_k = \left(\frac{\pi\rho_s}{6}\right)\sum_i x_{s,i} m_i d_{ii}^k \ , \quad k = 0,1,2,3. \tag{3.8}$$

with $x_{s,i}$ being the segment mole fraction of component 'i' represented by:

$$x_{s,i} = \frac{m_i x_i}{\sum_{k=1}^{n} m_k x_k} \tag{3.9}$$

The d_{ii} term in eq. (3.8) is defined as the effective diameter of segments of 'i' components. It was determined by the Barker and Henderson (1967) expression which expresses the effective diameter as a function of temperature:

$$d_{ii}(T) = \int_0^{\sigma_{ii}} \left(1 - exp\left(-\beta u_{ii}^{Mie}(r)\right)\right) dr \tag{3.10}$$

where $u_{ii}^{Mie}(r)$ is the Mie pair potential given by eq. (3.2).

The other part of the monomeric term accounts for attractive molecular interactions through mean Helmholtz free energy up to third order. The first order perturbation dispersive term is given by:

$$a_1 = \sum_{i=1}^{n}\sum_{j=1}^{n} x_{s,i} x_{s,j} a_{1,ij} \tag{3.11}$$

$$\begin{aligned} a_{1,ij} = C_{ij}\Big[x_{0,ij}^{\lambda_{a,ij}}\left(a_{1,ij}^{s}(\rho_s;\lambda_{a,ij}) + B_{ij}(\rho_s;\lambda_{a,ij})\right) \\ - x_{0,ij}^{\lambda_{r,ij}}\left(a_{1,ij}^{s}(\rho_s;\lambda_{r,ij}) + B_{ij}(\rho_s;\lambda_{r,ij})\right)\Big] \end{aligned} \tag{3.12}$$

where,

$$x_{0,ij} = \frac{\sigma_{ij}}{d_{ij}} \tag{3.13}$$

$$B_{ij}(\rho_s;\lambda_{ij}) = 2\pi\rho_s d_{ij}^3 \epsilon_{ij}\left[\frac{1-{\zeta_x}/{2}}{(1-\zeta_x)^3} I_{\lambda,ij} - \frac{9\zeta_x(1+\zeta_x)}{2(1-\zeta_x)^3} J_{\lambda,ij}\right] \tag{3.14}$$

with

$$\zeta_x = \frac{\pi\rho_s}{6}\sum_{i=1}^{n}\sum_{j=1}^{n} x_{s,i}x_{s,j}{d_{ij}}^3 \tag{3.15}$$

The terms $I_{\lambda,ij}$ and $J_{\lambda,ij}$ are mathematically expressed as:

$$I_{\lambda,ij} = -\frac{x_{0,ij}^{3-\lambda_{ij}} - 1}{\lambda_{ij}-3} \tag{3.16}$$

$$J_{\lambda,ij} = -\frac{\left(x_{0,ij}\right)^{4-\lambda_{ij}}\left(\lambda_{ij}-3\right) - \left(x_{0,ij}\right)^{3-\lambda_{ij}}\left(\lambda_{ij}-4\right) - 1}{\left(\lambda_{ij}-3\right)\left(\lambda_{ij}-4\right)} \tag{3.17}$$

The $a_{1,ij}^s$ term corresponds to the first order perturbation term for Sutherland (Sutherland, 1887) fluid and is given by:

$$a_{1,ij}^s(\rho_s;\lambda_{ij}) = -2\rho_s\left(\frac{\pi\epsilon_{ij}{d_{ij}}^3}{\lambda_{ij}-3}\right)\frac{1-\zeta_x^{eff}(\lambda_{ij})/2}{\left(1-\zeta_x^{eff}(\lambda_{ij})\right)^3} \tag{3.18}$$

where

$$\zeta_x^{eff}(\lambda_{ij}) = c_1(\lambda_{ij})\zeta_x + c_2(\lambda_{ij})\zeta_x{}^2 + c_3(\lambda_{ij})\zeta_x{}^3 + c_4(\lambda_{ij})\zeta_x{}^4 \tag{3.19}$$

with

$$\begin{pmatrix} c_1 \\ c_2 \\ c_3 \\ c_4 \end{pmatrix} = \begin{pmatrix} 0.81096 & 1.7888 & -37.578 & 92.284 \\ 1.0205 & -19.341 & 151.26 & -463.50 \\ -1.9057 & 22.845 & -228.14 & 973.92 \\ 1.0885 & -6.1962 & 106.98 & -677.64 \end{pmatrix} \cdot \begin{pmatrix} 1 \\ 1/\lambda_{ij} \\ 1/\lambda_{ij}{}^2 \\ 1/\lambda_{ij}{}^3 \end{pmatrix} \tag{3.20}$$

Similarly, for the second order perturbation term can be represented as:

$$a_2 = \sum_{i=1}^{n}\sum_{j=1}^{n} x_{s,i}x_{s,j}a_{2,ij} \tag{3.21}$$

where

$$\begin{aligned} a_{2,ij} = \frac{1}{2}K^{HS}(1+\chi_{ij})\epsilon_{ij}C_{ij}{}^2 \\ \times \Big[x_{0,ij}^{2\lambda_{a,ij}}\left(a_{1,ij}^{s}(\rho_s; 2\lambda_{a,ij}) + B_{ij}(\rho_s; 2\lambda_{a,ij})\right) \\ - 2x_{0,ij}^{\lambda_{a,ij}+\lambda_{r,ij}}\left(a_{1,ij}^{s}(\rho_s; \lambda_{a,ij}+\lambda_{r,ij}) + B_{ij}(\rho_s; \lambda_{a,ij}+\lambda_{r,ij})\right) \\ + x_{0,ij}^{2\lambda_{r,ij}}\left(a_{1,ij}^{s}(\rho_s; 2\lambda_{r,ij}) + B_{ij}(\rho_s; 2\lambda_{r,ij})\right)\Big] \end{aligned} \tag{3.22}$$

In eq. (3.22), $K^{HS}$is the isothermal compressibility of the mixtures of hard spheres and is mathematically represented by:

$$K^{HS} = \frac{(1-\zeta_x)^4}{1 + 4\zeta_x + 4\zeta_x{}^2 - 4\zeta_x{}^3 + 4\zeta_x{}^4} \tag{3.23}$$

with

$$\chi_{ij} = f_1(\alpha_{ij})\bar{\zeta}_x + f_2(\alpha_{ij})\bar{\zeta}_x{}^5 + f_3(\alpha_{ij})\bar{\zeta}_x{}^8 \tag{3.24}$$

where

$$\bar{\zeta}_x = \frac{\pi\rho_s}{6}\sum_{i=1}^{n}\sum_{j=1}^{n} x_{s,i}x_{s,j}\sigma_{ij}{}^3 \tag{3.25}$$

and

$$\alpha_{ij} = C_{ij}\left(\frac{1}{\lambda_{a,ij}-3} - \frac{1}{\lambda_{r,ij}-3}\right). \tag{3.26}$$

Finally, the third order mean free energy fluctuation term that is one of the major improvement of SAFT VR Mie is expressed in similar fashion of eq. (3.11) and (3.21). Its analytical expression is given by:

$$a_{3,ij} = -\epsilon_{ij}{}^3 f_4(\alpha_{ij})\bar{\zeta}_x \exp\left(f_5(\alpha_{ij})\bar{\zeta}_x + f_6(\alpha_{ij})\bar{\zeta}_x{}^2\right) \tag{3.27}$$

with

$$f_k(\alpha_{ij}) = \left(\sum_{n=0}^{n=3}\phi_{k,n}\alpha_{ij}{}^n\right)\Big/\left(1 + \sum_{n=4}^{n=6}\phi_{k,n}\alpha_{ij}{}^{n-3}\right) \tag{3.28}$$

3.4.1.2 Chain Term

The chain term was the result of Chapman et al. work (Jackson et al., 1988). The Helmholtz free energy contribution for chain term is usually expressed in a similar mathematical form for various versions of SAFT. The only difference lies in the determination of pair correlation function depending upon the selected reference. For Mie fluid, the chain term is given by:

$$a^{CHAIN} = -\sum_{i=1}^{n} x_i(m_i - 1) \ln g_{ii}^{Mie}(\sigma_{ii}) \tag{3.29}$$

The pair correlation function $g_{ij}^{Mie}(\sigma_{ij})$ for Mie chain segments at contact is determined by combination of hard sphere, first and second order radial distribution functions.

$$\begin{aligned} & g_{ij}^{Mie}(\sigma_{ij}) \\ &= g_{d,ij}^{HS}(\sigma_{ij}) exp\left[\beta\epsilon\, g_{1,ij}(\sigma_{ij})/\, g_{d,ij}^{HS}(\sigma_{ij}) + (\beta\epsilon)^2\, g_{2,ij}(\sigma_{ij})/\, g_{d,ij}^{HS}(\sigma_{ij})\right] \end{aligned} \tag{3.30}$$

where $g_{d,ij}^{HS}(\sigma_{ij})$ is a pair correlation function of mixtures of hard spheres and expressed by :

$$g_{d,ij}^{HS}(\sigma_{ij}) = exp\left(k_0 + k_1 x_{0,ij} + k_2 {x_{0,ij}}^2 + k_3 {x_{0,ij}}^3\right) \tag{3.31}$$

With k_0 , k_1 , k_2 and k_3 are the density-dependent coefficients that are given by:

$$k_0 = -ln(1 - \zeta_x) + \frac{42\zeta_x - 39{\zeta_x}^2 + 9{\zeta_x}^3 - 2{\zeta_x}^4}{6(1 - \zeta_x)^3} \tag{3.32}$$

$$k_1 = \frac{{\zeta_x}^4 + 6{\zeta_x}^2 - 12\zeta_x}{2(1 - \zeta_x)^3} \tag{3.33}$$

$$k_2 = \frac{-3{\zeta_x}^2}{8(1 - \zeta_x)^2} \tag{3.34}$$

$$k_3 = \frac{-{\zeta_x}^4 + 3{\zeta_x}^2 + 3\zeta_x}{6(1 - \zeta_x)^3} \tag{3.35}$$

The first order term $g_{1,ij}(\sigma_{ij})$ in eq. (3.30) is given by:

$$g_{1,ij}(\sigma_{ij}) = \frac{1}{2\pi d_{ij}^3 \epsilon_{ij}} \Bigg[3 \frac{\partial a_{1,ij}}{\partial \rho_s} - C_{ij} \lambda_{a,ij} x_{0,ij}^{\lambda_{a,ij}} \frac{a_{1,ij}^S(\rho_s; \lambda_{a,ij}) + B_{ij}(\rho_s; \lambda_{a,ij})}{\rho_s} + C_{ij} \lambda_{r,ij} x_{0,ij}^{\lambda_{r,ij}} \frac{a_{1,ij}^S(\rho_s; \lambda_{r,ij}) + B_{ij}(\rho_s; \lambda_{r,ij})}{\rho_s} \Bigg] \tag{3.36}$$

Similarly, the second order term $g_{2,ij}(\sigma_{ij})$ which contributes to the pair correlation function is expressed as:

$$g_{2,ij}(\sigma_{ij}) = (1 + \gamma_{c,ij}) g_{2,ij}^{MCA}(\sigma_{ij}) \tag{3.37}$$

where

$$\gamma_{c,ij} = \phi_{7,0} \left(-\tanh\left(\phi_{7,1} (\phi_{7,2} - \alpha_{ij}) \right) + 1 \right) \bar{\zeta}_x \theta_{ij} \times \exp\left(\phi_{7,3} \bar{\zeta}_x + \phi_{7,4} \bar{\zeta}_x^{\,2} \right) \tag{3.38}$$

with

$$\theta_{ij} = exp(\beta \epsilon_{ij}) - 1 \tag{3.39}$$

The values of $\phi_{7,0}, \phi_{7,1}, \phi_{7,2}, \phi_{7,3}$ and $\phi_{7,4}$can be found in literature (Lafitte et al., 2013). The term $g_{2,ij}^{MCA}(\sigma_{ij})$ in eq. (3.37) is represented by following equation:

$$g_{2,ij}^{MCA}(\sigma_{ij}) = \frac{1}{2\pi d_{ij}^3 \epsilon_{ij}{}^2}\Bigg[3\frac{\partial \frac{a_{2,ij}}{1+\chi_{ij}}}{\partial \rho_s} - \epsilon_{ij}C_{ij}{}^2 K^{HS}\lambda_{r,ij}x_{0,ij}^{2\lambda_{r,ij}} \times \frac{a_{1,ij}^s(\rho_s; 2\lambda_{r,ij}) + B_{ij}(\rho_s; 2\lambda_{r,ij})}{\rho_s} + \epsilon_{ij}C_{ij}{}^2 K^{HS}(\lambda_{r,ij}+\lambda_{a,ij})x_{0,ij}^{\lambda_{r,ij}+\lambda_{a,ij}} \times \frac{a_{1,ij}^s(\rho_s; \lambda_{r,ij}+\lambda_{a,ij}) + B_{ij}(\rho_s; \lambda_{r,ij}+\lambda_{a,ij})}{\rho_s} - \epsilon_{ij}C_{ij}{}^2 K^{HS}\lambda_{a,ij}x_{0,ij}^{2\lambda_{a,ij}} \times \frac{a_{1,ij}^s(\rho_s; 2\lambda_{a,ij}) + B_{ij}(\rho_s; 2\lambda_{a,ij})}{\rho_s}\Bigg] \tag{3.40}$$

3.4.1.3 Association Term

The major attribute of SAFT is to address the association molecular interactions. The Helmholtz free energy term for association interactions was the consequence of Wertheim TPT1.All of the SAFT variants employ the general form of association Helmholtz free energy term determined by Wertheim. As stated above, association term is computationally complicated, a simple interaction potential such as SW potential is commonly used for association sites across the SAFT variants. The general mathematical form of association term is given by:

$$a^{ASSOC} = \sum_{i=1}^{n} x_i \sum_{a=1}^{s_i} n_{ai}\left[lnX_{ai} - \frac{X_{ai}}{2} + \frac{1}{2}\right] \tag{3.41}$$

where s_i is the association site type, n_{ai} is the number of 'a' type sites on a molecule 'i' and X_{ai} is the fraction of component 'i' not bonded at site 'a'. This fraction is mathematically expressed as:

$$X_{ai} = \frac{1}{1 + \rho \sum_{j=1}^{n} x_j \sum_{b=1}^{s_j} n_{b,j} X_{bj} \Delta_{abij}} \tag{3.42}$$

The Δ_{abij} term signifies the association strength between sites of type 'a' on component 'i' and sites of type 'b' on component 'j'. The association strength is generally expressed as:

$$\Delta_{abij} = K_{abij} F_{abij} I_{abij} \tag{3.43}$$

where K_{abij} is a bonding volume parameter, I_{abij} is a dimensionless integral known as association kernel and F_{abij} is the Mayer function, which accounts for hydrogen bonding energy (ϵ_{abij}^{HB}), defined by:

$$F_{abij} = exp\left(\beta \epsilon_{abij}^{HB}\right) - 1 \tag{3.44}$$

The evaluation of association strength depends upon the type of reference fluid and pair potential for association sites. It was indicated before that association sites are characterized generally by SW interaction potential. Hence, the focus turns toward the selection of reference monomeric system. Each reference fluid has a particular radial distribution function which is required for the determination of association kernel (I_{abij}).

A recent study (Dufal, Lafitte, Haslam, et al., 2015) based on above indicated concept, has evaluated radial distribution functions based on diverse reference monomeric systems. These radial distribution functions were then used to calculate the association kernels and ultimately the association strengths. In this thesis work, association strengths determined by Dufal et al. (2015) have been applied for VLE in the equilibrium system including gas hydrate mixture. These association strengths are based on HS RDF, LJ RDF and Mie RDF.

The HS RDF association concept has been adopted by several versions of SAFT(Walter G. Chapman et al., 1990; Galindo, Whitehead, & Jackson, 1996; Gross & Sadowski, 2002) due to its simplicity and accuracy for HS fluids ranging from low to intermediate densities. It is the simplest association expression based on Wertheim concept, that led to physical interpretation of association interactions. It considers the reference fluid as a system of hard spheres with off-center SW association sites embedded on them. Primarily, this association concept was proposed in line with SAFT VR Mie EOS by Lafitte et al. (2013). Mathematically, association strength based on HS RDF is given by:

$$\Delta_{abij} = K_{abij} F_{abij}\, g_{d,ij}^{HS}(d) \tag{3.45}$$

where

$$K_{abij} = 4\pi d_{ij}^2 \Big[ln\big((r_{abij}^c + 2r_{abij}^d)/d_{ij}\big) \times \Big(6{r_{abij}^c}^3 + 18{r_{abij}^c}^2 r_{abij}^d - 24{r_{abij}^d}^3\Big) + \big(r_{abij}^c + 2r_{abij}^d - d_{ij}\big)\Big(22{r_{abij}^d}^2 - 5r_{abij}^c r_{abij}^d - 7r_{abij}^d d_{ij} - 8{r_{abij}^c}^2 + r_{abij}^d d_{ij} + d_{ij}^2\Big)\Big] / \Big(72{r_{abij}^d}^2\Big) \quad (3.46)$$

with 'r_{ab}^c' the cutoff range of SW interaction between association sites a and b, 'r_{ab}^d' the distance of each association site from the center of considered segment and $g_{d,ij}^{HS}(d)$ is based on the Boublik (Boublík, 1986)expression:

$$g_{d,ij}^{HS}(d) = \frac{1}{1-\zeta_3} + 3\frac{d_{ii}d_{jj}}{d_{ii}+d_{jj}}\frac{\zeta_2}{(1-\zeta_3)^2} + 2\left(\frac{d_{ii}d_{jj}}{d_{ii}+d_{jj}}\right)^2 \frac{{\zeta_2}^2}{(1-\zeta_3)^3} \quad (3.47)$$

The RDF of LJ reference monomeric system was already determined by Muller and Gubbins (1995). Dufal et al (2015) took the advantage of Muller and Gubbins work (Müller & Gubbins, 1995) for LJ RDF. They proposed a new simple association kernel based on LJ RDF using a different fixed geometry for association sites. The algebraic expression of novel LJ association kernel is presented by:

$$I(T^*, \rho^*) = \sum_{i=0}^{i+j\leq 10} \sum_{j=0} c_{ij} [\rho^*]^i [T^*]^j \quad (3.48)$$

where c_{ij} are 66 adjustable parameters (Dufal, Lafitte, Haslam, et al., 2015) , $\rho^*$is dimensionless density that implicitly accounts for segment diameter 'σ' and given by:

$$\rho^* = \rho\sigma_{vdW1,x}^3 \tag{3.49}$$

with ρ as total number density and $\sigma_{vdW1,x}^3$ is defined through following mixing rule:

$$\sigma_{vdW1,x}^3 = \sum_i \sum_j x_i x_j \sigma_{ij}^3 \tag{3.50}$$

T_{ij}^* is the dimensionless temperature that accounts for interaction energy and represented as :

$$T_{ij}^* = \frac{k_B T}{\epsilon_{ij}} \tag{3.51}$$

Another achievement of the study of Dufal et al. (2015) was the determination of Mie association kernel using the RDF of Mie fluids. The molecular geometry is characterized by Mie monomeric segments with off center SW association sites. In a similar approach employed for novel LJ association kernel, novel Mie association kernel is determined. The latter association kernel accounts for repulsive exponent (λ_r) in addition to dimensionless temperature and number density. Mathematically, novel Mie association kernel is given by:

$$I(T^*, \rho^*, \lambda_r) = \sum_{i=0}^{i+j\leq 10} \sum_{j=0} a_{ij}(\lambda_r)[\rho^*]^i[T^*]^j \tag{3.52}$$

where $a_{ij}(\lambda_r)$ are 66 adjustable coefficients. Their functional dependence on Mie repulsive exponent is represented by:

$$a_{ij}(\lambda_r) = \sum_{k=0}^{6} b_{i,j,k} \, [\lambda_r]^k \tag{3.53}$$

where $b_{i,j,k}$ are 462 adjustable coefficients that can be found in the literature (Dufal, Lafitte, Haslam, et al., 2015).

The above indicated association terms have been evaluated for accurate prediction of gas hydrate VLE mixtures in Chapter 4.

3.5 Combining Rules

In a thermodynamic mixture, a molecule either interacts with the similar molecule or a different molecule. The interaction potential parameters for pure components are available. However, in order to address the effects of unlike molecular interactions, a combining rule is required. A combining rule defines the unlike molecular interaction potential parameters through a linear function of like molecular interaction parameters (Luongo-Ortiz & Starling, 1997). Almost all the SAFT VR Mie adjustable parameters, except number of segments 'm', require combining rules to cater the effects of molecular interactions.

The most common Lorentz-Berthelot combining rules have been used in determination of unlike SAFT VR Mie parameters. Lorentz combining rule uses simple arithmetic mean expression for the determination of unlike parameters. On the contrary, Berthelot combining rules uses a geometric mean sort of expression.

In this work, Lorentz-like combining rules are generally used for size or distance based parameters. The mathematical expressions for combining rules of size based parameters are as following:

a. Segment diameter (σ)

$$\sigma_{ij} = \frac{\sigma_{ii} + \sigma_{jj}}{2} \tag{3.54}$$

b. Barker Henderson effective diameter (d)

$$d_{ij} = \frac{d_{ii} + d_{jj}}{2} \tag{3.55}$$

c. Cutoff range of SW interaction between association sites a and b (r^c_{abij})

$$r^c_{abij} = \frac{r^c_{abii} + r^c_{abjj}}{2} \tag{3.56}$$

d. Distance of each association site from the center of considered segment(r^d_{abij})

$$r^d_{abij} = \frac{r^d_{abii} + r^d_{abjj}}{2} \tag{3.57}$$

e. Bonding volume parameter

$$K_{abij} = \left(\frac{{K_{abii}}^{1/3} + {K_{abjj}}^{1/3}}{2}\right)^3 \tag{3.58}$$

On the other hand, Berthelot-like combining rules are employed for energy and interactions based parameters. Some of which are mathematically represented in following manner.

f. Dispersive energy (ϵ_{ij}) with a binary interaction parameter (k_{ij}) for highly non-ideal fluids

$$\epsilon_{ij} = \left(1 - k_{ij}\right) \frac{\sqrt{\sigma_{ii}^3 \sigma_{jj}^3}}{\sigma_{ij}^3} \sqrt{\epsilon_{ii}\epsilon_{jj}} \tag{3.59}$$

g. Association Energy (ϵ_{abij}^{HB})

$$\epsilon_{abij}^{HB} = \sqrt{\epsilon_{abii}^{HB} \epsilon_{abjj}^{HB}} \tag{3.60}$$

h. Repulsive or Attractive exponents ($\lambda_{a,ij}\ or\ \lambda_{r,ij}$)with a binary interaction parameter

$$\lambda_{k,ij} - 3 = \sqrt{\left(\lambda_{k,ii} - 3\right)\left(\lambda_{k,jj} - 3\right)}\ , \qquad k = a, r \tag{3.61}$$

CHAPTER 4

VLE PREDICTION OF NON-ASSOCIATIVE MIXTURES USING SAFT-VR MIE EOS

4.1 Introduction

Vapor-liquid equilibrium (VLE) is an integral part of gas hydrate calculations due to the co-existence of the three phases (vapor, liquid and hydrate) when gas hydrates form at certain conditions. The accuracy of vapor-liquid equilibrium influences the accuracy of the gas hydrate incipient conditions. This is why the SAFT-VR Mie EOS, which is expected to be more accurate than other SAFT versions, is selected for this purpose.

This chapter presents the methodology and results of VLE related to gas hydrate mixtures using the SAFT-VR Mie EOS. The chapter addresses the VLE of hydrate former-hydrate former systems that are normally non-associating in nature. The organization of the chapter is as follows: Section 4.2 gives a summary about the determination of the adjustable parameters of the SAFT VR Mie EOS for non-associating components (hydrate formers) considered in this thesis. At the end, Section 4.3 presents the correlated VLE results for non-associative systems.

4.2 SAFT-VR Mie Adjustable Parameters for Non Associating Components

As stated in Chapter 3, there are five adjustable parameters for non-associating molecules. They include number of Mie segments (m), segment diameter (σ), dispersive energy (ϵ), repulsive (λ_r) and attractive (λ_a) exponents of Mie pair potential. These adjustable parameters are found by fitting against the experimental pressure-volume-temperature (PVT) data for each pure component. An objective function is minimized to reduce the difference between the experimental and calculated vapor pressure and liquid density:

$$obj = \sum \left[\left(\frac{P_{cal} - P_{exp}}{P_{exp}} \right)^2 + \left(\frac{\rho^L_{cal} - \rho^L_{exp}}{\rho^L_{exp}} \right)^2 \right] \tag{4.1}$$

To validate the accuracy of the adjustable parameters, Average Absolute Deviation in vapor pressure ($AADP(\%)$) and liquid density ($AADL(\%)$) are calculated. These AAD (%) are given by:

$$AADP(\%) = \left(\sum \left| \frac{P_{exp} - P_{cal}}{P_{exp}} \right| / N \right) \times 100 \tag{4.2}$$

$$AADL(\%) = \left(\sum \left| \frac{\rho^L_{exp} - \rho^L_{cal}}{\rho^L_{exp}} \right| / N \right) \times 100 \tag{4.3}$$

where P_{exp} is experimental vapor pressure,P_{cal} is the calculated vapor pressure, N represents the number of data points, ρ^L_{exp} is the experimental liquid density and ρ^L_{cal} is the calculated liquid density.

The calculations of vapor pressure and liquid density are carried out by satisfying the equilibrium conditions, specifically thermal, mechanical and chemical equilibrium. Appendix B demonstrates the calculation procedure along with the chemical equilibrium equations used. The Nelder-Mead simplex direct search algorithm is used for minimizing the objective function (eq. (4.1)).

The hydrate formers are usually non-associating in nature except few molecules such as hydrogen sulfide. Hydrogen sulfide is an associating molecule with weak hydrogen bonding forces. For this reason, different studies (Dufal, Lafitte, Haslam, et al., 2015; Perez, Valtz, Coquelet, Paricaud, & Chapoy, 2016) have predicted the fluid behavior of hydrogen sulfide with fairly good accuracy by ignoring the effect of association. Therefore, this thesis work treats hydrogen sulfide as a non-associating molecule as well.

In this thesis work, the adjustable SAFT-VR Mie parameters are taken from the literature. In case they are not available, we develop an optimization procedure using the simplex method to minimize eq. (4.1). Table 4-1 summarizes the adjustable parameters found in the literature. The estimated SAFT VR Mie adjustable parameters in this work are given in Table 4-2. The average absolute deviations for vapor pressure and liquid density are also reported along with the reference of experimental data.

Table 4-1: The SAFT VR Mie adjustable parameters for pure components taken from the literature.

Component	m_s	σ (Å)	ϵ/k (K)	λ_r	λ_a	Data Reference
Methane	1.0000	3.7412	153.36	12.6500	6.0000	(Lafitte et al., 2013)
Ethane	1.4373	3.7257	206.12	12.4000	6.0000	(Lafitte et al., 2013)
Propane	1.6845	3.9056	239.89	13.0060	6.0000	(Lafitte et al., 2013)
Carbon dioxide	1.5000	3.1916	231.88	27.5570	5.1646	(Lafitte et al., 2013)
Argon	1.0000	3.4038	117.84	12.0850	6.0000	(Dufal, Lafitte, Galindo, et al., 2015)
Ethene	1.7972	3.2991	142.64	9.6463	6.0000	(Dufal, Lafitte, Galindo, et al., 2015)
Nitrogen	1.4214	3.1760	72.43	9.8749	6.0000	(Dufal, Lafitte, Galindo, et al., 2015)
Oxygen	1.4283	2.9671	81.47	8.9218	6.0000	(Dufal, Lafitte, Galindo, et al., 2015)
Hydrogen Sulfide	1.0000	3.7783	387.28	22.4510	6.0000	(Perez et al., 2016)

Table 4-2: The SAFT VR Mie adjustable parameters for pure components calculated in this work.

Component	Temperature Range (K)	m_s	σ (Å)	ϵ/k (K)	λ_r	λ_a	AADP (%)	AADL (%)	Data Reference
Isobutane	170-340	2.0102	3.9686	231.46	11.9	6	0.4630	0.1763	(Stefan Glos, Kleinrahm, & Wagner, 2004)
Ethyne	190-302	2.126	2.9496	165.65	11.342	6	0.5086	0.1534	(Yaws, 2015)

4.3 VLE Results of Non-Associating Systems

After evaluating the SAFT VR Mie adjustable parameters for pure components, their application to determine the VLE of hydrate formers' mixtures is evaluated in this section. The SAFT-VR Mie is extended to mixtures by the mixing and combining rules, given in Chapter 3.

The main purpose of assessing the VLE of hydrate former mixtures is to extend the application of the SAFT VR Mie EOS to single and mixed gas hydrate systems. Accurate VLE is usually obtained with the introduction of binary interaction parameters (k_{ij}) (Fateen, Khalil, & Elnabawy, 2013). The k_{ij} is determined by minimizing the following objective function based on the experimental and calculated pressures:

$$obj = \left(\sum \left|\frac{P_{cal} - P_{exp}}{P_{ex}}\right| / N\right) \tag{4.4}$$

The gas hydrate formers are usually light hydrocarbons such as methane, ethane, propane, isobutane, ethene and light gases like carbon dioxide, nitrogen, hydrogen sulfide. The binary VLE behavior of most of these hydrate former mixtures is classified as type I phase behavior as per classification of Van Konyenburg and Scott (Konynenburg & Scott, 1980) .Type I phase behavior depicts a continuous gas-liquid critical line without any liquid-liquid miscibility. This type of phase behavior is usually found in non-polar and chemically similar substances. Similar type of phase behavior of various binary hydrate former mixtures is usually predicted in the present work, unless otherwise specified, using the SAFT VR Mie EOS.

The VLE calculations are carried using the equality of fugacities of each component in vapor and liquid phase at constant temperature and pressure. The residual Helmholtz energy expression of the SAFT VR Mie EOS is used to determine the fugacity by the equations summarized in Appendix B. In order to assess the accuracy of VLE calculations of binary mixtures considered in this work, they are compared with experimental data. The experimental data are taken from the literature.

4.3.1 Hydrocarbon VLE Mixtures

The first four components in alkane series are essential components of natural gas that contribute significantly in the formation of natural gas hydrates. The VLE of the binary systems forming from these four compounds is studied in this section.

Figures 4.1, 4.2 & 4.3 depict the VLE prediction of methane-based mixtures, namely methane-ethane, methane-propane and methane-isobutane at temperatures of 199.92, 214 and 310.93 K; respectively. The VLE of these systems shows excellent agreement with the experimental data at low pressures. The k_{ij} values for methane-ethane, methane-propane and methane-isobutane systems are -0.0084, -0.0055 and -0.0087; respectively.

On the other hand, an overestimation of VLE behavior is observed at high pressures; particularly for methane-isobutane system. This deficiency is commonly found in almost all equations of state (McCabe & Jackson, 1999). However, in a recent study by Lafitte et al (2013), much improved prediction was obtained at high pressure for a more complex hydrocarbon system (ethane-decane) using the SAFT VR Mie EOS as compared to the SAFT VR-SW EOS. This improvement in VLE prediction was the result of

consideration of a higher order perturbation term for dispersion forces in SAFT-VR Mie EOS as compared to other versions of SAFT.

Another observation while studying the VLE results of methane based systems is that with an increase in segment number 'm', the degree of overestimation of bubble pressure increases too. This is clear from AADP values of methane-ethane, methane-propane and methane-isobutane systems provided in Table 4-3. The values are 0.0164%, 2.3977% and 3.5956%; respectively. This is not limited to the SAFT-VR Mie but also to other models whenever there is a dissymmetry in size or energy of binary components (Blas & Vega, 1998; McCabe & Jackson, 1999).

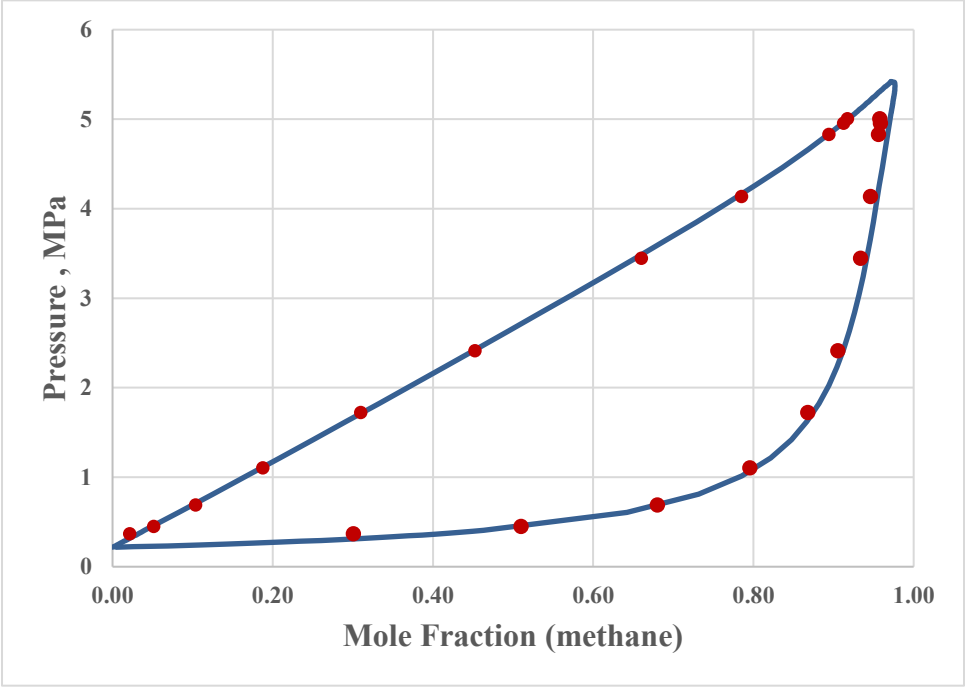

Figure 4.1: The VLE of Methane-Ethane system at 199.92 K with k_{ij} = - 0.0084. The solid line is the correlation of the SAFT VR Mie EOS. The points represent experimental VLE data (Wichterle & Kobayashi, 1972a).

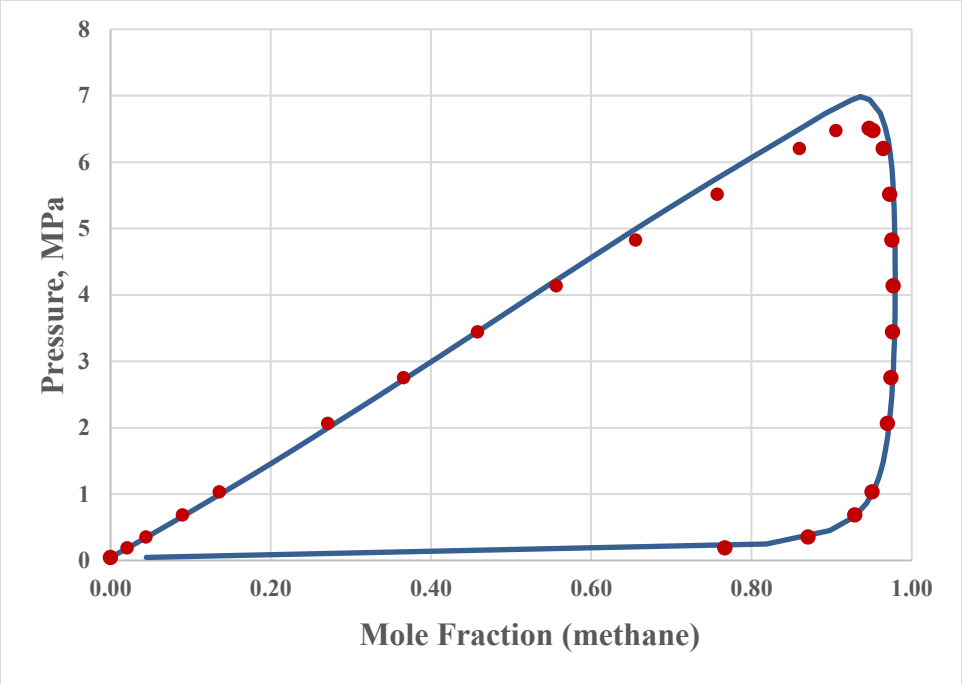

Figure 4.2: The VLE of Methane-Propane system at 214 K with k_{ij} = -0.0055 . The solid line is the correlation of the SAFT-VR Mie EOS. The points represent experimental VLE data (Wichterle & Kobayashi, 1972b).

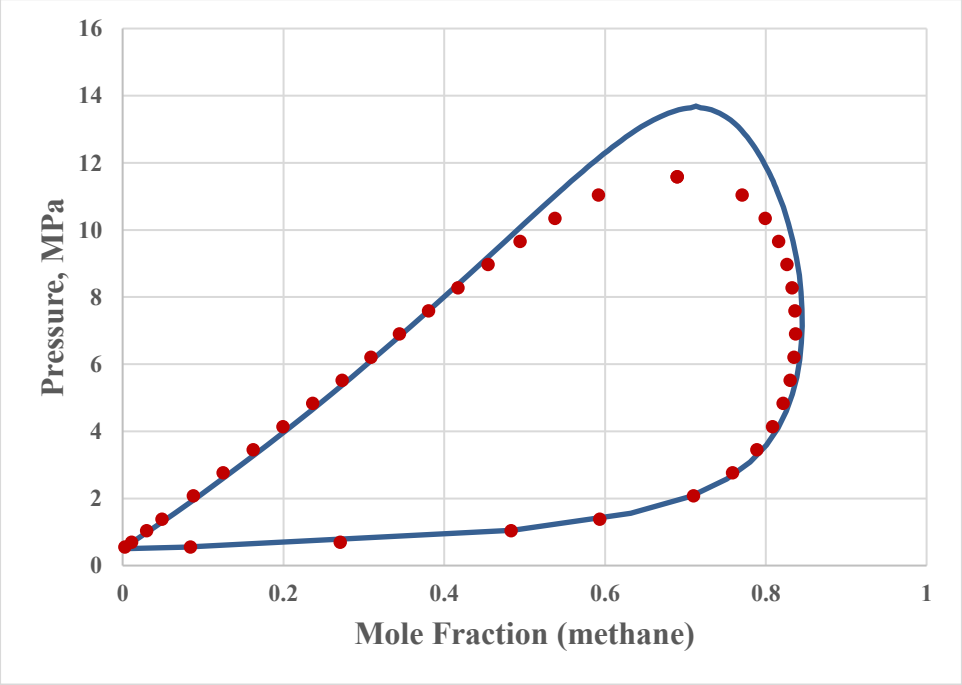

Figure 4.3: The VLE of Methane-Isobutane system at 310.93 K with k_{ij} = -0.0087. The solid line is the correlation of the SAFT-VR Mie EOS. The points represent experimental VLE data (Olds, Sage, & Lacey, 1942).

The VLE study is extended to ethane-propane, propane-isobutane and ethane-isobutane systems, as shown in Figures 4.4, 4.5 & 4.6. The VLE behavior of these systems is predicted at 270, 273.15 and 311.26 K; respectively. The VLE prediction, for each of these mixtures, is quite accurate with k_{ij} values of -0.0068, -0.0011 and -0.0103. The segment numbers 'm' and attractive energy values of ethane, propane and isobutane are close to each other, which make them ideal mixtures. As given in Table 4-3, the AADP values of ethane-propane, propane-isobutane and ethane-isobutane are less than 2%. Similarly, the vapor mole fraction variation of these systems are 0.0539, 0.0242 and 0.0087; respectively.

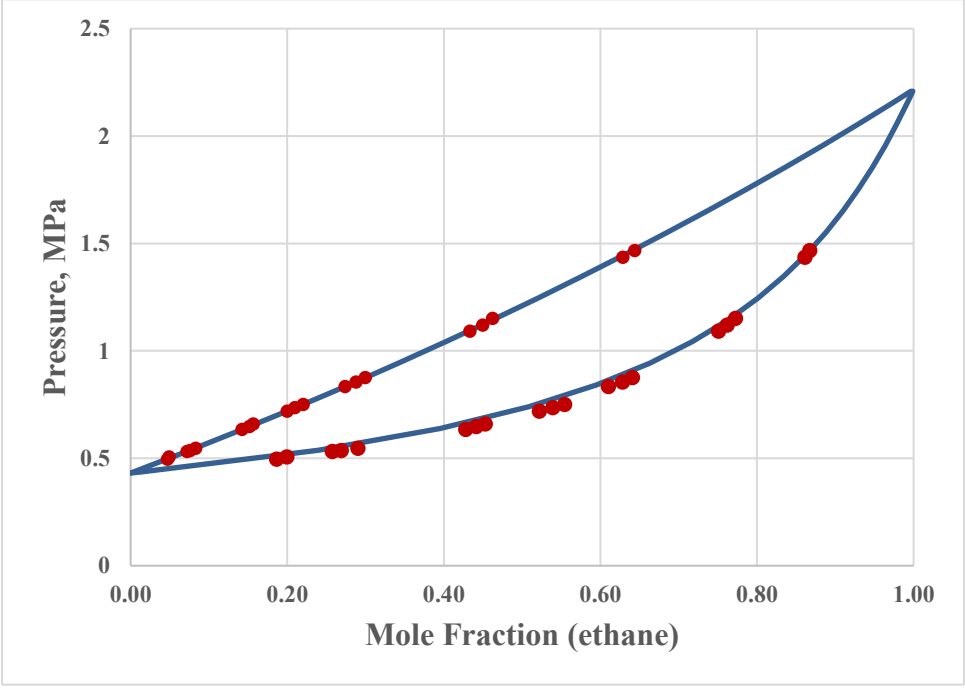

Figure 4.4: The VLE of Ethane-Propane system at 270 K with k_{ij} = -0.0068. The solid line is the correlation of the SAFT-VR Mie EOS. The points represent experimental VLE data (Blanc & Setier, 1988).

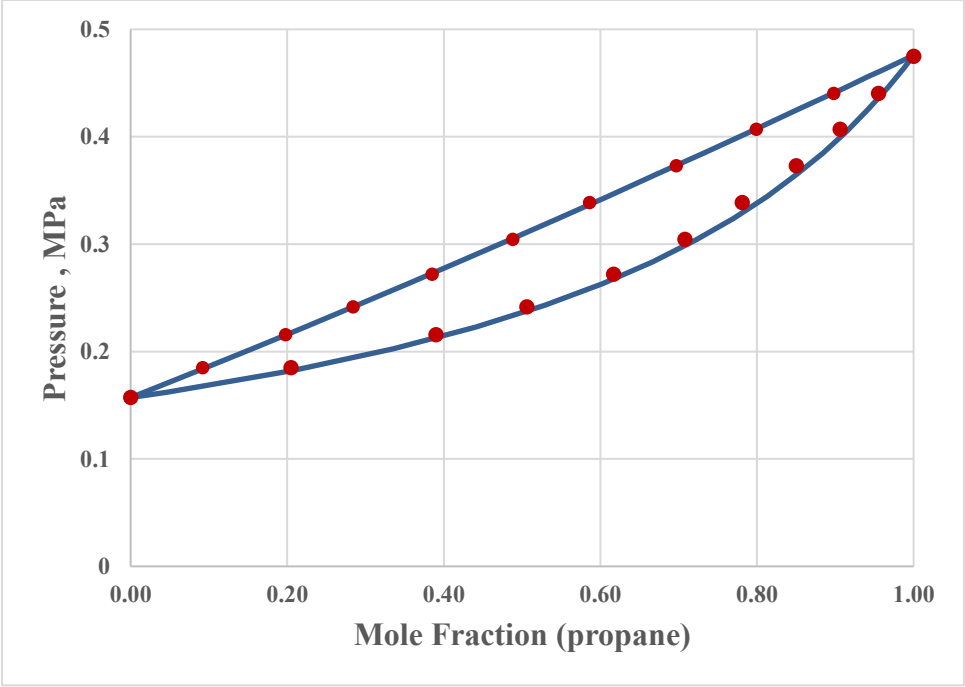

Figure 4.5: The VLE of Propane-Isobutane system at 273.15 K with k_{ij} = -0.0011. The solid line is the correlation of the SAFT-VR Mie EOS. The points represent experimental VLE data (Lim, Ho, Park, & Lee, 2004).

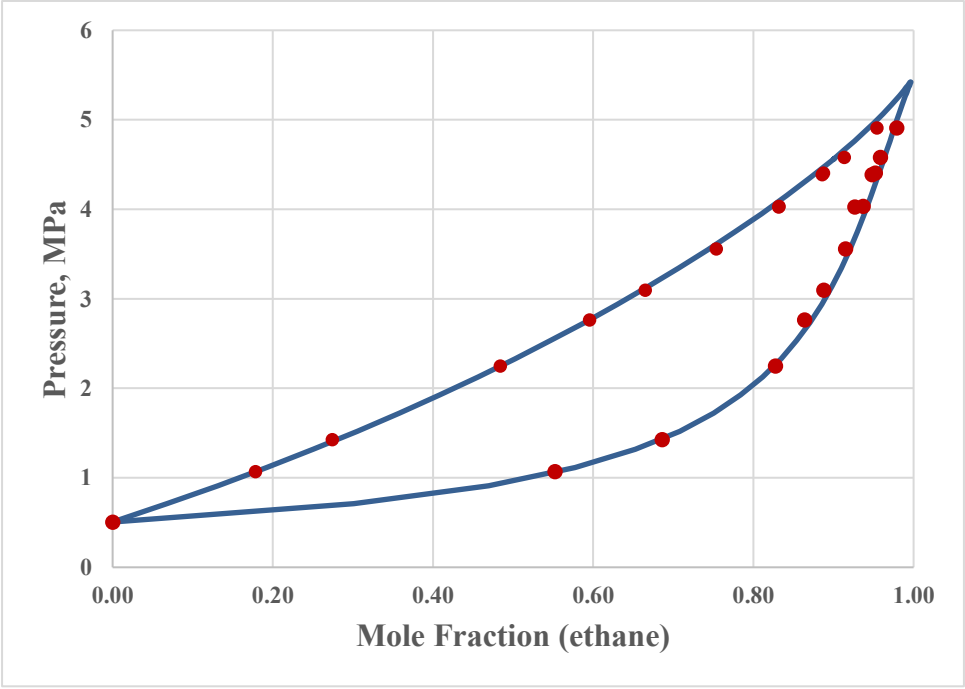

Figure 4.6: The VLE of Ethane-Isobutane system at 311.26 K with k_{ij} = -0.0103. The solid line is the correlation of the SAFT-VR Mie EOS. The points represent experimental VLE data (Besserer & Robinson, 1973b).

Our objective is to test the SAFT-VR Mie applicability on systems containing unsaturated hydrocarbons as well since they could form gas hydrates such as methane-ethene system. Methane-ethene mixtures are commonly found in petroleum refining and

petrochemical processes (Ma et al., 2001). Figure 4.7 illustrates an accurate estimation of VLE behavior of methane-ethene mixture at 180 K. The bubble pressure and vapor mole fraction deviations for methane-ethene mixture are respectively 0.0046% and 0.0184 (see Table 4-3).

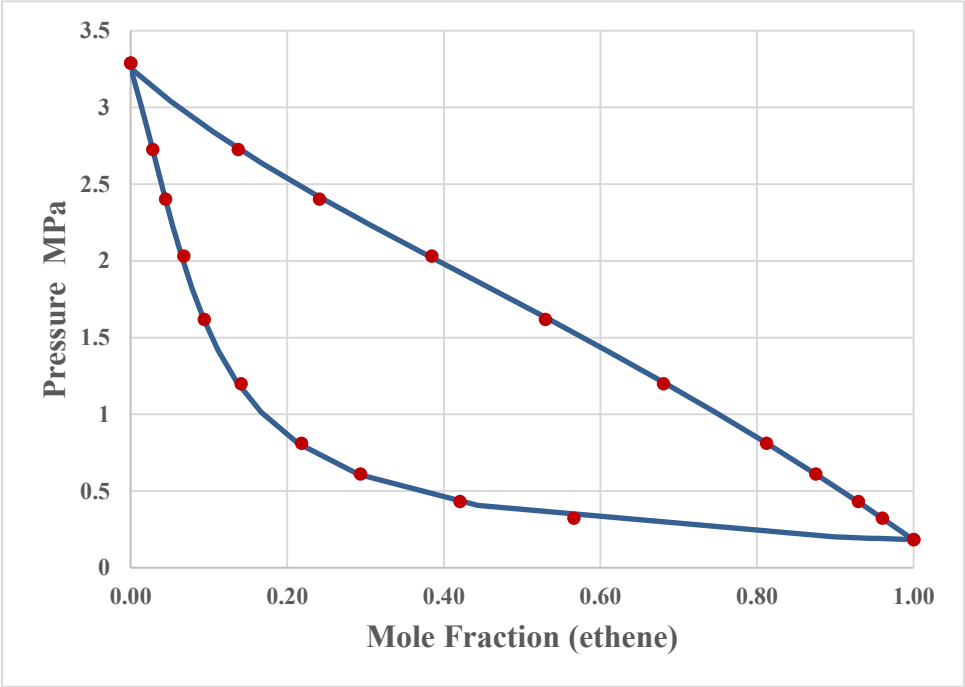

Figure 4.7: The VLE of Methane-Ethene system at 180 K with k_{ij} = 0.0061. The solid line is the correlation of the SAFT-VR Mie EOS. The points represent experimental VLE data (R. C. Miller, Kidnay, & Hiza, 1977).

A summary of the previous VLE systems are provided in Table 4-3. The references of the VLE experimental data are listed in the table.

Table 4-3: VLE results summary of hydrocarbon mixtures

System	T (K)	k_{ij}	AADP (%)	AADY	Exp. Points (N)	Data Reference
Methane-Ethane	200.00	-0.0084	0.0164	0.0141	15	(Wichterle & Kobayashi, 1972a)
Methane-Propane	214.00	-0.0055	2.3977	0.0061	14	(Wichterle & Kobayashi, 1972b)
Methane-Isobutane	310.93	-0.0087	3.5956	0.0272	19	(Olds et al., 1942)
Ethane-Propane	270.00	-0.0068	0.3081	0.0539	23	(Blanc & Setier, 1988)
Propane-Isobutane	273.15	-0.0011	0.1971	0.0242	11	(Lim et al., 2004)
Ethane-Isobutane	311.26	-0.0103	1.0948	0.0087	11	(Besserer & Robinson, 1973b)
Methane-Ethene	180.00	0.0061	0.0046	0.0184	11	(R. C. Miller et al., 1977)

4.3.2 Hydrocarbon-Nonhydrocarbon VLE Mixtures

Carbon dioxide, nitrogen and hydrogen sulfide are some of the non-hydrocarbon substances that are commonly present as impurities in natural gases (Shimekit & Mukhtar, 2012). Their presence in natural gas creates problems like severe corrosion in

pipelines, reduction of natural gas calorific value and many others. Hence, they are removed from natural gas based on certain specifications (Jusoh, N.W., 2012). They interact with hydrocarbons in fuel burning environments as well as in petrochemical industries. Therefore, the VLE behavior of these nonhydrocarbons with light hydrocarbons is of prime interest.

Starting with CO_2-Hydrocarbon mixtures, whose VLE behavior prediction is termed as complex due to the quadrupole nature of CO_2. The study of quadrupole-quadrupole interactions needs an additional perturbation term (Nguyen-Huynh, Passarello, Tobaly, & de Hemptinne, 2008). However, recent studies by Lafitte et al. (2013) and Gonzales et al. (2016) showed that the SAFT-VR Mie gave good prediction of VLE of CO_2-decane and CO_2-n-butane systems without employing the quadrupole interactions. For this reason, the quadrupole interactions of CO_2 are ignored in this study.

Figures 4.8, 4.9 & 4.10 represent the CO_2-hydrocarbon mixtures. These mixtures include CO_2-methane, CO_2-propane and CO_2-isobutane at 220, 252.95 and 310.93 K; respectively. The accuracy of these mixtures is assessed by the AADP (%) and AADY values provided in Table 4-4. The AADP of pressure prediction is less than 2% while the vapor mole fraction deviations range from 0.0119 to 0.0303. The k_{ij} value of CO_2-methane mixture is 0.0066 which is relatively smaller than the k_{ij} values of CO_2-propane and CO_2-isobutane that are 0.059 and 0.060; respectively. The values of k_{ij} for these systems and those available in the literature (Gonzalez, Pereira, Paricaud, Coquelet, & Chapoy, 2015; Lafitte et al., 2013) reveal that the k_{ij} values of CO_2-n-alkanes varies between 0.05 and 0.06 at different temperatures.

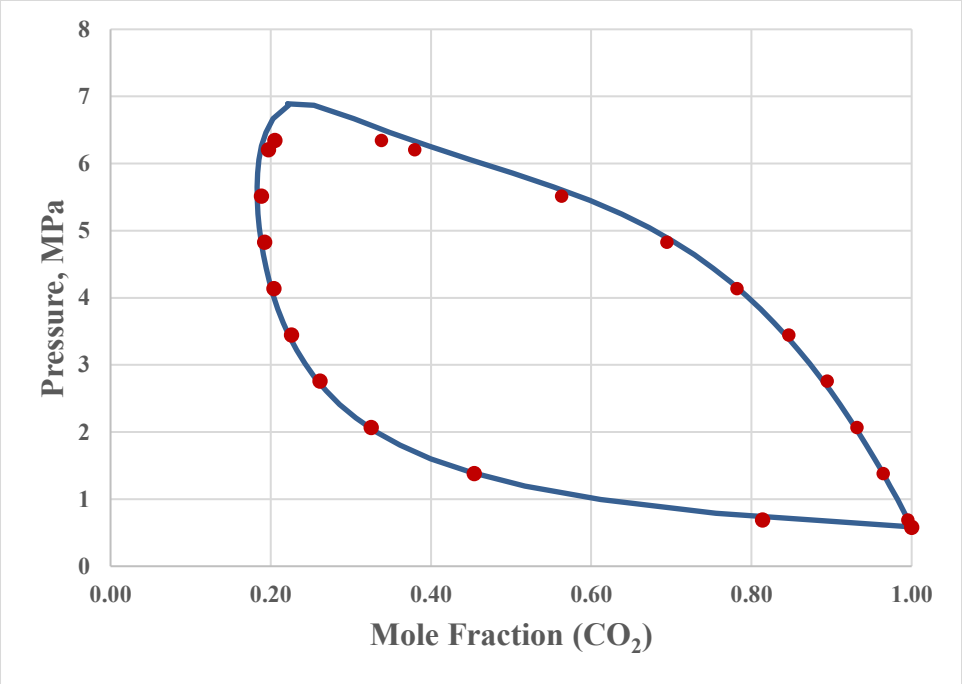

Figure 4.8: The VLE of CO_2-Methane system at 220 K with k_{ij} = 0.0066. The solid line is the correlation of the SAFT-VR Mie EOS. The points represent experimental VLE data (R. C. Miller et al., 1977).

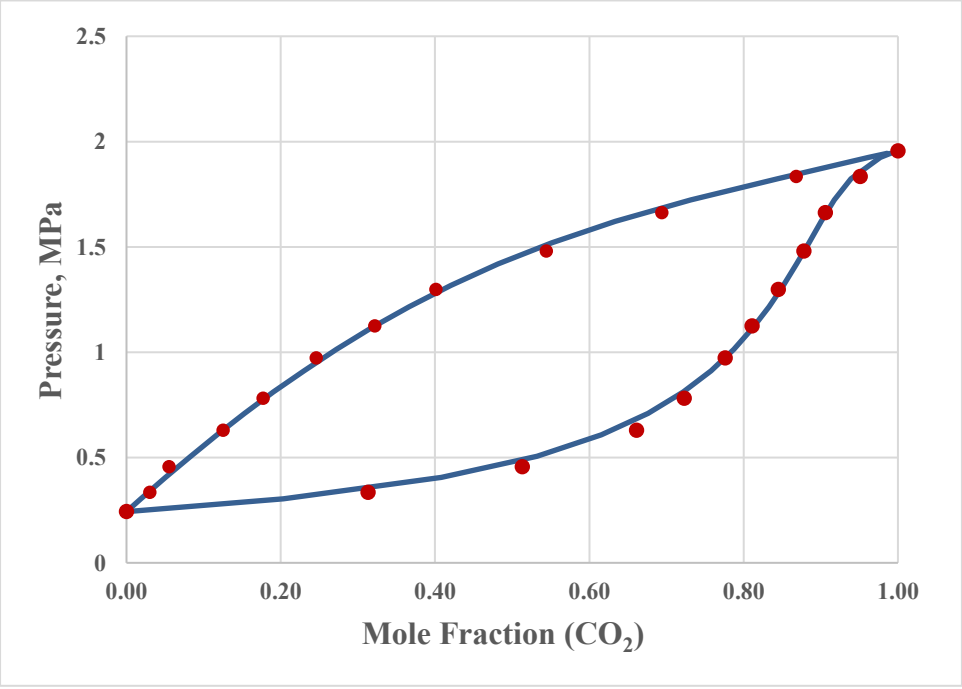

Figure 4.9: The VLE of CO_2-Propane system at 252.95 K with k_{ij} = 0.0599 .The solid line is the correlation of the SAFT-VR Mie EOS. The points represent experimental VLE data (Nagahama, Konishi, Hoshino, & Hirata, 1974).

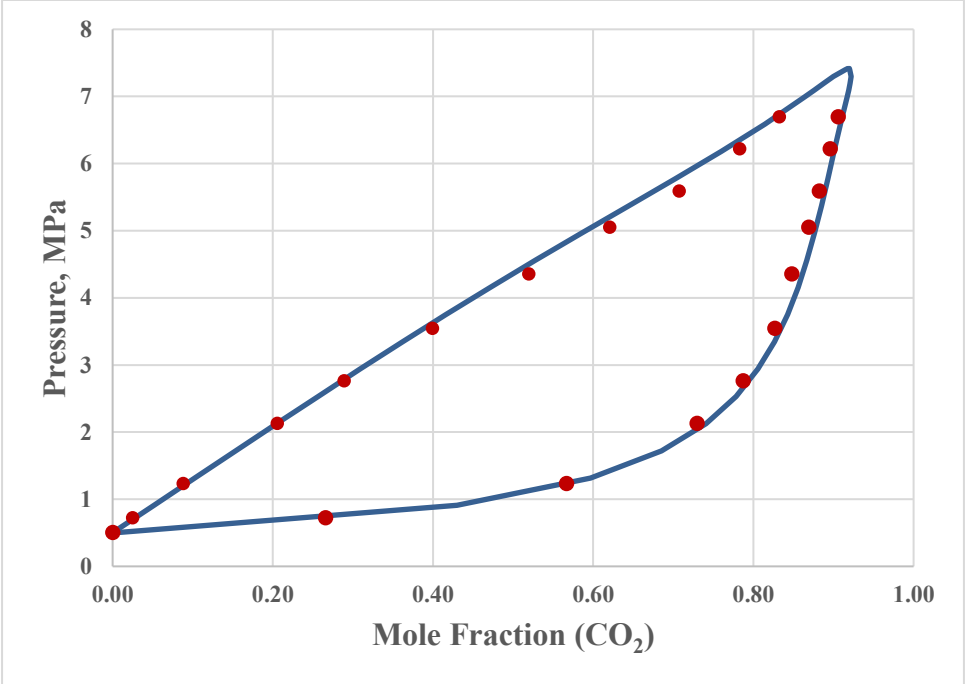

Figure 4.10: The VLE of CO_2-Isobutane system at 310.93 K with k_{ij} = 0.0600.The solid line is the correlation of the SAFT-VR Mie EOS. The points represent experimental VLE data (Besserer & Robinson, 1973a).

Another important compound in gas hydrates is nitrogen (N_2). Nitrogen forms gas hydrates alone or in the presence of hydrocarbons. Thus, it is important to study the prediction capability of VLE for N_2-hydrocarbon systems.

Figure 4.11 shows the predicted VLE diagram of N_2-methane mixture at 122 K. The quantitative prediction of VLE is quite precise with a k_{ij} value of 0.0324. The AADP (%) and AADY values for N_2-methane mixture, as given in Table 4-4, are 0.998% and 0.0176; respectively. In the similar manner, the VLE result of N_2-propane is shown in Figure 4.12 at 270 K with k_{ij} of 0.0172. The VLE prediction for vapor phase is quite good but considerable deviation from liquid mole fraction at higher pressures is observed with AADP of 5.472 %.

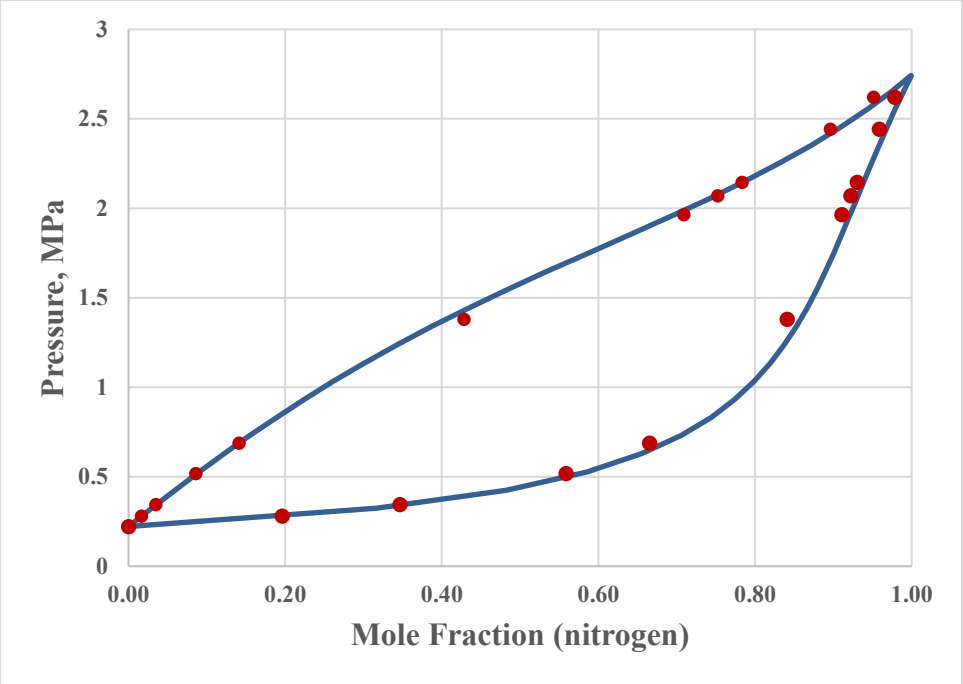

Figure 4.11: The VLE of Nitrogen-Methane system at 122 K with k_{ij} = 0.0324. The solid line is the correlation of the SAFT-VR Mie EOS. The points represent experimental VLE data (Stryjek, Chappelear, & Kobayashi, 1974).

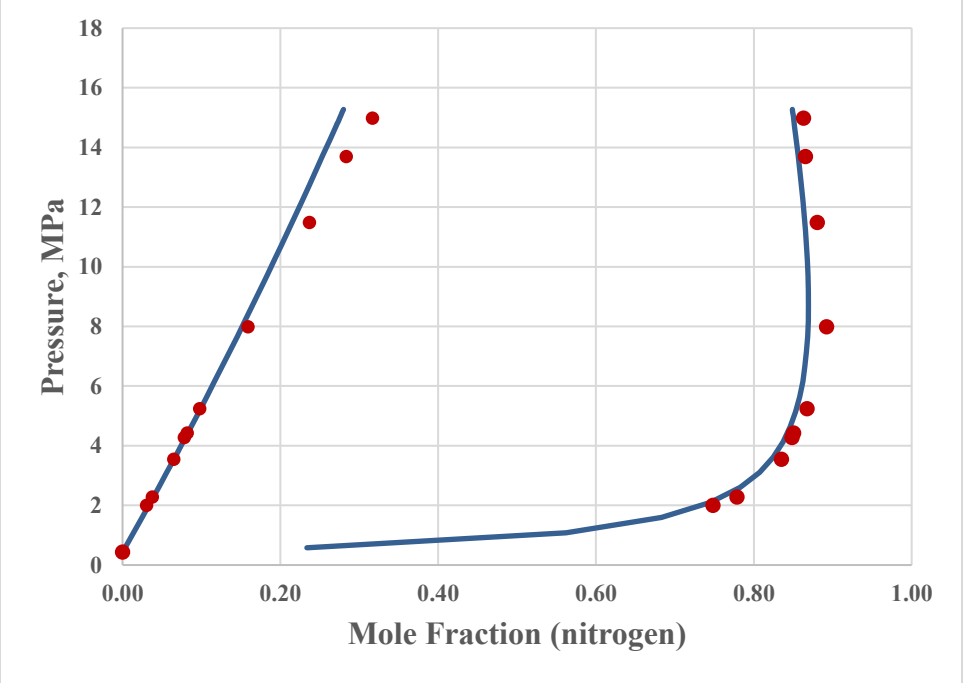

Figure 4.12: The VLE of Nitrogen-Propane system at 270 K with k_{ij} = 0.0172. The solid line is the correlation of the SAFT-VR Mie EOS. The points represent experimental VLE data (Yucelen & Kidnay, 1999).

Methane and H_2S are important components of reservoir fluid and their accurate VLE behavior is of prime interest in oil and gas industry (Coquelet et al., 2014). The presence of H_2S enhances the tendency of formation of gas hydrates (Noaker & Katz, 1954). Figure 4.13 demonstrates the VLE of methane-H_2S mixture using the SAFT-VR Mie EOS at 273.54 K with a binary interaction parameter of 0.0314. The binary interaction parameter is based on the work A.G. Perez et al. (2016). The AADP (%) and AADY values are 3.1202% and 0.0464; respectively.

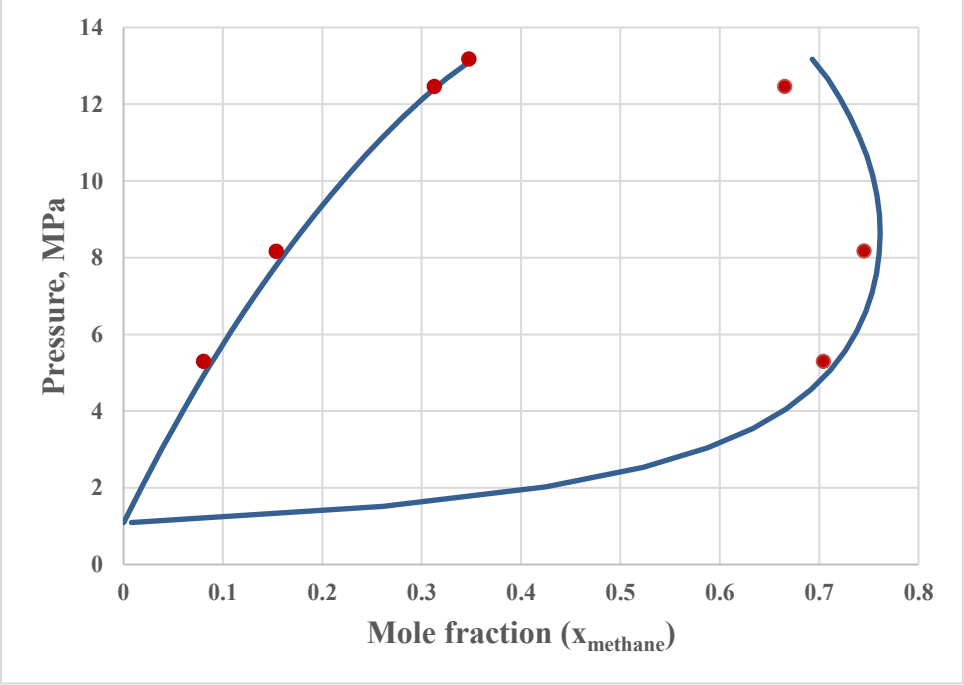

Figure 4.13: The VLE of Methane-H_2S system at 273.54 K with k_{ij}=0.0314. The solid line is the correlation of the SAFT-VR Mie EOS. The points represent experimental VLE data (Coquelet et al., 2014).

Table 4-4 summarizes the VLE results of considered hydrocarbon-nonhydrocarbon mixtures. Experimental data references are also reported in this table.

Table 4-4: Summary of VLE results of hydrocarbon-nonhydrocarbon mixtures

System	T (K)	k_{ij}	AADP (%)	AADY	Exp. Points (N)	Data Reference
CO_2-Methane	220.00	0.0066	1.460	0.0186	13	(Mraw, Hwang, & Kobayashi, 1978)
CO_2-Propane	252.95	0.0599	1.533	0.0303	12	(Nagahama et al., 1974)
CO_2-isobutane	310.93	0.06	1.711	0.0119	13	(Besserer & Robinson, 1973a)
Nitrogen-Methane	122.00	0.0324	0.998	0.0176	13	(Stryjek et al., 1974)
Propane-Nitrogen	270.00	0.0172	5.472	0.0218	11	(Yucelen & Kidnay, 1999)
Methane-H_2S	273.54	0.0314	3.1202	0.0464	4	(Coquelet et al., 2014)

4.3.3 Nonhydrocarbon VLE mixtures

Apart from hydrocarbon mixtures, gas hydrates form in the presence of non-hydrocarbon gaseous mixtures as well. These non-hydrocarbon mixtures include light gases such as nitrogen, carbon dioxide as well as noble gases like argon, krypton etc.

The VLE result for N_2-argon mixture is carried out at 122.89 K, and illustrated in Figure 4.14. As indicated in the previous section, the effect of quadrupolar interactions in N_2 and CO_2 mixtures is weak. As a result, an excellent VLE prediction of N_2-argon using the SAFT VR Mie EOS is obtained with kij value of 0.0013. This remarkable accuracy is seen by analyzing pressure and vapor mole fraction deviation values of N_2-argon mixtures given in Table 4-5.

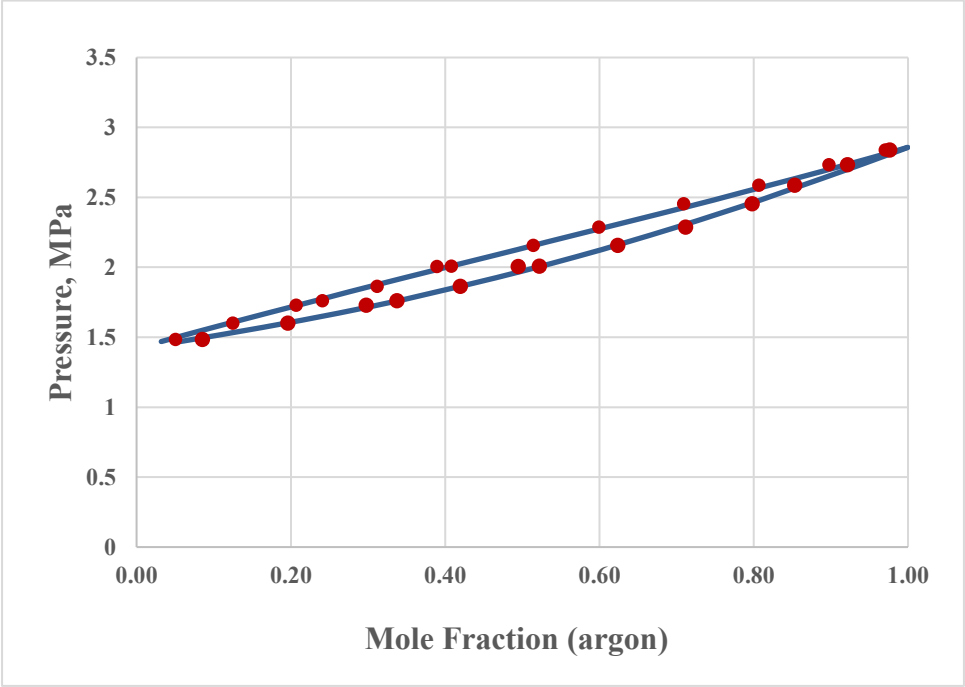

Figure 4.14: The VLE of Nitrogen-Argon system at 122.89 K with k_{ij}=0.0013. The solid line is the correlation of the SAFT-VR Mie EOS. The points represent experimental VLE data (Jin, Liu, & Sheng, 1993).

Quantitative VLE prediction for N_2-CO_2 mixture is shown in Figure 4.15 at 270 K with a binary interaction parameter of -0.1130. The k_{ij} value for this mixture is consistent with the ones obtained in the literature (Gonzalez et al., 2015). As shown in Table 4-5, AADP (%) and AADY values of this mixture are respectively 1.412% and 0.0117.

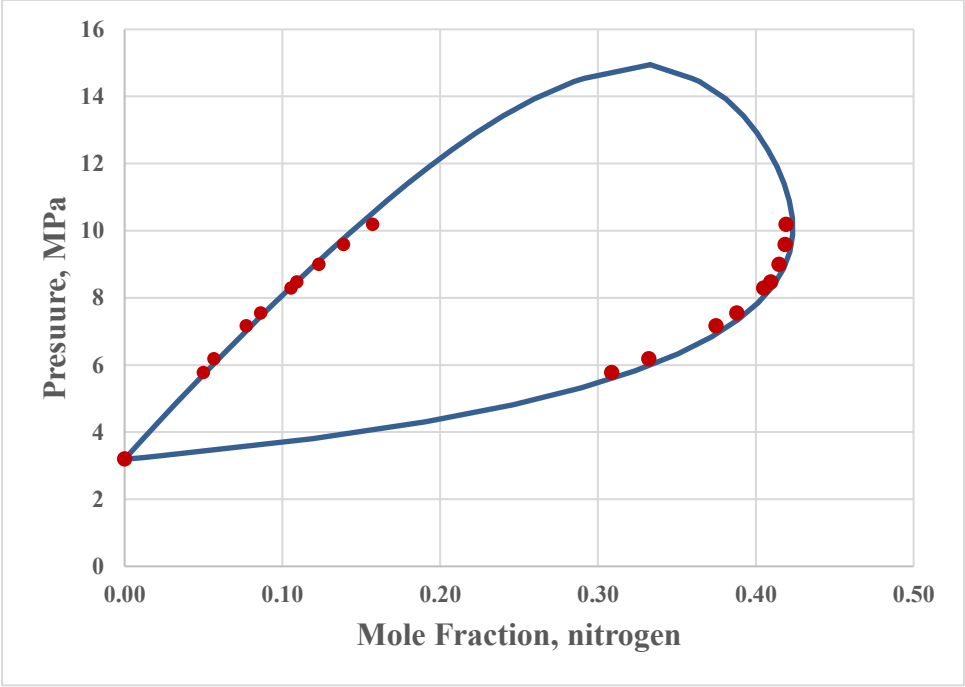

Figure 4.15: The VLE of Nitrogen-CO_2 system at 270 K with k_{ij}= -0.1130.The solid line is the correlation of the SAFT-VR Mie EOS. The points represent experimental VLE data (Brown, Sloan, & Kidnay, 1989).

Table 4-5 represents the summary of VLE results of nonhydrocarbon mixtures along with the references of experimental data.

Table 4-5 VLE result summary of nonhydrocarbon mixtures

System	T (K)	k_{ij}	AADP (%)	AADY	Exp. Points (N)	Data Reference
Nitrogen-Argon	122.89	0.0013	0.0067	0.0182	13	(Jin et al., 1993)
CO_2-Nitrogen	270	-0.113	1.412	0.0117	10	(Brown et al., 1989)

The deviations at higher pressures nearing critical locus are observed in different non-polar systems like methane-isobutane, propane-nitrogen, methane-H_2S, studied in this chapter. This behavior is common with EOS that are analytical in the free energy. The analytical EOSs usually fail to reproduce the singular behavior of fluids in the critical region due to long-scale fluctuations in density (Sengers & Sengers, 1986). SAFT-VR Mie being analytical in nature also exhibit this behavior. However, as compared to other SAFT variants and other analytical EOS, SAFT-VR Mie results in improved prediction of VLE at higher pressures nearing critical locus due to consideration of higher order perturbation term for dispersion forces (Lafitte et al., 2013).

To sum up, the SAFT-VR Mie EOS is very successful in predicting accurate VLE of various systems including methane-ethane, methane-propane, methane-isobutane, ethane-propane, propane-isobutane, ethane-isobutane, methane-ethene, CO_2-methane, CO_2-propane, CO_2-isobutane, propane-nitrogen, nitrogen-methane, methane-H_2S, nitrogen-argon and nitrogen-CO_2. Although the studied mixtures were selected based on the components involved in the formation of gas hydrate, these mixtures have different types of Van Konyenburg and Scott (1980) classification. VLE mixtures including methane-ethane, methane-propane, methane-isobutane, ethane-propane, propane-isobutane, ethane-isobutane, methane-ethene, CO_2-methane, CO_2-propane, CO_2-isobutane, nitrogen-argon exhibit Type I phase behavior classification. Type III VLE behavior classification is exhibited by propane-nitrogen, nitrogen-methane and methane-H_2S mixtures.

The quantitative VLE results of these classifications make the SAFT-VR Mie EOS an excellent candidate to study more complex systems in future studies.

CHAPTER 5

VLE PREDICTION OF WATER-NON-ASSOCIATING COMPOUNDS USING SAFT-VR MIE EOS

5.1 Introduction

Water is an important component and its presence with the hydrate formers contributes to the formation of gas hydrates. It acts as a host molecule that encapsulates hydrate formers to form gas hydrates. In addition, in gas hydrate system, water interacts with hydrate formers in the aqueous and gas phases. Therefore, accurate VLE behavior of host (water) and guest (hydrate formers) mixtures is of prime importance in the calculations of incipient conditions of gas hydrates.

This chapter focusses on the determination of VLE behavior of water-nonpolar compounds. Section 5.2 summarizes the adjustable parameters of water using the SAFT-VR Mie EOS based on different association schemes. It is followed by section 5.3, which has further three sub-sections. Section 5.3.1 evaluates the effect of the change of pairwise potential in the association term on the accuracy of VLE of water-nonpolar systems. Sections 5.3.2 & 5.3.3 are dedicated for VLE results of water-hydrocarbon systems and water-non-hydrocarbon systems; respectively.

5.2 SAFT-VR Mie Adjustable Parameters for Water

Water is an associating compound and could reasonably be characterized by four off-center association sites (Clark, Haslam, Galindo, & Jackson, 2006; Nezbeda, Kolafa, & Kalyuzhnyi, 1989; Nezbeda & Pavlíček, 1996), as illustrated in Figure 5.1. Associating components, in comparison to non-associating components, are characterized by two additional parameters depending on the association scheme. Therefore, seven adjustable parameters are used for associating compounds. One of the association parameters is either the association volume (K_{ab}) or the cutoff range of SW interaction between association sites a and b (r_{ab}^{c}). The other one is the association energy (ϵ_{ab}^{HB}) which is the same parameter in all association schemes. Table 5-1 lists the SAFT-VR Mie adjustable parameters of water for HS, Novel LJ and Novel Mie association schemes found in the literature.

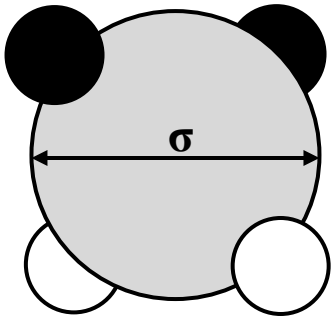

Figure 5.1 General schematic of water molecule with four off-center association sites representing hydrogen atoms (black) and electron lone pairs on oxygen atom (white).

5.3 VLE of Water-Hydrate Former Systems

The water-hydrate former VLE mixtures are considered as challenging non-ideal binary mixtures. Their VLE behavior is classified as Type III phase behavior as per van

Konynenburg and Scott classification (Konynenburg & Scott, 1980). They exhibit large regions of vapor-liquid and liquid-liquid fluid-phase equilibria with a discontinuous vapor-liquid critical locus (Dufal, Lafitte, Haslam, et al., 2015).

As water is an association compound, both dispersion and association interactions need to be considered in the VLE calculations. Hydrate formers that are generally known can be both associating and non-associating. Hence, both self-association and cross association effects account in prediction of water-hydrate formers mixtures. This work considers non-associating hydrate formers which focusses on self-association in water-hydrate formers VLE mixtures.

In water-nonpolar mixtures, the accurate determination of vapor and liquid mole fractions are difficult due to the hydrophobic nature of the system. In addition, nonpolar have very low solubilities in water. The accuracy of such systems depends on the k_{ij} values which are determined by flash calculation based on the following objective function:

$$obj = \left(\sum \left(\frac{\left(x_{cal} - x_{exp}\right)^2}{x_{exp}} + \frac{\left(y_{cal} - y_{exp}\right)^2}{y_{exp}} \right) / N \right) \tag{5.1}$$

where x_{exp} and y_{exp} are experimental liquid and vapor mole fractions, x_{cal} and y_{cal} are calculated liquid and vapor mole fractions and N represents the number of experimental data points.

Table 5-1: The SAFT VR Mie adjustable parameters for water taken from the literature.

Component	m_s	σ (Å)	ϵ/k (K)	λ_r	λ_a	r_{ab}^c	K_{ab}	ϵ_{ab}^{HB}	Data Reference
Water-HS [a]	1.0	3.1610	488.75	52.367	6.0	0.5834	-	1210.0	(Dufal, Lafitte, Haslam, et al., 2015)
Water-LJ [a]	1.0	3.0063	266.68	17.020	6.0	-	101.69	1985.4	(Dufal, Lafitte, Haslam, et al., 2015)
Water-Mie [a]	1.0	3.0555	418.00	35.823	6.0	-	496.66	1600.0	(Dufal, Lafitte, Haslam, et al., 2015)

[a] Water with four association sites

However, due to the complex nature of water containing system, a single binary interaction parameter does not give quantitative VLE results. This is why two binary interactions parameters are utilized; one is for the vapor phase and the other is for the aqueous phase.

5.3.1 Association Term Evaluation for Water-Hydrate Former Systems

There are three association schemes used with the SAFT VR Mie EOS in the literature (Dufal, Lafitte, Haslam, et al., 2015). A general SAFT description for the molecular structure of water is considered by these association schemes that consist of a spherical repulsive core with four off-center SW association sites (Clark et al., 2006; Nezbeda et al., 1989; Valtz, Chapoy, Coquelet, Paricaud, & Richon, 2004). These association schemes use Wertheim's original TPT1 procedure with different radial distribution functions (RDF), namely HS, Novel LJ and Novel Mie RDFs. Mathematical representation of each of these association schemes is already demonstrated in Chapter 3. The SAFT-VR Mie parameters of water are reported in Table 5-1 for each association scheme**.** On the other hand, the SAFT-VR Mie parameters for non-associating hydrate formers can be found in Table 4-1.

In order to evaluate the accuracy of each association scheme indicated above, the VLE behavior of water-methane and water-ethane is studied.

The VLE of water-methane mixture is studied at 283.15 K by the SAFT VR Mie EOS. Each scheme gives quantitative VLE prediction of this mixture with the adjustment of k_{ij} values. The values of vapor and liquid k_{ij} parameters along with predicted mole fraction deviations for water-methane are provided in Table 5-2. Each scheme predicts

reasonably well the VLE behavior of water-methane mixture with different phase dependent k_{ij} values. The Novel LJ association scheme gives almost the same accuracy compared to the other two schemes but with a smaller kij for the liquid phase.

Similar comparison is carried out for water-ethane mixture at 293.11 K. The phase dependent k_{ij} values and mole fraction deviation are present in Table 5-3. Accurate VLE is obtained by the SAFT-VR Mie with the three schemes. However, the Novel LJ association scheme has the smaller k_{ij} values.

Above indicated comparisons among association schemes for the prediction of VLE behavior of water-methane and water-ethane systems point towards the selection of Novel LJ association scheme with the SAFT VR Mie EOS.

The SAFT VR Mie methodology uses Mie potential to address the chain and dispersion molecular effects. If the Mie RDF for association is not implemented with the SAFT-VR Mie, other RDFs cause theoretical inconsistency (Dufal, Lafitte, Haslam, et al., 2015). However, as long as accurate and realistic thermodynamic properties and phase equilibrium are predicted, the application of Novel LJ association scheme in line with SAFT VR Mie is practically acceptable and unproblematic.

Table 5-2: Association schemes comparison for VLE prediction of Water-Methane system at 283.15 K

Association Scheme	k_{ijv}	k_{ijl}	AADX	AADY	Data Reference
HS	-0.0050	-0.3733	2.2185×10^{-05}	0.0852	(A. Chapoy, Coquelet, & Richon, 2005; A. Chapoy, Mohammadi, Chareton, Tohidi, & Richon, 2004; Wang, Chen, Han, Guo, & Guo, 2003)
Novel LJ	-0.0784	-0.0167	2.2151×10^{-05}	0.0854	
Novel Mie	-0.0123	-0.1774	2.2172×10^{-05}	0.0857	

Table 5-3: Association schemes comparison for VLE prediction of Water-Ethane system at 293.11 K

Association Scheme	k_{ijv}	k_{ijl}	AADX	AADY	Data Reference
HS	0.1022	-0.2195	3.2238×10^{-05}	0.0850	(Antonin Chapoy, Coquelet, & Richon, 2003; Mohammadi, Chapoy, Tohidi, & Richon, 2004)
Novel LJ	0.0543	-0.0881	2.8116×10^{-05}	0.0803	
Novel Mie	0.1102	-0.1567	2.9104×10^{-05}	0.0673	

5.3.2 VLE of Water-Hydrocarbon Systems

This section evaluates the VLE behavior of water-hydrocarbon mixtures. The hydrocarbon hydrate formers taken in consideration are lighter alkanes including methane, ethane, propane and ethene.

Figures 5.2 (a) & (b) illustrate the phase behavior of water-methane system at 283.15 K. The AADX and AADY values for water methane system, provided in Table 5-4, illustrate the reasonable accuracy of VLE prediction using the SAFT VR Mie-Novel LJ EOS. The k_{ij} value for vapor phase is -0.0784 and for liquid phase is -0.0167.

Water-ethane is another system studied in this work. VLE behavior of water-ethane mixture at about 293.11 K is predicted in Figures 5.3 (a) & (b) using the SAFT VR Mie-Novel LJ EOS. The adjusted k_{ij} values for water-rich and ethane-rich phases are -0.0881 and 0.0543; respectively. For water-ethane system, the mole fraction deviation values for vapor phase is 0.0803 and for liquid phase is 2.811×10^{-05}, as reported in Table 5-4.

In a similar fashion, water-propane system VLE prediction is evaluated using the SAFT VR Mie-Novel LJ EOS (see Figures 5.4 (a) & (b)). The system is studied at two different temperatures due to the lack of vapor and liquid experimental data at the same temperature. For the aqueous phase, the system is studied at 293.13 K for liquid phase while it is studied at 338.71 K for vapor phase. Remarkable accuracy of VLE prediction, with k_{ijv} and k_{ijl} values of 0.0437 and -0.1338, is clear from AADX and AADY values for water-propane system provided in Table 5-4.

(a)

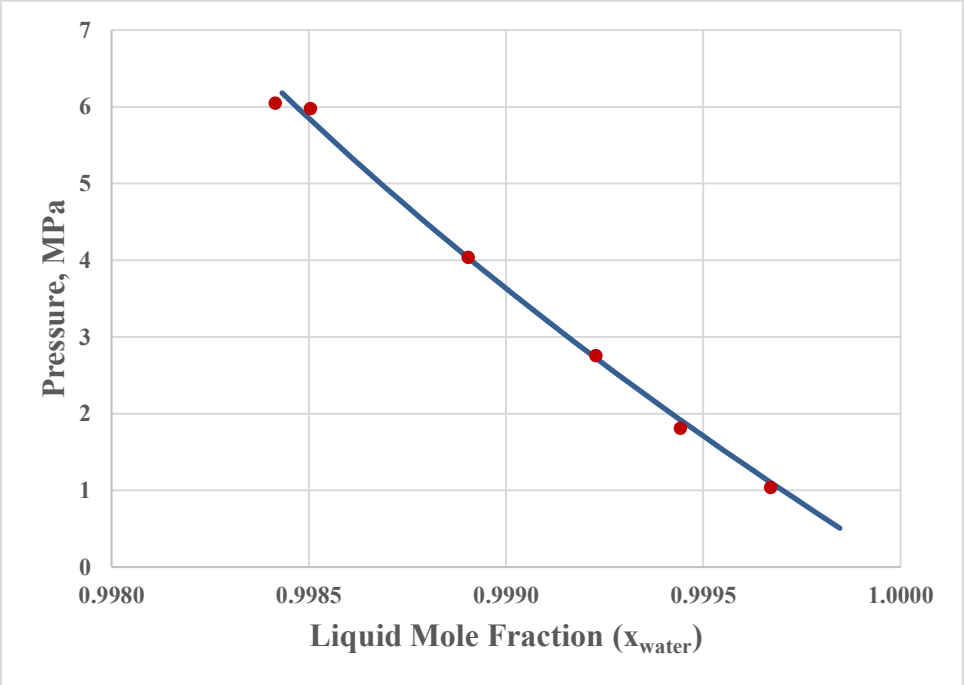

(b)

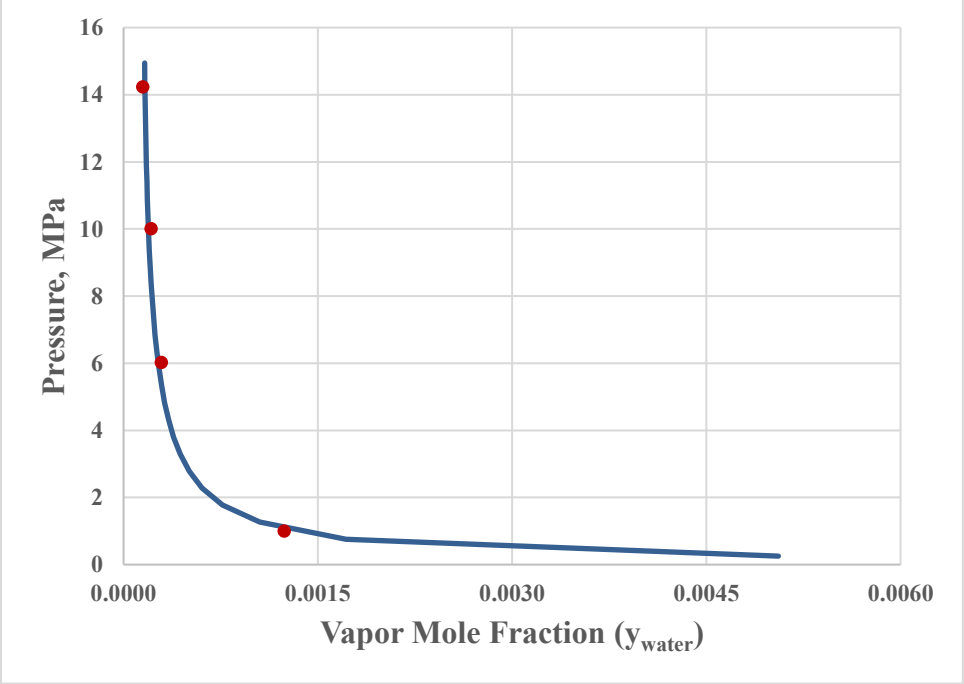

Figure 5.2: The VLE of Water-Methane system at 283.15 K (a) water-rich phase with k_{ijl}=-0.0167 (b) methane rich phase with k_{ijv}=-0.0784. The solid line is the correlation of the SAFT-VR Mie-Novel LJ EOS. The points represent experimental VLE data (A. Chapoy et al., 2005, 2004; Wang et al., 2003).

When analyzing the results of lighter alkanes mixtures with water through Figures 5.1 ,5.2, 5.3 & Table 5-4, various observations are noted. AADX and AADY values for all water-lighter alkane systems give very slight deviation from the experimental data. As the vapor phase of light alkanes-water mixture is almost completely pure in lighter alkanes, hence accurate vapor phase behavior is achieved using small k_{ij} values. On the other hand, while assessing the k_{ij} parameters for liquid phase, an increase in k_{ijl} value is noted with the increase in carbon number of alkane series. Probable reason for this increase can be dissymmetry of molecules of water and light alkanes molecules.

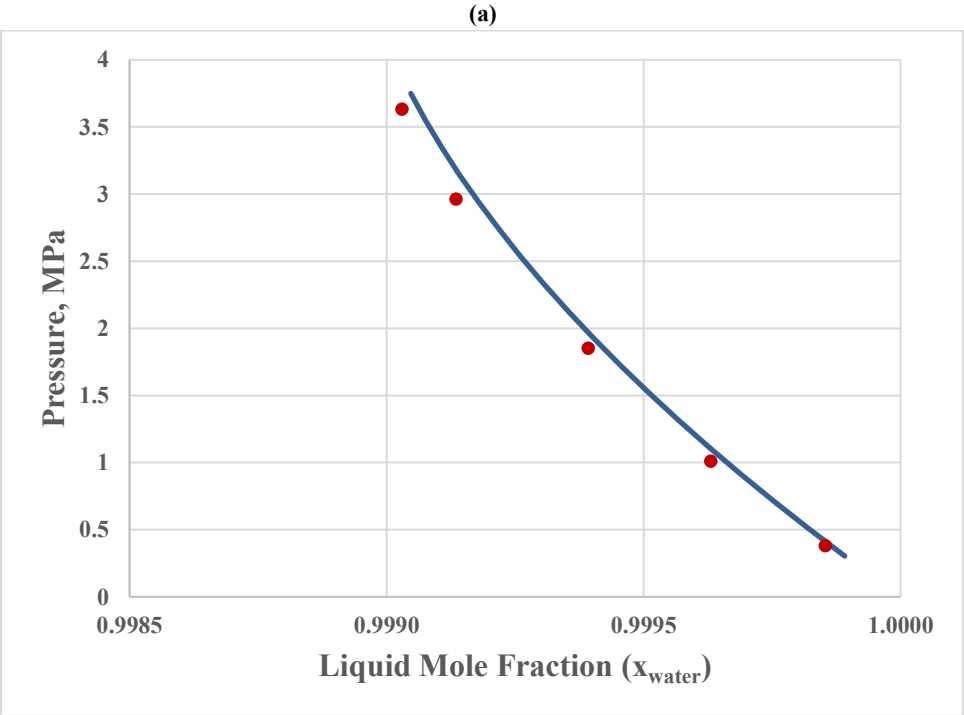

(b)

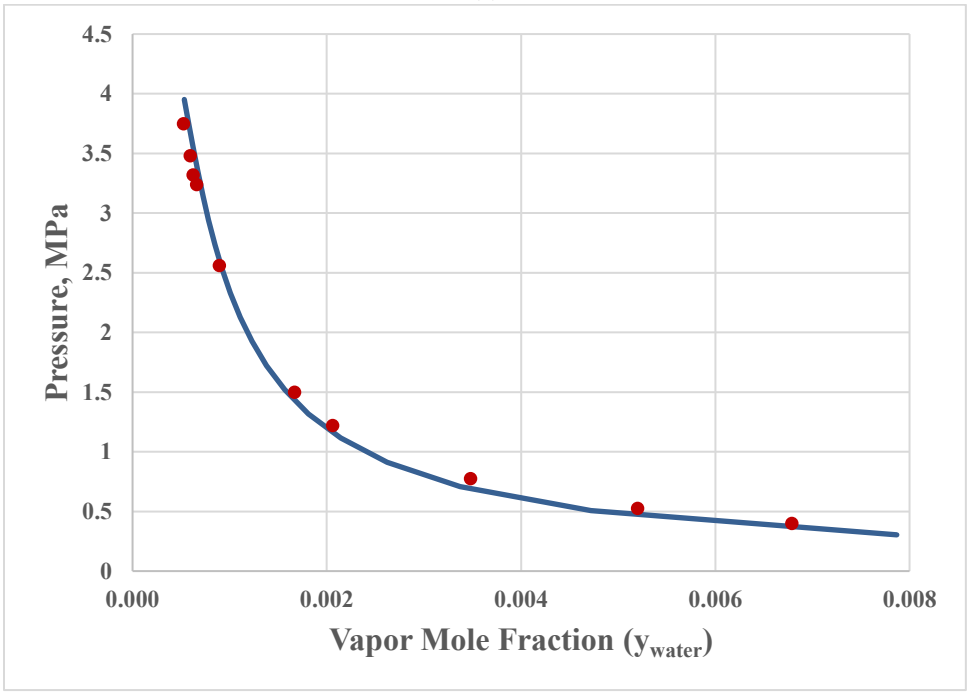

Figure 5.3: The VLE of Water-Ethane system at 293.11 K (a) water-rich phase with k_{ijl}=-0.0881 (b) ethane rich phase with k_{ijv}=0.0543. The solid line is the correlation of the SAFT-VR Mie-Novel LJ EOS. The points represent experimental VLE data (Antonin Chapoy et al., 2003; Mohammadi et al., 2004).

(a)

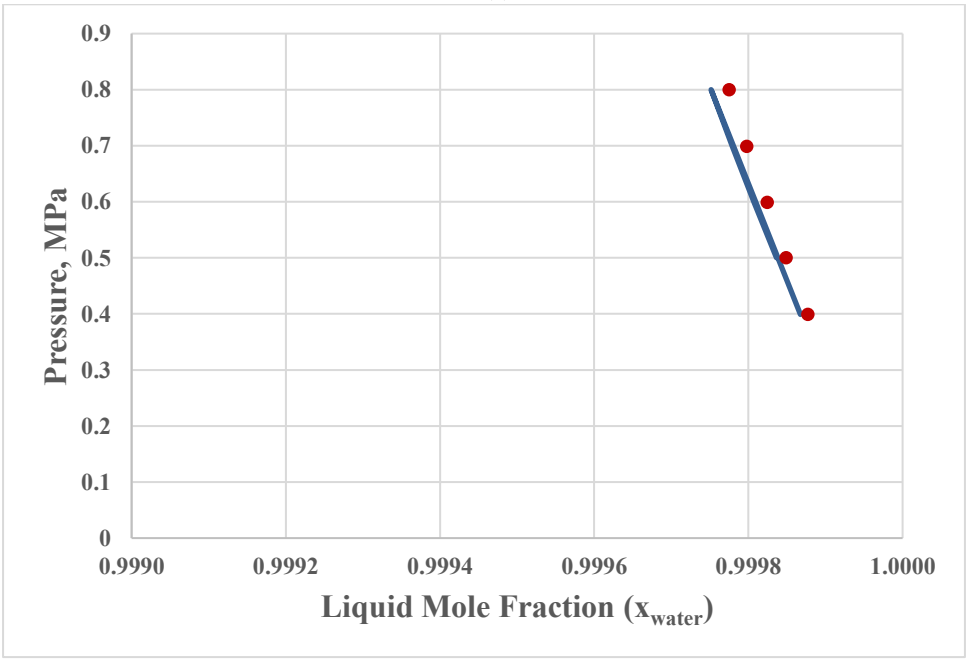

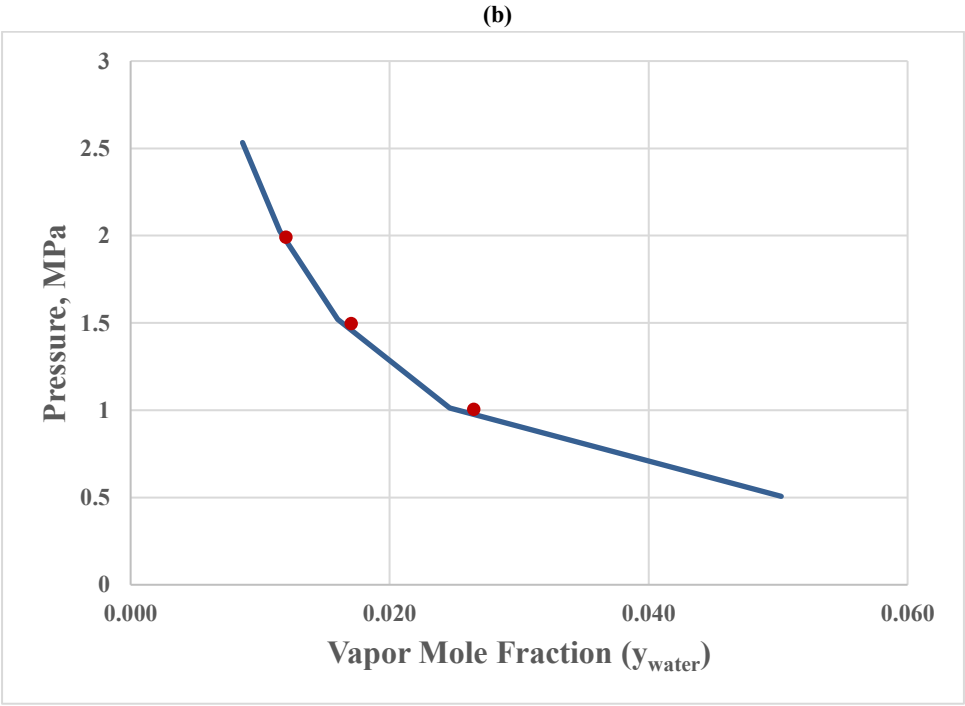

Figure 5.4: The VLE of Water-Propane system (a) water-rich phase at 293.13 K with k_{ijl}=-0.1338 (b) propane rich phase at 338.71 K with k_{ijv}=0.0437. The solid line is the correlation of the SAFT-VR Mie-Novel LJ EOS. The points represent experimental VLE data (Antonin Chapoy, Mokraoui, et al., 2004; Kobayashi & Katz, 1953).

Apart from alkanes, ethene is studied with water. The prediction of the VLE of water-ethene mixture is shown in Figure 5.5 at 344.26 K. The mole fraction deviation is provided in Table 5-4. The k_{ij} values of vapor and liquid phases are -0.19256 and -0.2028; respectively. These k_{ij} values are high compared to alkane systems studied above. A plausible reason for these high k_{ij} values is that ethene is an unsaturated hydrocarbon with double bonds, but the SAFT theory conceives the compounds as single covalent bond molecules.

(a)

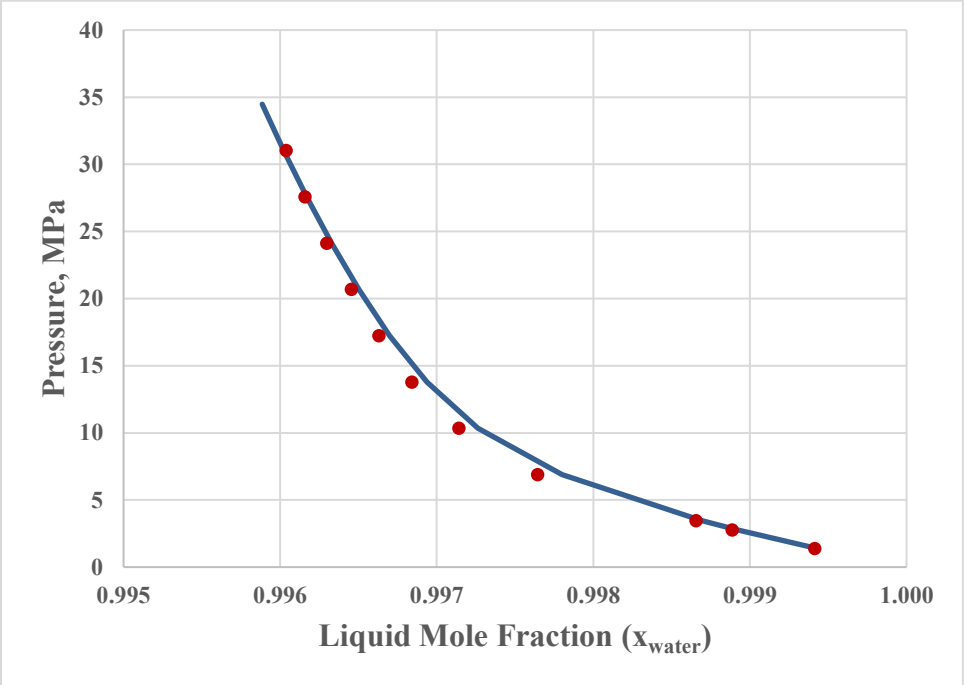

(b)

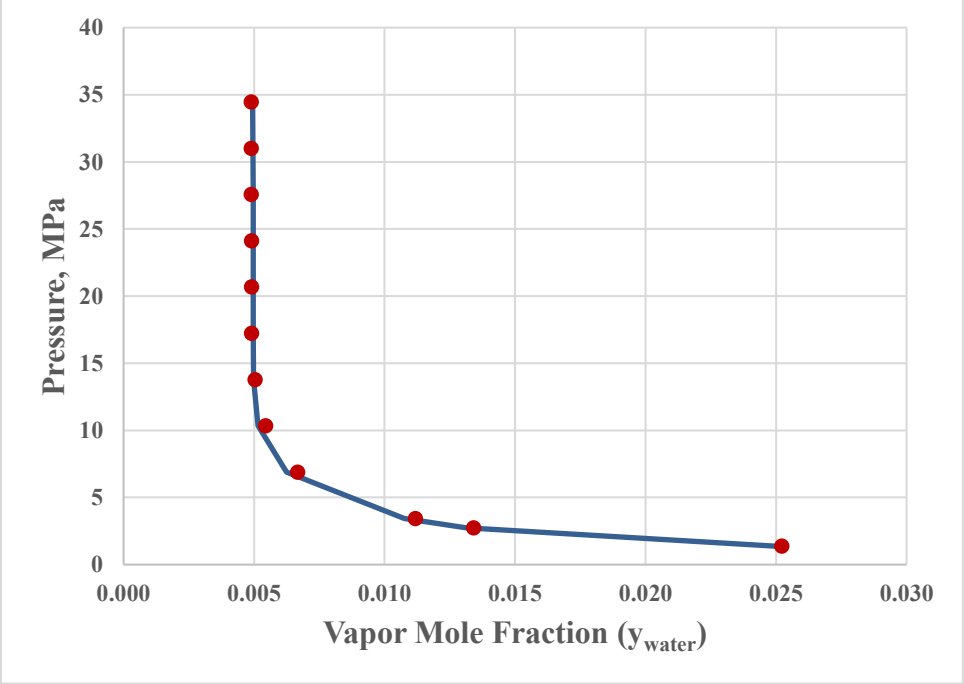

Figure 5.5: The VLE of Water-Ethene system at 344.26 K (a) water-rich phase with k_{ijl}=-0.1926 (b) ethene rich phase with k_{ijv}=-0.2028. The solid line is the correlation of the SAFT-VR Mie-Novel LJ EOS. The points represent experimental VLE data (Anthony & McKetta, 1967).

Table 5-4: VLE results summary of water-hydrocarbon systems

System	T(K)	k_{ijv}	k_{ijl}	AADX	AADY	Data Reference
Water-Methane	283.15	-0.0784	-0.0167	2.220×10^{-05}	0.0854	(A. Chapoy et al., 2005, 2004; Wang et al., 2003)
Water-Ethane	293.11	0.0543	-0.0881	2.811×10^{-05}	0.0803	(Antonin Chapoy et al., 2003; Mohammadi et al., 2004)
Water-Propane	338.71 293.13	0.0437 (at 338.71 K)	-0.1338 (at 293.13 K)	1.700×10^{-05}	0.0421	(Antonin Chapoy, Mokraoui, et al., 2004; Kobayashi & Katz, 1953)
Water-Ethene	344.26	-0.1925	-0.2028	5.520×10^{-05}	0.0227	(Anthony & McKetta, 1967)

5.3.3 VLE of Water-Nonhydrocarbon Systems

As discussed earlier about the nonhydrocarbon components that take part in gas hydrate mixtures. Here, in this section, the VLE behavior of water-nonhydrocarbon mixtures is studied. The nonhydrocarbons considered in this section include argon, nitrogen and carbon dioxide.

Figures 5.6 (a) & (b) show an accurate prediction of VLE behavior of water argon-mixture at 298.15 K. Argon is a non-associating and spherical molecule, its interaction with water molecules only occur in form of dispersion forces. The VLE prediction is obtained with small k_{ij} value for both vapor and liquid phases. The k_{ij} values in both phases are around 0.026. The k_{ij} values and mole fraction deviation values for water-argon mixture is found in Table 5-5.

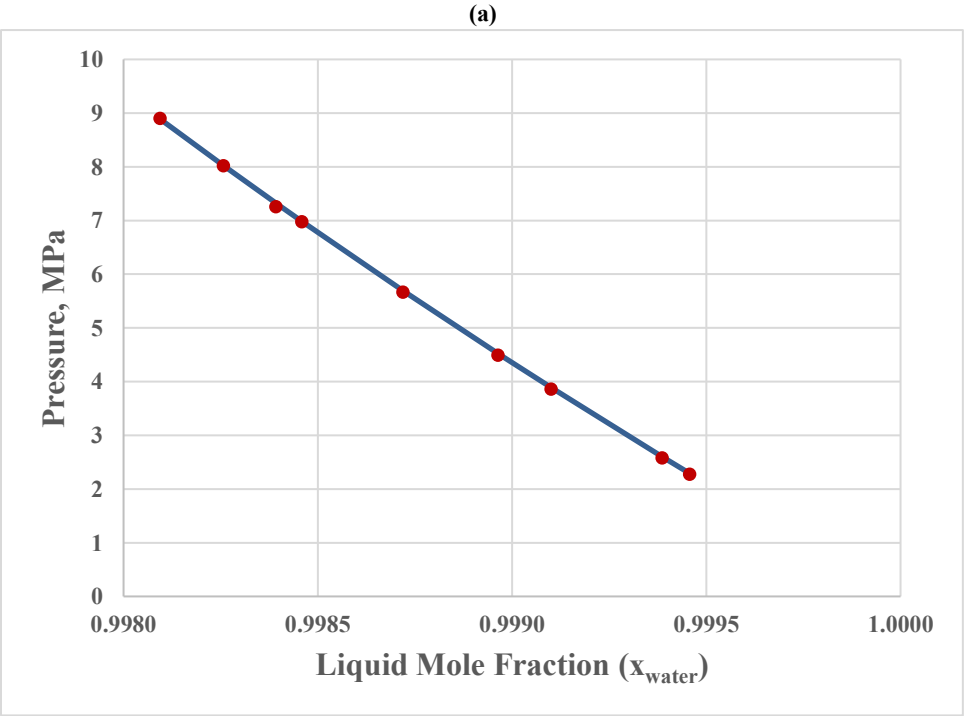

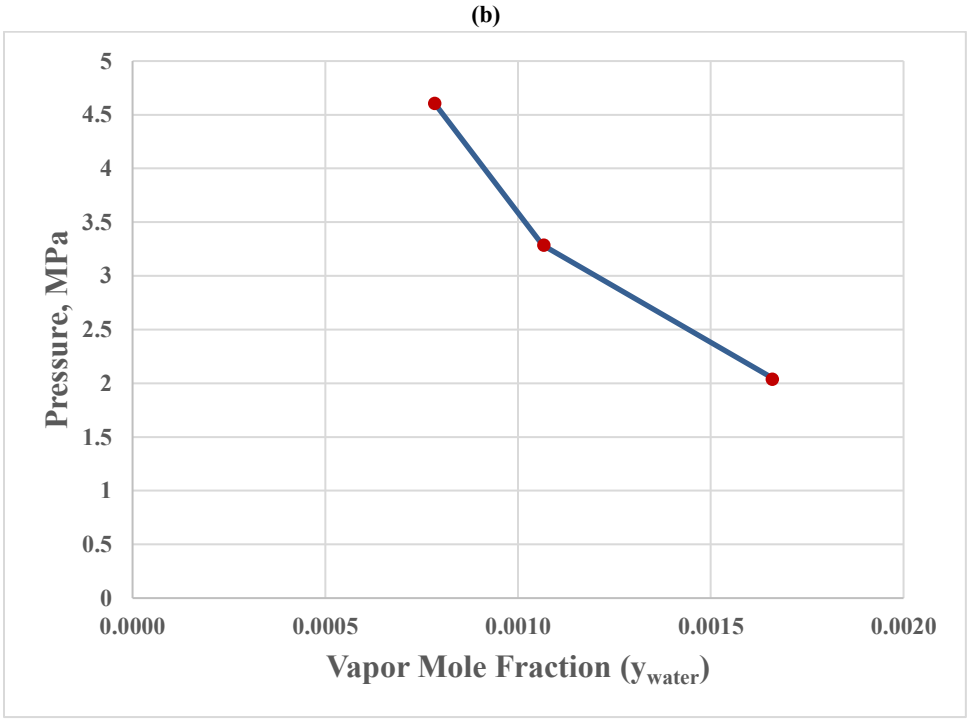

Figure 5.6: The VLE of Water-Argon system at 298.15 K (a) water-rich phase with k_{ijl}=-0.0268 (b) argon rich phase with k_{ijv}=-0.0262. The solid line is the correlation of the SAFT-VR Mie-Novel LJ EOS. The points represent experimental VLE data (Kennan & Pollack, 1990; Rigby & Prausnitz, 1968).

Figures 5.7 (a) & (b) depict the VLE behavior prediction of water-nitrogen mixture at 283.2 K. The AADX and AADY values provided in Table 5-5 indicate reasonable accuracy of water-nitrogen VLE prediction. The k_{ij} value of vapor phase is 0.0673 whereas that of liquid phase is -0.2326. These high k_{ij} values is due to the approximation of nitrogen molecule as a single covalent bond molecule. Moreover, low temperatures contribute to the increase in strength of self-association especially in liquid phase which is mostly water (Chaplin, 2000).

(a)

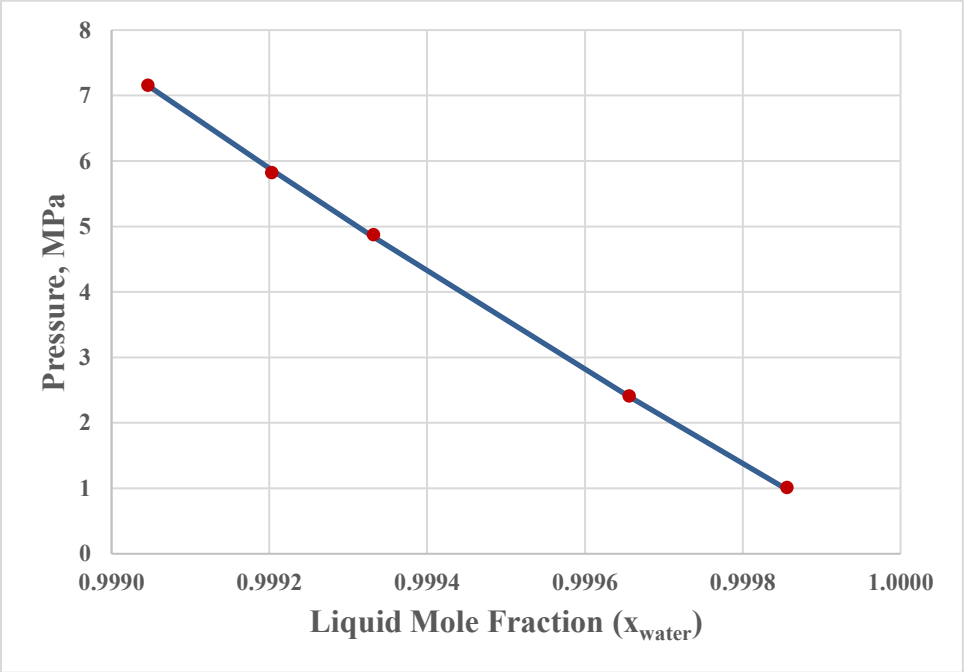

(b)

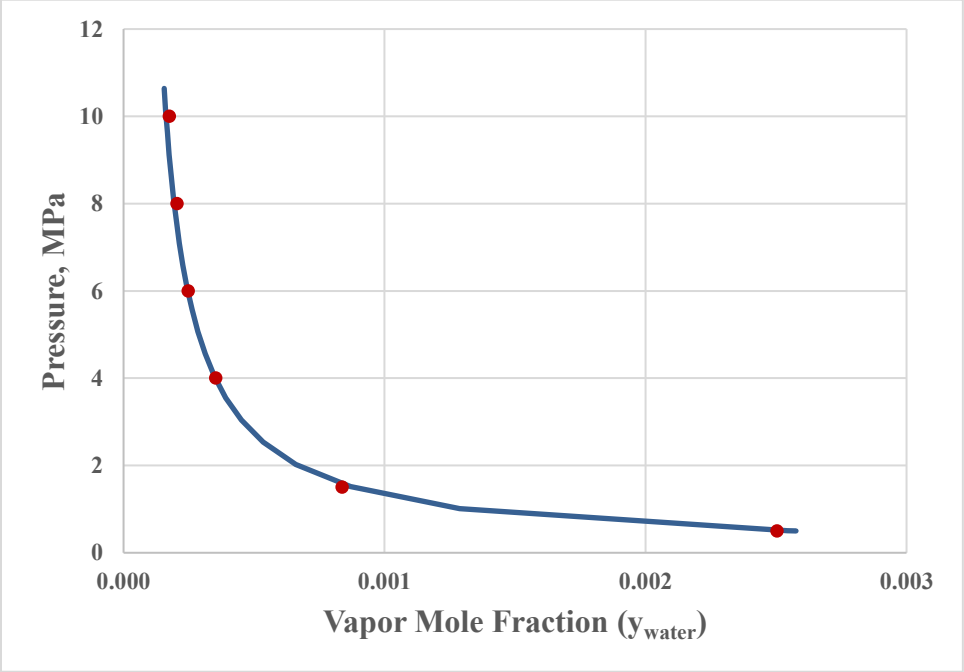

Figure 5.7: The VLE of Water-Nitrogen system at 283.2 K (a) water-rich phase with k_{ijl}=-0.2326 (b) nitrogen rich phase with k_{ijv}=0.0673. The solid line is the correlation of the SAFT-VR Mie-Novel LJ EOS. The points represent experimental VLE data (Antonin Chapoy, Mohammadi, Tohidi, & Richon, 2004).

The most complex system assessed in this section is water-carbon dioxide mixture shown by Figure 5.8. The k_{ijv} and k_{ijl} values for water-CO_2 mixture are -0.358 and -0.145; respectively. The vapor and liquid mole fraction deviation values are very small and given in Table 5-5. However, when compared to the AADX and AADY values of other water-nonhydrocarbon systems, water-CO_2 VLE behavior shows less accurate results even after the consideration of k_{ij} values. There can be various reasons for slightly deviating VLE as compared to other mixtures. Firstly, as it is known that CO_2 and water readily reacts at ambient conditions to form carbonic acid. Hence, there is a possibility of carbonic acid formation at higher pressures as well (Pan & Galli, 2016). However, the SAFT does not consider any chemical reaction effects while predicting VLE behavior. Moreover, CO_2 is a compound with double bonds but SAFT conceives it as a single covalent bonded molecule.

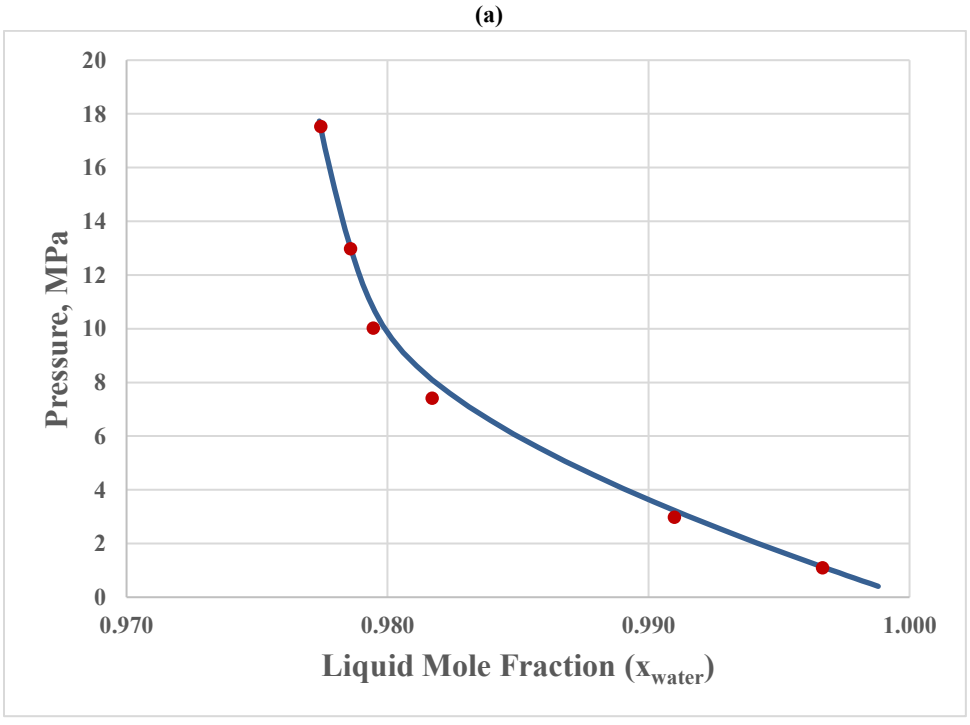

(b)

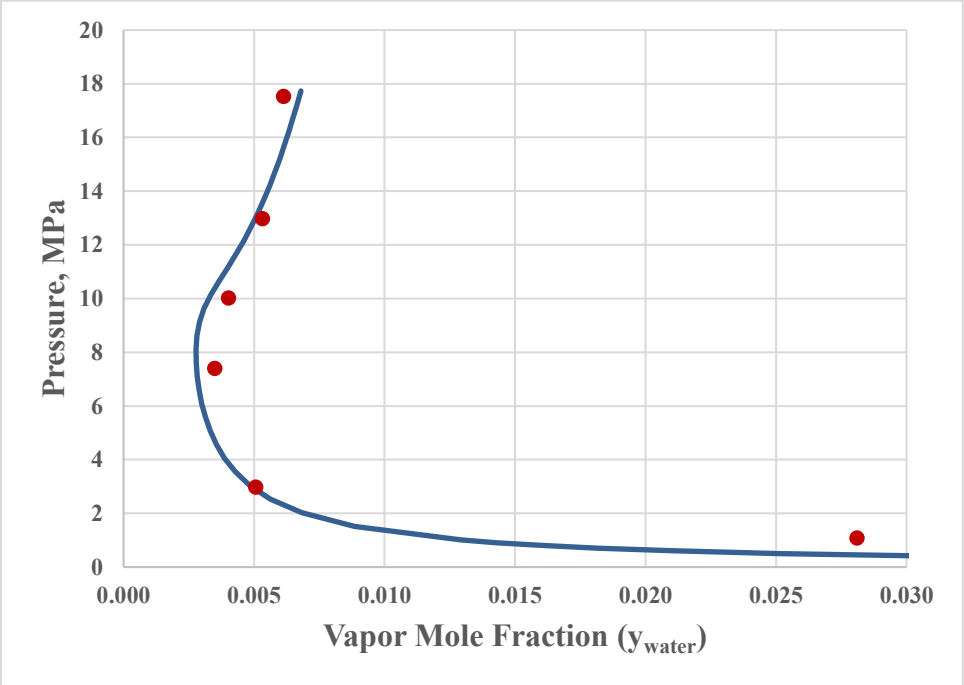

Figure 5.8: The VLE of Water-CO_2 system at 323.15 K (a) water-rich phase with k_{ijl}=-0.1450 (b) CO_2 rich phase with k_{ijv}=-0.3580. The solid line is the correlation of the SAFT-VR Mie-Novel LJ EOS. The points represent experimental VLE data (Hou, Maitland, & Trusler, 2013).

H_2S has a high tendency for gas hydrate formation (Noaker & Katz, 1954). For this very reason, it is important to study phase behaviour of water-H_2S, so that accurate gas hydrate equilibrium can be predicted. Figures 5.9 (a) & (b) represent the predicted VLE behaviour of water-H_2S system at 310.93 K. This accurate VLE prediction is obtained by adjusting the k_{ij} values. The adjusted k_{ij} values for vapour and liquid phases are -1.0256 and -0.0144; respectively. The high k_{ij} value of vapour phase accommodates the ignored effects of association in H_2S rich phase. AADX and AADY values provided in Table 5-5 confirms high accuracy achieved in prediction of VLE of water-H_2S system.

(a)

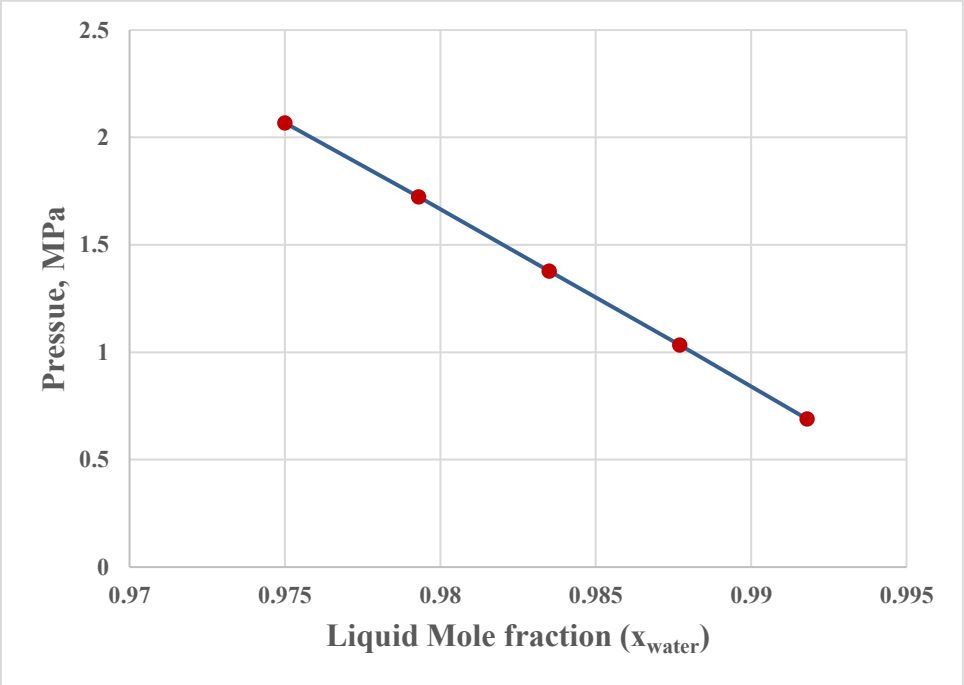

(b)

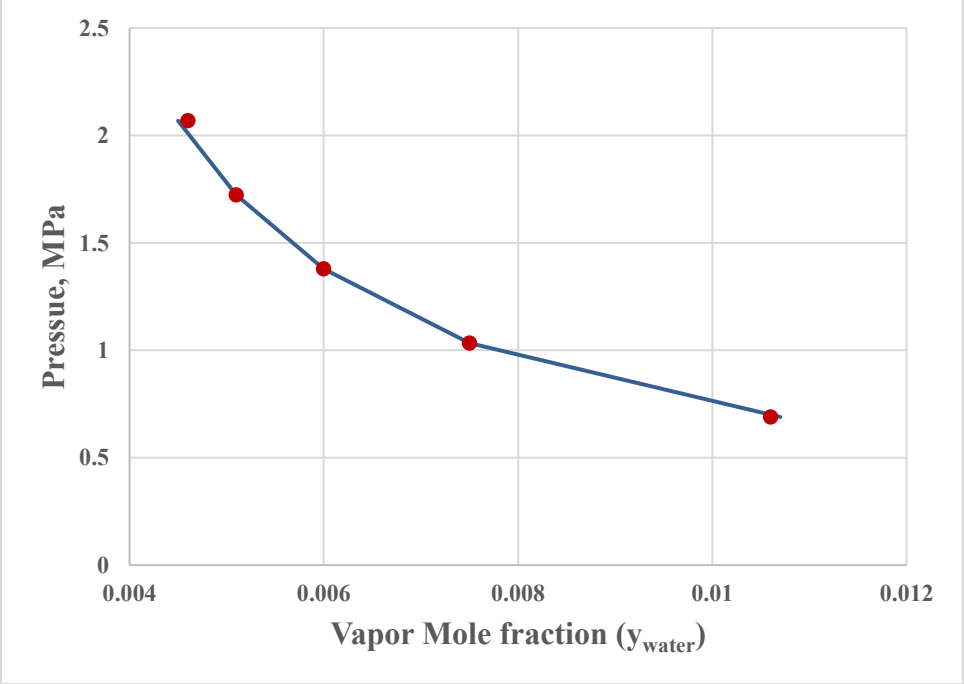

Figure 5.9: The VLE of Water-H_2S system at 310.93 K (a) water-rich phase with k_{ijl}=-0.0144 (b) H_2S rich phase with k_{ijv}=-1.0256. The solid line is the correlation of the SAFT-VR Mie-Novel LJ EOS. The points represent experimental VLE data (Selleck et al., 1952).

Table 5-5: VLE results summary of water-nonhydrocarbon mixtures

System	T(K)	k_{ijv}	k_{ijl}	AADX	AADY	Data Reference
Water-Argon	298.15	0.0268	0.0262	4.55×10^{-06}	0.0023	(Kennan & Pollack, 1990; Rigby & Prausnitz, 1968)
Water-N_2	283.2	0.0673	-0.2326	3.22×10^{-06}	0.0368	(Antonin Chapoy, Mohammadi, et al., 2004)
Water-CO_2	323.15	-0.3580	-0.145	0.00035	0.1901	(Hou et al., 2013)
Water-H_2S	310.93	-1.0256	-0.0144	3.00×10^{-05}	0.0053	(Selleck et al., 1952)

CHAPTER 6

GAS HYDRATE EQUILIBRIUM CALCULATIONS

6.1 Introduction

The previous two chapters provided the capability of the SAFT-VR Mie EOS to predict VLE of various gas hydrate mixtures. Quantitative prediction of VLE were achieved by the introduction of binary interaction parameter. The accurate VLE obtained in the previous two chapters will definitely contribute to the accuracy of gas hydrates calculations. This chapter utilizes the remarkable accuracy achieved in the previous two chapters to contribute to the results of gas hydrate incipient conditions with the aid of vdWP model. Gas hydrate equilibrium is determined for both single and mixed gas hydrates. Single gas hydrate system indicates that the system is water and one gas former (e.g. methane). Mixed gas hydrate system consists of water and at least two gases (e.g. methane and ethane).

The organization of this chapter starts with determination of optimum parameters of Langmuir constants in Section 6.2. It is followed by the selection of reference thermodynamic parameters required for gas hydrate calculations in Section 6.3. Section 6.4 evaluates the accuracy of incipient conditions of single gas hydrates. Mixed gas hydrates equilibrium results are then reported and assessed accordingly (see Section 6.5). At the end, achieved gas hydrate results are compared with other EOS models in Section 6.6.

6.2 Langmuir Constant Adjustable Parameters

As indicated in Chapter 2, this work focusses on the prediction of incipient conditions of L_w-H-V gas hydrate equilibrium. For most natural gas hydrate formers, the experimental data range extends between 273.15 K to about 300 K. This temperature range makes the use of eq. (2.9) applicable for the determination of Langmuir constants for gas hydrate equilibrium calculations. Eq. (2.9) consists of adjustable parameters that depend on size of cavity in each gas hydrate structure. This work uses both the literature and calculated adjustable parameters for Langmuir constants. The literature based adjustable parameters are given in Table 2-3 and they provide accurate results except for some compounds. This is why we proposed new sets of adjustable parameters given in Table 6-1. Table 6-1 also contains ethyne parameters that are not available in the literature.

6.3 Thermodynamic Reference Properties

The significance and description of reference thermodynamic properties is explained in details in Chapter 2. There are different values of these reference thermodynamic properties available in the literature. Some of frequently used literature values are given in Table 2-4. In order to select the best possible reference energy parameters, this work tests several combinations of the values given in Table 2-4 to predict the incipient conditions of single gas hydrates. The combination of reference energy values with the lowest AADP (%) is selected for the calculations of the incipient conditions.

Table 6-1: The Langmuir constant adjustable parameters for hydrate formers calculated in this thesis.

Guest	Temperature Range, K	Small $A_{ml} \times 10^3$, K	Large $B_{ml} \times 10^{-3}$, K	Small $A_{ml} \times 10^2$, K	Large $B_{ml} \times 10^{-3}$, K	Data Reference
Structure I hydrates						
Argon	274.30 -296.71	33.645	2.558	3.515	2.016	(D. R. Marshall et al., 1964)
Ethane	273.7-286.5	0	0	0.200	4.010	(Deaton & Frost, 1946)
Oxygen	273.8-284.55	17.500	2.109	4.548	2.066	(van Cleeff & Diepen, 1960)
Ethyne	273.2-285.5	3.010	4.790	0.030	3.680	(Tumba et al., 2013)
Carbon dioxide	274.3-282.9	1.200	2.860	0.900	3.280	(Adisasmito et al., 1991)

The reference chemical potential and enthalpy difference values for structure I are first evaluated. There are five values of these references given in Table 2-4. The combination of these values is classified in sets as given in Table 6-2.

Table 6-2: Structure 1 Reference energy values sets

Sets	$\Delta\mu_w^0$ (J/mol)	Δh_w^0 (J/mol)	**Reference**
Set 1	1235±10	-4327	(Holder et al., 1980; Ng & Robinson, 1985)
Set 2	1297	-4622	(Dharmawardhana et al., 1980)
Set 3	1264	-4860	(Parrish & Prausnitz, 1972)
Set 4	1299.5±10	-4150	(Holder et al., 1984)
Set 5	1287	-5080	(Handa & Tse, 1986)

Each of the sets in Table 6-2 is tested in parallel with either one of the heat capacity difference and β values given in Table 2-4 to predict the pressure dissociation of structure I systems with single gas hydrates. Table 6-3 shows the dissociation pressure deviation relative to experimental values for all sets given in Table 6-2. The heat capacity difference and β values considered here are -38.13 J / mol.K and 0.141 J/mol.K^2; respectively. The overall AADP (%) values are calculated using the weighted average formula.

Table 6-3: Comparison of Structure 1 AADP (%) values for the selection of reference chemical potential difference and enthalpy difference values

Hydrate formers	Exp. Points	AADP (%)				
		Set 1	Set 2	Set 3	Set 4	Set 5
Methane	17	18.005	2.708	5.720	2.905	3.710
Ethane	20	22.738	1.334	8.905	3.350	2.492
Carbon dioxide	9	24.914	1.849	12.334	4.959	1.798
Argon	11	27.715	1.462	9.436	8.675	7.005
Oxygen	21	22.361	1.839	9.647	3.865	1.359
Ethene	11	27.462	2.529	11.825	8.378	3.648
Ethyne	8	20.046	0.651	8.496	3.180	2.088
Nitrogen.	21	18.539	2.912	7.293	3.896	1.534
Hydrogen Sulfide	8	22.751	3.784	8.104	10.154	2.262
Overall	**126**	**22.169**	**2.131**	**8.800**	**4.907**	**2.713**

By analyzing the AADP (%) values for different sets for structure I gas hydrates, set 2 gives the lowest AADP (%) at consistent basis. The overall AADP (%) value for set 2 is 2.131% that directs towards the accurate prediction of single gas hydrate equilibrium. Therefore, the selected values of $\Delta\mu_w^o$ and Δh_w^o for structure I are 1297 J/mol and -4622 J/mol; respectively.

Next step is to conduct the same analysis for the selection of reference chemical potential difference and enthalpy difference value for structure II. There are three values given for structure II gas hydrates for chemical potential difference and enthalpy difference given in Table 2-4. The intent was to conduct the similar AADP (%) analysis for structure II reference chemical potential difference and enthalpy difference values. However, due to highly overestimated prediction of structure II gas hydrates by the values of Dharmawardhena et al. (1980) and Handa & Tse (1986), the only choice of Parish and Prausnitz values were left. The overall AADP (%) for the prediction of structure II gas hydrates through Parish & Prausnitz values is 1.5421 %. Moreover, Parish and Prausnitz concerned values are also employed by different studies in the prediction of gas hydrates (Barkan & Sheinin, 1993; Englezos et al., 1991; Li, Wu, & Englezos, 2006). As a consequence, the selected reference chemical potential difference and enthalpy difference values for structure II gas hydrates are 883 J/mol.K and -5203.5 J/mol.K^2; respectively.

Table 6-4: Structure II AADP (%) values for the selection of reference chemical potential difference and enthalpy difference values

Hydrate formers	**Exp. Points**	**Parish & Prausnitz AADP (%)**
Propane	10	0.9594
Isobutane	9	1.2328
Nitrogen	21	1.9522
Overall	40	**1.5421**

The selection of optimum heat capacity difference and β values are also explored for both structure I and II. Incipient conditions of each of the considered single gas hydrates are predicted using the heat capacity difference and β values provided in Table 6-5. The set with the lowest AADP (%) value is selected. An overall comparison is conducted for both structures I and II to decide the optimum heat capacity difference and β values.

Table 6-5: Structure I and II heat capacity difference and β values

Structure	**Sets**	ΔCp_w^o $(J/mol.K)$	β $(J/mol.K^2)$	**Data Reference**
I, II	Set A	-38.13	0.141	(Parrish & Prausnitz, 1972)
I	Set B	-34.583	0.189	(V. T. John et al., 1985)
II		-36.8607	0.1809	

Table 6-6 shows the comparison between both sets based on the prediction of dissociation pressure of gas hydrate systems. From the AADP values, it is apparent that Set A is slightly better than Set B. As a result, the selected values of heat capacity difference and β for both the structures I and II are -38.13 J/mol.K and 0.141 J/mol.K^2; respectively.

Table 6-6: Comparison of AADP (%) values of all considered single gas hydrate systems,for the selection of heat capacity difference and β values

Hydrate formers	Structure	Exp. Points	AADP (%)	
			Set A	Set B
Methane	I	17	2.7078	2.5436
Ethane	I	20	1.3341	1.2618
Carbon dioxide	I	9	1.8494	1.9700
Argon	I	11	1.4617	1.6851
Oxygen	I	21	1.8386	1.8862
Ethene	I	11	2.5294	2.9390
Ethyne	I	8	0.6515	0.6936
Nitrogen (SI)	I	21	2.9116	2.9437
Hydrogen Sulfide	I	8	3.7840	4.3712
Nitrogen (SII)	II	21	2.9116	2.9437
Propane	II	10	0.9594	0.9611
Isobutane	II	9	1.2328	1.2330
Overall	**-**	**166**	**1.9891**	**2.0451**

6.4 Single Gas Hydrates

This section uses the selected Langmuir constant parameters and reference thermodynamic properties in the preceding sections to predict the single gas hydrates equilibrium. Moreover, determination of gas hydrate structure of each considered hydrate former is reported. Eleven single hydrate systems are studied in this work. The systems are natural gas hydrate formers including methane, ethane, propane, isobutane, carbon dioxide and nitrogen. Moreover, single hydrate systems such as ethene and ethyne are considered for their application in petrochemical industries. Other single hydrate systems studied in this work include oxygen and argon. The predicted incipient pressure of considered gas hydrates is compared with the experimental data to evaluate the prediction capability of vdWP model with SAFT-VR Mie.

As discussed in Chapter 4, adequate and effective phase equilibrium calculations contribute to improvement in prediction of gas hydrate equilibrium. The binary interaction parameters (k_{ij}) of hydrate former-water system are therefore taken into account in the equilibrium calculations of H-V-L mixtures.

The VLE data for some systems such as water-isobutane, water-oxygen and water-ethyne are not found in the literature. The k_{ij} values for isobutane hydrate are thus adjusted with the gas hydrate equilibrium data. For ethyne and oxygen hydrates, the vdWP with SAFT-VR Mie gives quantitative prediction with k_{ij} equal to zero.

6.4.1 Single Gas Hydrate Equilibrium Curves

The first studied gas hydrate system is water-methane. As per the literature (Carroll, 2009; Sloan & Koh, 2008), methane forms structure I. It is found that the prediction of dissociation pressures using the vdWP with SAFT-VR Mie models compares very well with experimental data as shown in Figure 6.1. For the range from 274.25 to 285.78 K, the AADP for this system is 2.7078% as shown in Table 6-7.

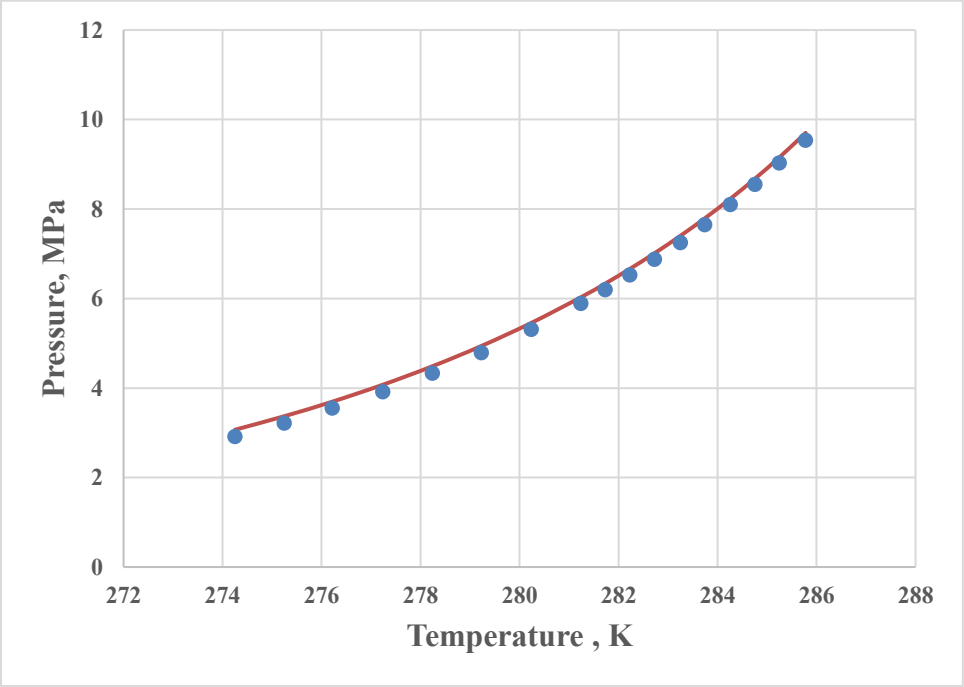

Figure 6.1: Incipient conditions prediction of Methane hydrate for temperatures 274.25-285.78 K. The solid line is the correlation of the vdWP model. The points represent experimental gas hydrate equilibrium data (Nakamura et al., 2003).

Another common system of gas hydrates is water-ethane. Ethane has a larger diameter compared to methane, hence they can enter only large cavities of structure I (Carroll, 2009; Sloan & Koh, 2008). Due to this reason, the Langmuir constant parameters for small cavities are taken zero, as given in Table 6-1. Excellent prediction of L_w-H-V equilibrium of ethane is seen in Figure 6.2 for temperatures ranging from 273.7-

286.5 K. The AADP (%) is 1.334% as given in Table 6-7, which confirms the remarkable accuracy the vdWP and SAFT-VR Mie model.

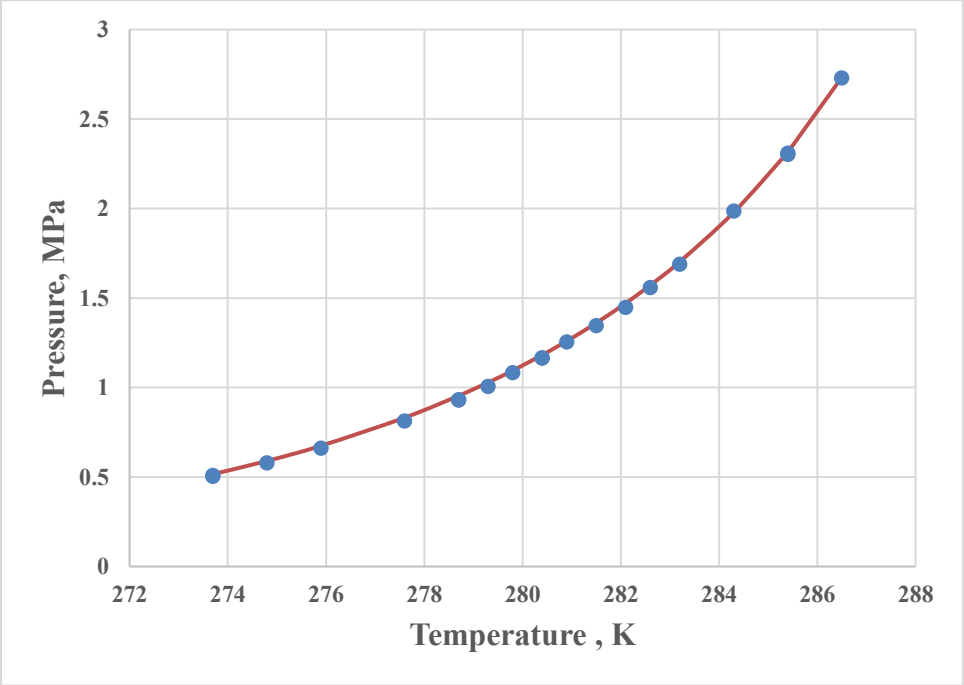

Figure 6.2: Incipient conditions prediction of Ethane hydrate for temperatures 273.7-286.5 K. The solid line is the correlation of the vdWP model.The points represent experimental gas hydrate equilibrium data (Deaton & Frost, 1946).

Propane and isobutane are other higher gaseous alkanes that form gas hydrates. Due to their large sizes, they cannot form structure I. However, they occupy only the large cavities of structure II, as can be seen in Table 2-3 where all values of Langmuir constant parameters are zero except the large cavities of structure II. Figures 6.3 & 6.4 illustrate the precise incipient conditions curves of propane and isobutane. The temperature range for propane hydrate is from 273.2-278 K, whereas for isobutane hydrate is from 273.2-275.1 K. The adjusted k_{ij} values across the aforementioned isobutane hydrate experimental data temperature range are 0.0073 for vapor phase and -

0.2474 for liquid phase. The AADP (%) values for propane and isobutane hydrates are less than 2% as provided in Table 6-7.

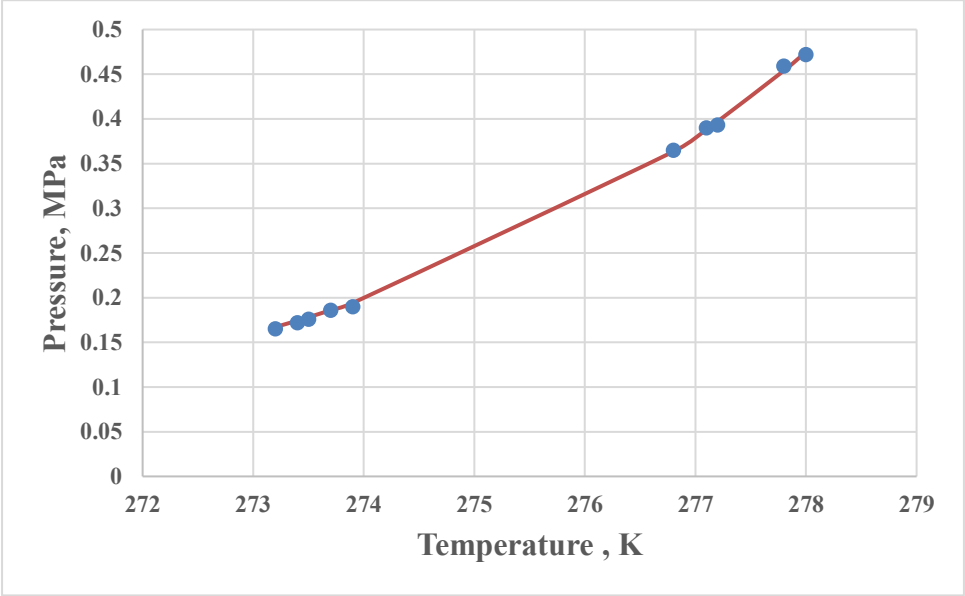

Figure 6.3: Incipient conditions prediction of Propane hydrate for temperatures 273.2-278 K. The solid line is the correlation of the vdWP model.The points represent experimental gas hydrate equilibrium data (B. Miller & Strong, 1946).

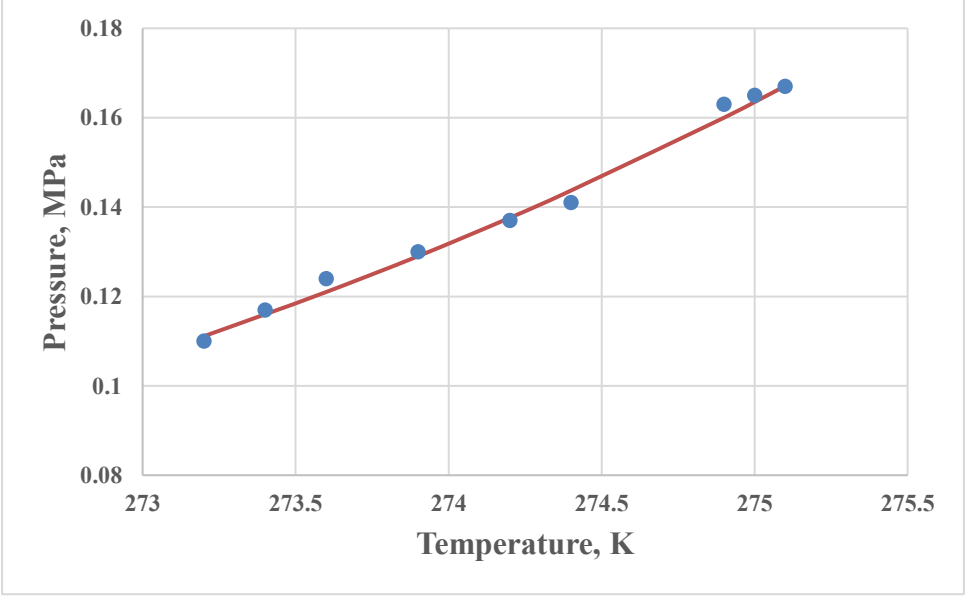

Figure 6.4: Incipient conditions prediction of Isobutane hydrate for temperatures 273.2-275.1 K. The solid line is the correlation of the vdWP model. The points represent experimental gas hydrate equilibrium data (Schneider & Farrar, 1968)

Carbon dioxide hydrates are considered as potential and cheaper methods for carbon dioxide capturing (Castellani, Filipponi, Nicolini, Cotana, & Rossi, 2013). Hydrate technology, apart from gas separation, is also being used for the storage of carbon dioxide capture under sea floors or in old petroleum wells as well (Klauda & Sandler, 2000). These applications primarily require an accurate gas hydrate equilibrium curve of carbon dioxide. Figure 6.5 illustrates a remarkable prediction of incipient conditions of carbon dioxide gas hydrates using SAFT VR Mie-Novel LJ EOS and vdWP model. The temperature range for gas hydrate equilibrium prediction is 274.3-282.9 K. Figure 6.5 shows very accurate prediction at low temperatures due to low solubility of carbon dioxide in the hydrate formation zone (Servio & Englezos, 2001). On the other hand, a slight deviation at higher temperatures above 280 K is noted as compared with the experimental data. This is because at higher temperatures in the presence of hydrates, solubility of carbon dioxide in water increases, in turn effecting the water activity. However, looking at the AADP (%) of 1.8494%, the overall prediction of L_w-H-V equilibrium of carbon dioxide is extraordinary.

Ethene is another gaseous component that form hydrates at low temperatures and high pressures. Ethene forms structure I gas hydrates (Sloan & Koh, 2008; Tumba et al., 2013). Figure 6.6 represents quantitative prediction of ethene hydrate equilibrium diagram for structure I, with a temperature range from 273.3-289.6 K. The AADP for ethane hydrate is 2.529%, which points toward the adequate behavior of SAFT VR Mie-Novel LJ EOS and vdWP model.

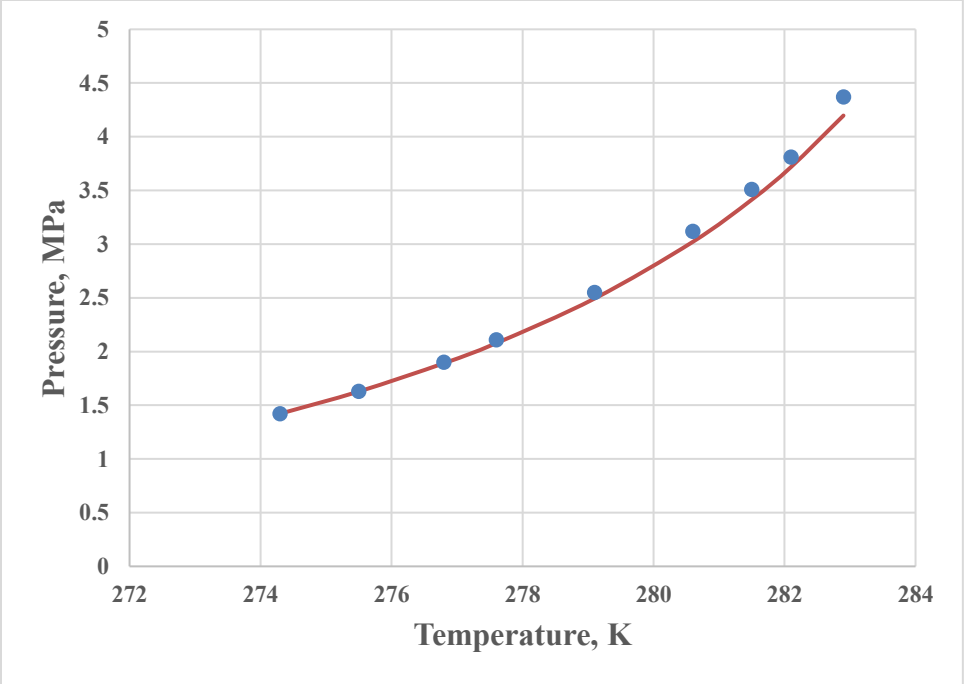

Figure 6.5: Incipient conditions prediction of CO_2 hydrate for temperatures 274.3-282.9 K. The solid line is the correlation of the vdWP model.The points represent experimental gas hydrate equilibrium data (Adisasmito et al., 1991).

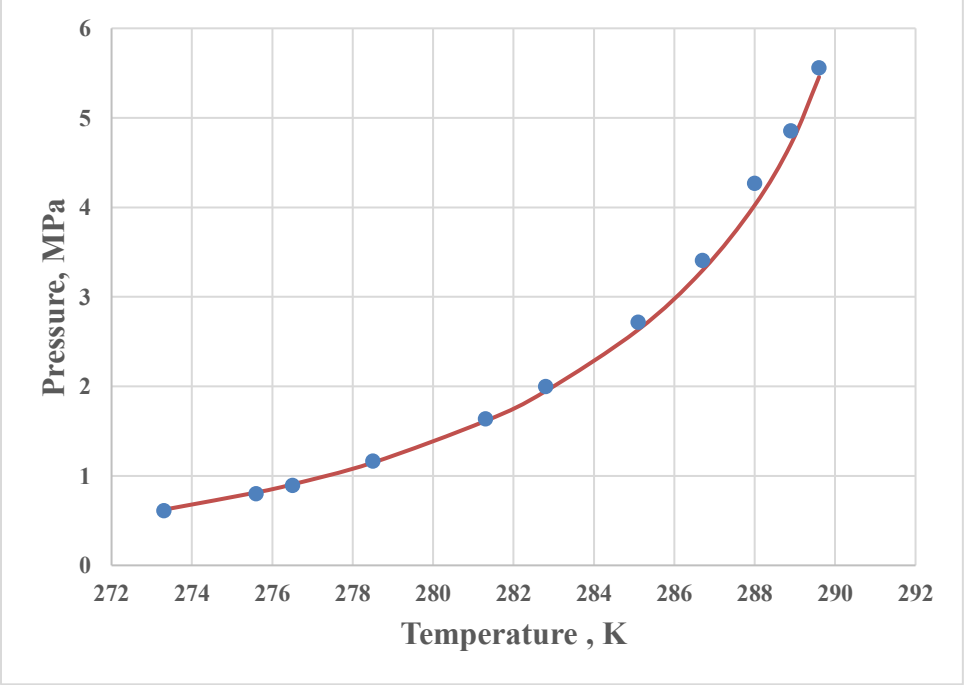

Figure 6.6 Incipient conditions prediction of Ethene hydrate for temperatures 273.3-289.6 K. The solid line is the correlation of the vdWP model.The points represent experimental gas hydrate equilibrium data (Tumba et al., 2013).

Ethyne gas hydrate system is also studied in this work. Unlike previous systems, the Langmuir constant parameters of ethyne were not available in the literature. Therefore, these parameters are optimized in this thesis with the combination of ethyne hydrate experimental data given in Table 6-1. After the determination the Langmuir constant parameters, ethyne hydrate incipient conditions are predicted as illustrated in Figure 6.7. This excellent prediction of incipient pressures is achieved using structure I hydrate parameters for temperatures ranging from 273.2 to 285.5 K. A small AADP (%) value of 0.6515% provided in Table 6-7, endorses the high level of accuracy of prediction of the SAFT VR Mie-Novel LJ EOS and vdWP model as illustrated in Figure 6.7.

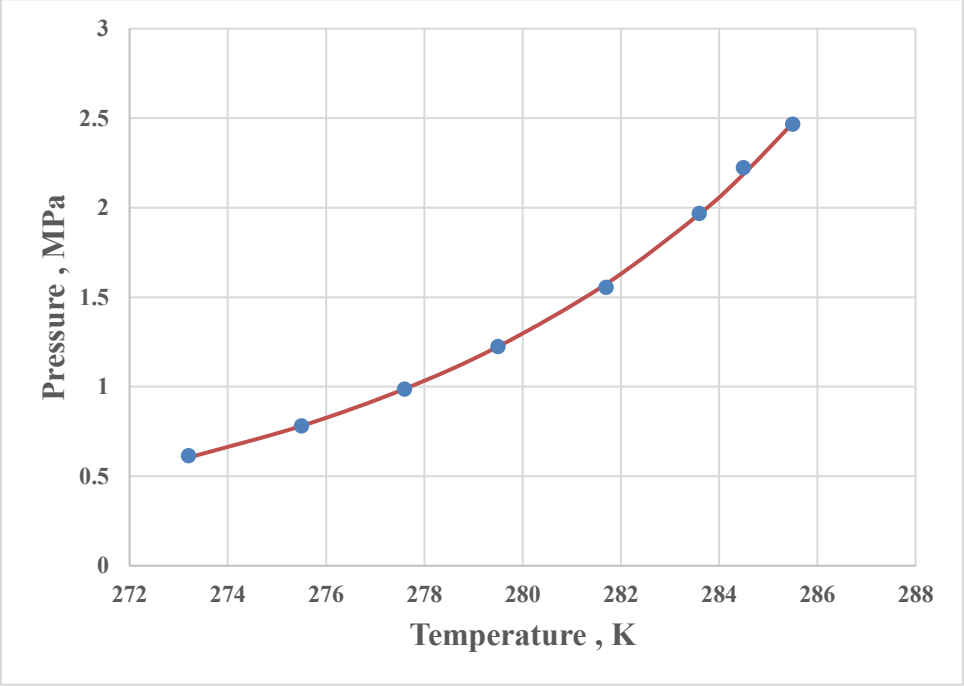

Figure 6.7: Incipient conditions prediction of Ethyne hydrate for temperatures 273.2-285.5 K. The solid line is the correlation of the vdWP model. The points represent experimental gas hydrate equilibrium data (Tumba et al., 2013).

Argon is a noble gas that is supposed to form Structure II hydrates as per the crystallographic studies of Davidson et al. (1984a). However, these crystallographic

studies were carried out at low temperature of 100 K. When the gas hydrate equilibrium calculations of argon were carried out in this thesis at temperatures above ice point, structure I hydrates were formed. This is supported by the literature studies by Parish and Prausnitz (1972) and Holder et al. (1980). Figure 6.8 is the remarkable estimation of dissociation conditions of argon gas hydrates from 278.32-298.76 K. The AADP (%) for the predicted argon gas hydrate equilibrium is 1.4617%, which is given in Table 6-7.

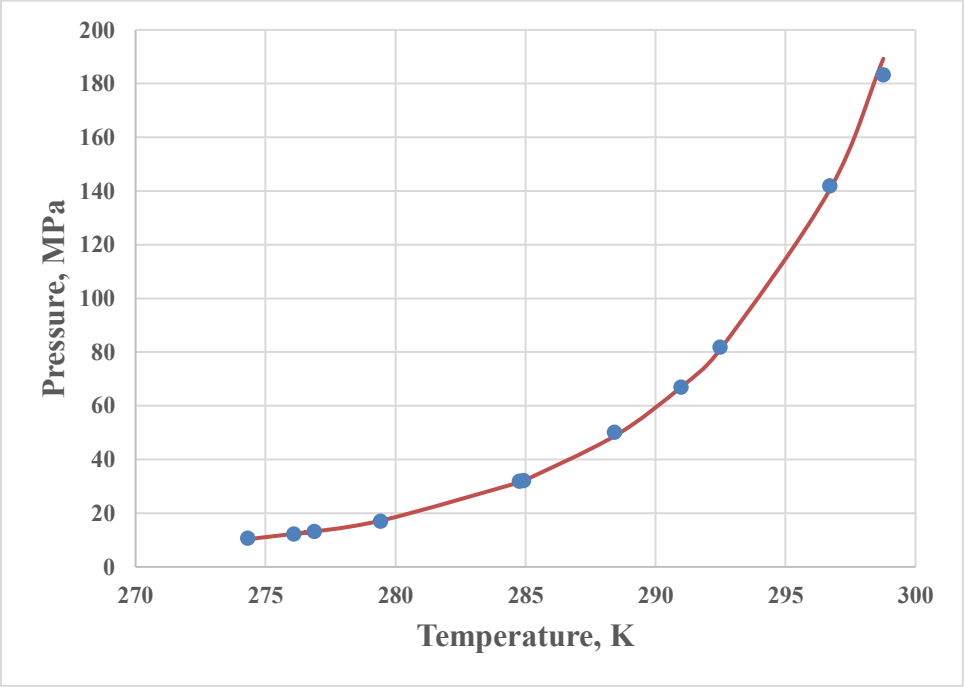

Figure 6.8: Incipient conditions prediction of Argon hydrate for temperatures 278.32-298.76 K. The solid line is the correlation of the vdWP model. The points represent experimental gas hydrate equilibrium data (D. R. Marshall et al., 1964).

Oxygen hydrates are also said to form structure II hydrates as per crystallographic studies (Davidson et al., 1981; J.S. Tse C.I. Ratcliffe & Powell, 1986). However, these studies are carried at very low temperatures below ice point. On the other hand, while predicting the oxygen hydrate structure at temperatures above ice point, we find that oxygen forms structure I. This result is also supported by Parish and Prausnitz (1972) and

Mohammadi et al. (2003) studies. Using structure I hydrate parameters, the oxygen gas hydrate equilibrium curve is quantitatively predicted by the SAFT VR Mie-Novel LJ EOS and vdWP model as shown in Figure 6.9 from 273.15-284.15 K. Table 6-7 contains the AADP (%) of oxygen hydrate that is 1.8386%.

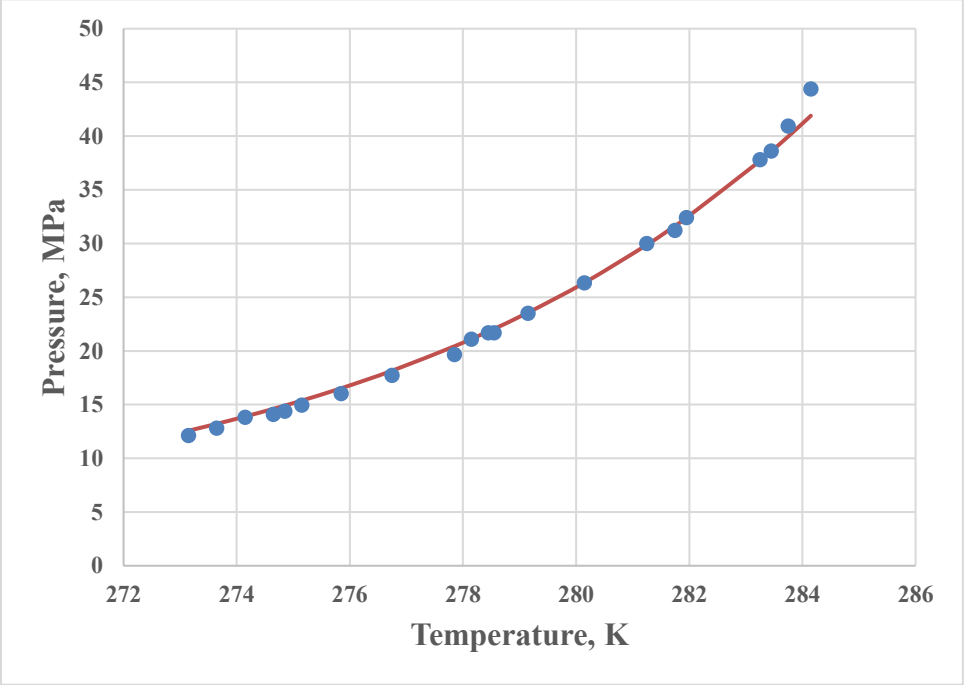

Figure 6.9: Incipient conditions prediction of Oxygen hydrate for temperatures 273.15-284.15 K. The solid line is the correlation of the vdWP model.The points represent experimental gas hydrate equilibrium data (van Cleeff & Diepen, 1965).

H_2S has a high tendency of hydrate formation (Noaker & Katz, 1954), which makes it an important single hydrate system to study. H_2S hydrate is commonly known to form structure I hydrate (Carroll, 2009; Antonin Chapoy, Mohammadi, Tohidi, Valtz, & Richon, 2005; Sloan & Koh, 2008). Figure 6.10 predicts the incipient conditions of H_2S hydrates for a temperature range of 277.6- 299.8 K, with a hydrate structure of type I. There is a slight deviation noted at higher temperatures above 291.8 K, as compared to

experimental data. The AADP (%) of 3.7840% for the prediction of H_2S hydrate equilibrium, portrays the remarkable prediction of vdWP model.

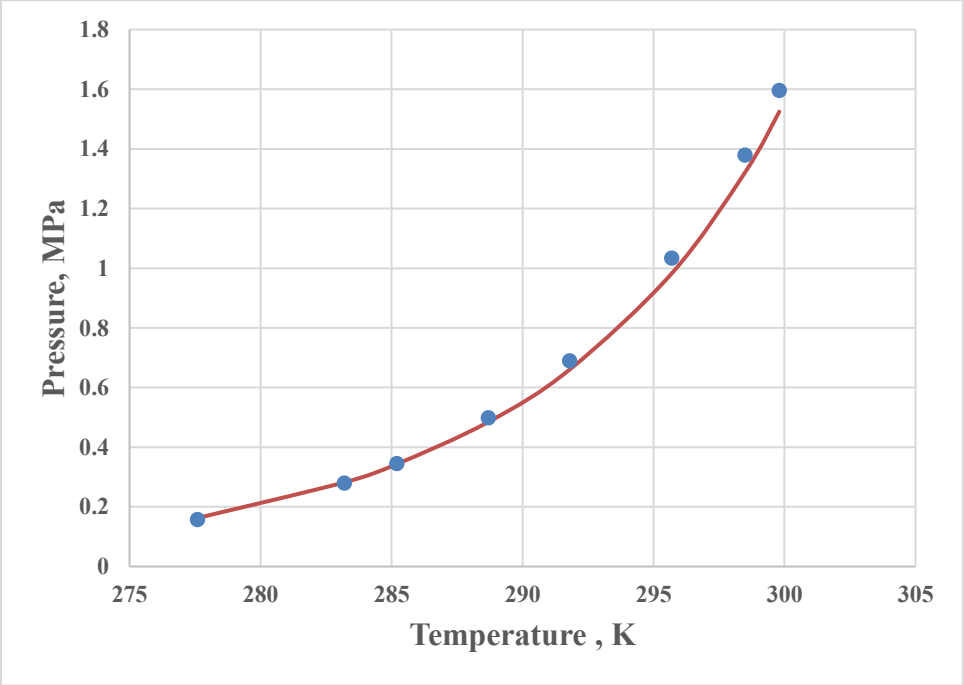

Figure 6.10: Incipient conditions prediction of H_2S hydrate for temperatures 277.6- 299.8 K. The solid line is the correlation of the vdWP model. The points represent experimental gas hydrate equilibrium data (Selleck et al., 1952).

6.4.1.1 Nitrogen gas hydrate structures

Nitrogen gas hydrate system is given special attention compared to the previous systems due to the uncertainty of its structure type. There is a debate on the hydrate structure of nitrogen hydrate. Davidson et al. (1984a) crystallographic studies at 100 K reported that nitrogen forms structure II hydrates. Another study conducted by Hendriks et al. (1996) who reported that a transition at 134 K occurs from structure II to structure I on the ice-hydrate-vapor line. Sughara et al. (2002) through Raman spectroscopy technique determined that nitrogen hydrate forms structure II at temperatures ranging from 285-305 K. Saito et al. (1964), Mohammadi et al. (2003), Hendriks et al. (1996) and

Tohidi-Kalorazi (1995) have suggested that nitrogen forms structure I hydrate for L_w-H-V equilibrium.

In this work, we test our approach not only for predicting the incipient conditions but also for predicting the types of the structures. Figures 6.11 (a) & (b) depict the incipient condition prediction of nitrogen hydrate for structure I and II; respectively. The AADP (%) values for both the structures are provided in Table 6-7 that are 2.912% for structure I and 1.9522% for structure II. These small AADP (%) values suggest remarkable prediction of nitrogen gas hydrate equilibrium for both structures.

This work takes into account the stability analysis of the two structures of nitrogen to find out which structure is more stable at L_w-H-V conditions. For this purpose, Gibb's free energy for both structures (I & II) are determined and plotted against temperature in Figure 6.12. From temperatures 273.2 to 278.6 K, it is found that structure I is more stable as per the minimum Gibb's free energy criterion. On the other hand, a transition is observed from temperatures above 278.6 K, which suggests that structure II is more stable at higher temperatures. This observation regarding the structure II stability is confirmed by Sughara et al. (2002) study as well. Hence, based on stability criteria, the formation of nitrogen hydrate structures depends on temperature.

(a)

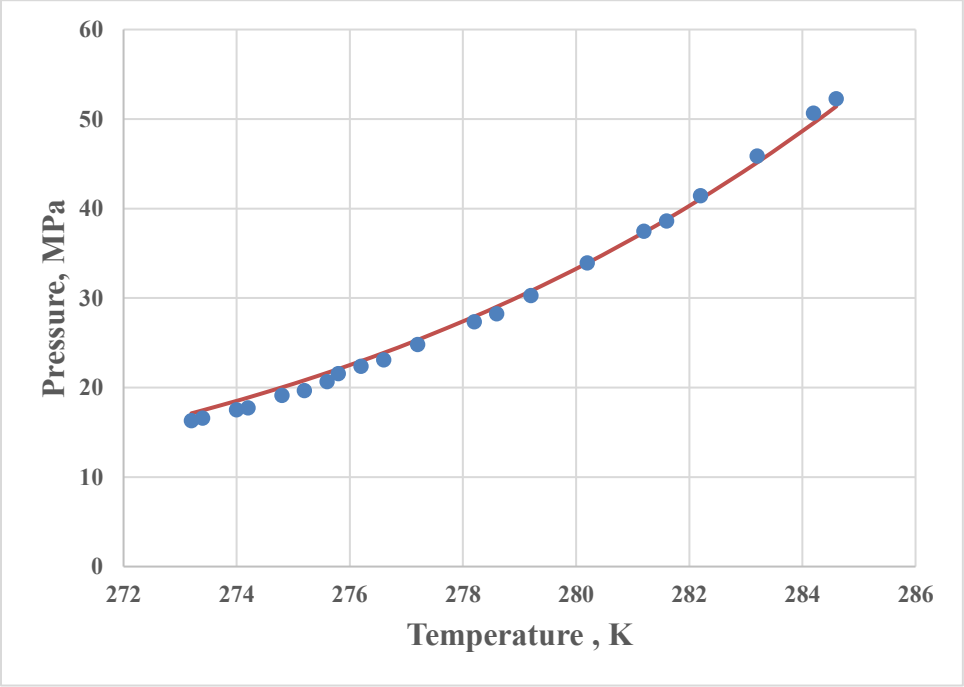

(b)

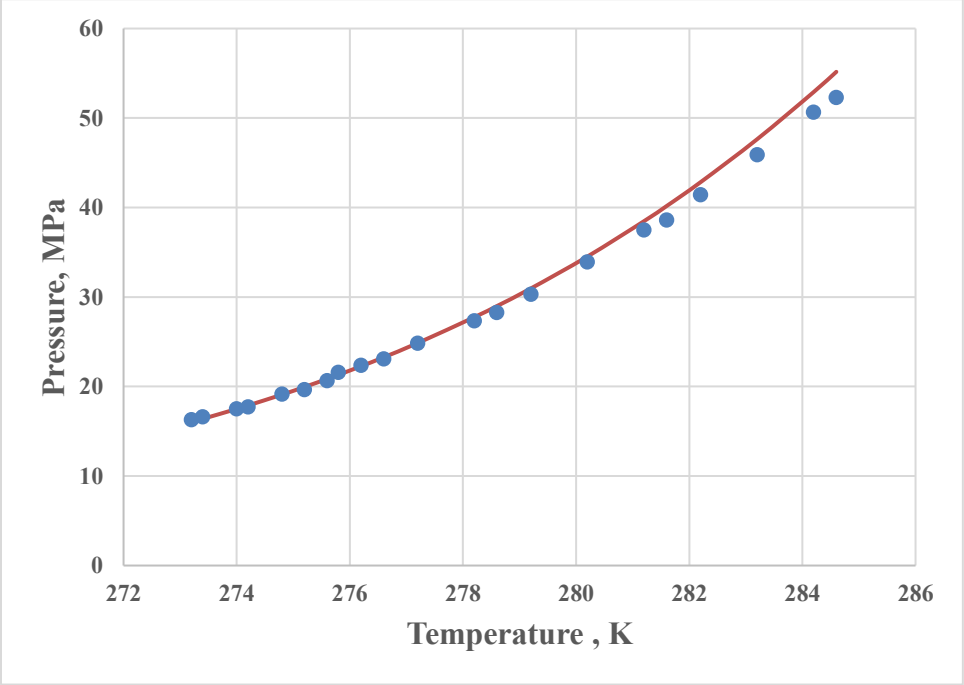

Figure 6.11: Incipient conditions prediction of Nitrogen hydrate for temperatures 273.2-284.6 K for (a) Structure I (b) Structure II. The solid line is the correlation of the vdWP model.The points represent experimental gas hydrate equilibrium data (van Cleeff & Diepen, 1960).

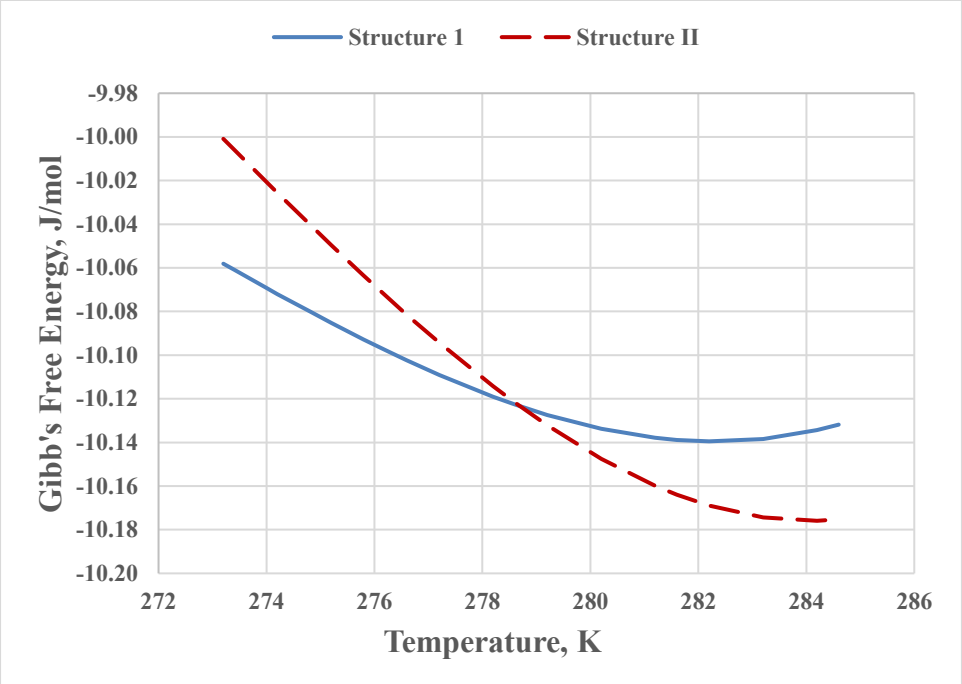

Figure 6.12: Stability assessment of Nitrogen hydrate structures

To sum up, Table 6-7 provides a complete summary of the results of dissociation pressures of the single gas hydrates. The AADP (%) is less than 4 % for each studied system. The overall AADP (%) value of 1.9891% highlights the excellent prediction of the SAFT VR Mie-Novel LJ EOS and vdWP model in this work.

Table 6-7: Gas hydrate equilibrium results summary for single hydrate systems

Gas hydrate	Temperature Range (K)	Exp. Points	Structure	AADP%	Data Reference
Methane	274.25-285.78	17	I	2.7078	(Nakamura et al., 2003)
Ethane	273.7-286.5	20	I	1.3340	(Deaton & Frost, 1946)
Propane	273.2-278	10	II	0.9594	(B. Miller & Strong, 1946)
Isobutane	273.2-275.1	9	II	1.2330	(Schneider & Farrar, 1968)
Carbon Dioxide	274.3-282.9	9	I	1.8494	(Adisasmito et al., 1991)
Ethene	273.3-289.6	11	I	2.5290	(Tumba et al., 2013)
Ethyne	273.2-285.5	8	I	0.6515	(Tumba et al., 2013)
Oxygen	273.15-284.15	21	I	1.8386	(van Cleeff & Diepen, 1965)
Argon	278.32-298.76	11	I	1.4617	(D. R. Marshall et al., 1964)
Hydrogen Sulfide	277.6- 299.8	8	I	3.7840	(Selleck et al., 1952)
Nitrogen	273.2-284.6	21	I / II	2.9120/1.9522	(van Cleeff & Diepen, 1960)
Overall	**-**	**166**	**-**	**1.9891**	**-**

6.5 Mixed Gas Hydrates

The excellent prediction of the incipient conditions of single gas hydrates motivated us to test the combination of SAFT-VR Mie-Novel LJ EOS and vdWP model for mixed gas hydrates systems. Mixed gas hydrates are further classified into binary gas hydrate and multicomponent gas hydrate systems.

The mixed gas hydrate systems are highly dependent on the feed gas composition. A slight change in gas composition can result in a change of gas hydrate equilibrium conditions as well as the type of hydrate structure. The feed composition is reported for the studied mixed gas hydrate systems.

6.5.1 Binary Gas Hydrate Systems

A total number of 10 binary gas hydrate systems are studied. The systems are given in Table 6-8.

The first binary gas hydrate system studied is methane-ethane system. Both are major components of natural gas, with methane composition vary from 55-99% and ethane composition up to 10 % (Zhdanov et al., 2010). The feed mixture considered in this work contains about 94.6% methane and 5.4% ethane content. Figure 6.13 illustrates excellent prediction of dissociation pressure of methane-ethane mixture for temperatures 284.9-299.1 K. Structure I provides better prediction and more stability for the methane-ethane mixture. The AADP (%) is 2.4501% and given in Table 6-8.

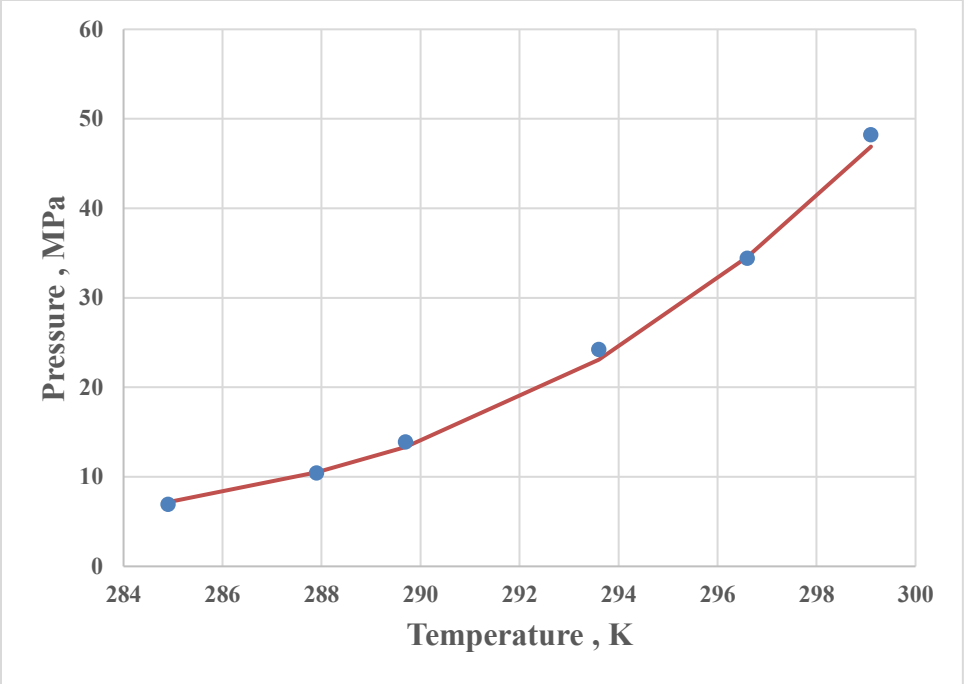

Figure 6.13: Incipient conditions prediction of Methane (94.6%) – Ethane (5.4%) mixed hydrate for temperatures 284.9- 299.1 K. The solid line is the correlation of the vdWP model.The points represent experimental gas hydrate equilibrium data (McLeod Jr. & Campbell, 1961).

The second binary gas hydrate system studied is methane-propane. This system is very important due to the existence of propane in natural gas mixture. The methane-propane mixture studied in this work contains 71.2% methane and 28.8% propane. The gas hydrae equilibrium diagram of methane-propane mixtures at temperatures varying from 274.8-283.2 K, is depicted in Figure 6.14. The accuracy of methane-propane hydrate equilibrium prediction is quite remarkable with an AADP (%) of 0.9856%. This mixture forms structure II, which was confirmed by the fact that even the slightest addition of propane content with methane results in structure II (Zhdanov et al., 2010).

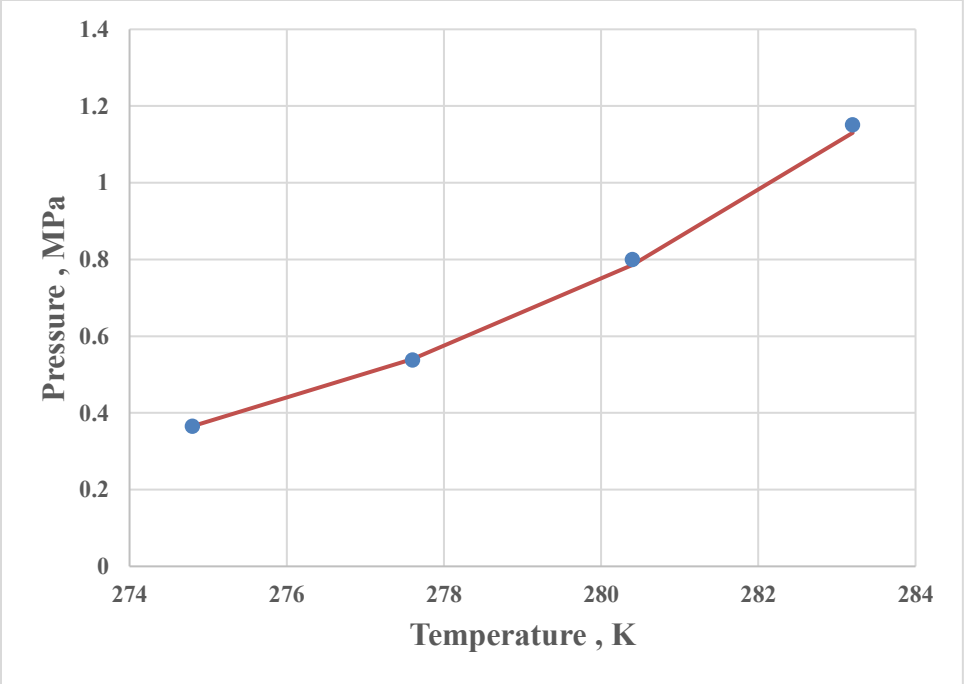

Figure 6.14: Incipient conditions prediction of Methane (71.2%) – Propane (28.8%) mixed hydrate for temperatures 274.8-283.2 K. The solid line is the correlation of the vdWP model.The points represent experimental gas hydrate equilibrium data (Deaton & Frost, 1946).

Methane-isobutane hydrate mixture is another mixture that has found application not only in natural gas environments but also in the LPG production pipelines. Wu et al. (1976), who considered the possibility of hydrate formation in LPG production pipelines, reported the experimental hydrate data for methane-isobutane mixtures. This work compares the SAFT VR Mie-Novel LJ EOS with one of the mixtures reported by Wu et al. (1976). The considered mixture contains 36.4% methane and 63.6% isobutane for a temperature range of 273.8 to 276.9 K. The result of dissociation pressure is shown in Figure 6.15. The AADP (%) for methane-isobutane mixture provided in Table 6-8 is 1.6503%. This small pressure deviation shows the precise prediction of our model in predicting the gas hydrate equilibrium of methane-isobutane mixture.

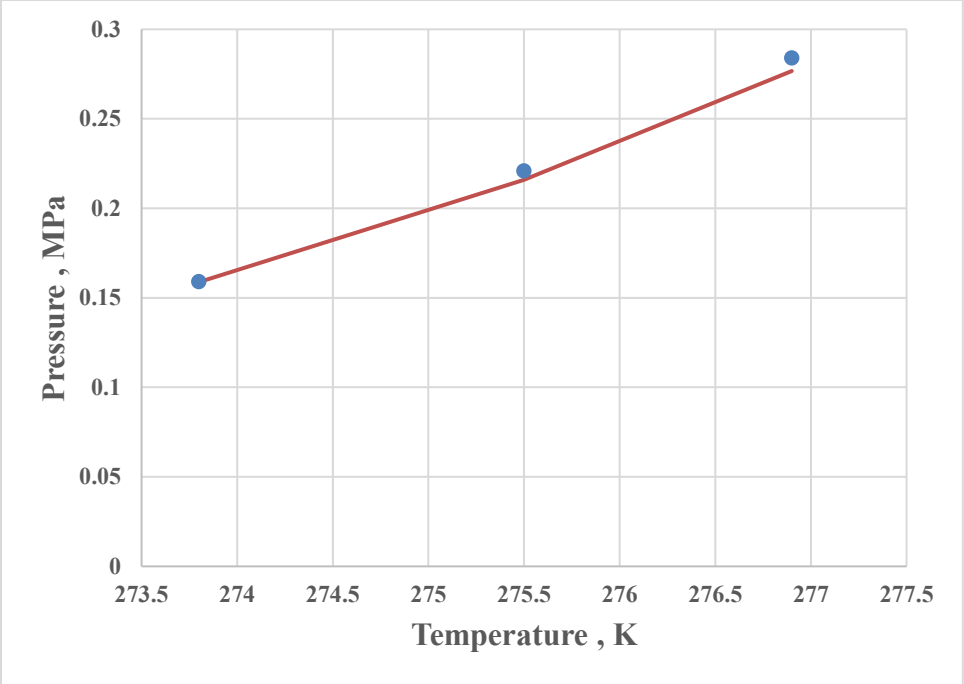

Figure 6.15: Incipient conditions prediction of Methane (36.4%) – Isobutane (63.6%) mixed hydrate for temperatures 273.8-276.9 K. The solid line is the correlation of the vdWP model.The points represent experimental gas hydrate equilibrium data (Wu et al., 1976).

Next gas hydrate mixture studied is ethane-propane mixture, which is very important mixture in LPG production lines. The studied mixture includes 28% ethane content and 72% propane. An accurate prediction of gas hydrate equilibrium of SAFT VR Mie-Novel LJ EOS is shown in Figure 6.16 for a temperature range of 276.5-277.9 K. The AADP (%) is 1.7387%. Our calculation suggests that ethane-propane mixture forms structure II. Our results are in alignment with the work of Holder et al. (1982).

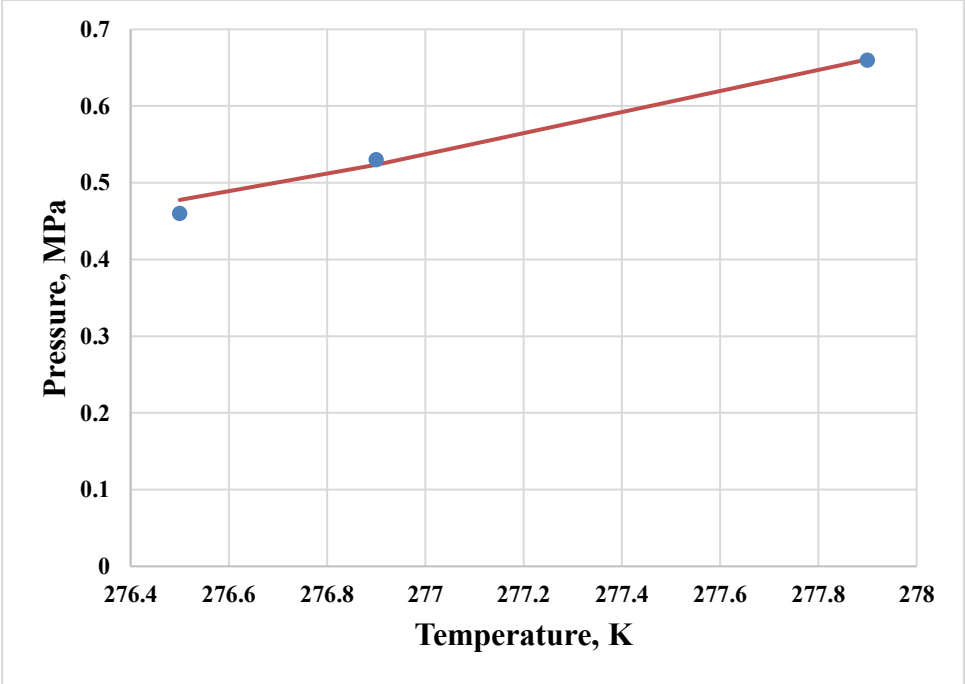

Figure 6.16: Incipient conditions prediction of Ethane (28%) –Propane (72%) mixed hydrate for temperatures 276.5-277.9 K. The solid line is the correlation of the vdWP model. The points represent experimental gas hydrate equilibrium data (Holder & Hand, 1982).

Carbon dioxide and nitrogen usually act as unwanted contents when they coexist with alkanes as mixtures. The reason for this is that most of the alkanes are used as fuels. Efficient fuels must have high calorific value. Carbon dioxide and nitrogen lower the calorific value of alkanes. The gas hydrate technology may be helpful in gas separation application to remove the unwanted content. Apart from this, a mixture of carbon dioxide and nitrogen is injected in insitu methane hydrates, to enhance methane recovery form these deposits (Sapate, 2015). Methane-CO_2 hydrate mixture is studied with a feed composition of 92% for methane. The predicted dissociation pressure at temperatures 277.8-285.1 K is seen in Figure 6.17. The SAFT VR Mie-Novel LJ EOS and vdWP model results compare very well with the experimental data with AADP of 2.17 %. The results of methane-CO_2 hydrate mixture are obtained using structure I parameters.

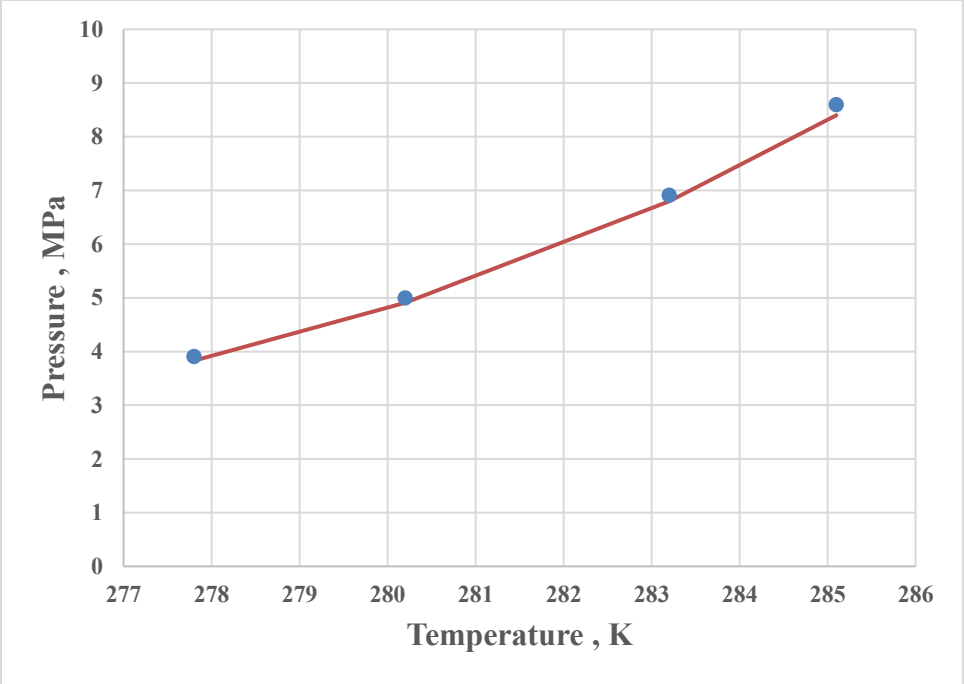

Figure 6.17: Incipient conditions prediction of Methane (92%) – CO_2(8%) mixed hydrate for temperatures 277.8-285.1 K. The solid line is the correlation of the vdWP model. The points represent experimental gas hydrate equilibrium data (Adisasmito et al., 1991).

The gas hydrate mixtures containing nitrogen are a bit complex, as their predicted hydrate equilibrium is acceptable for both structure I and II. As shown in Section 6.4.1.1 for water-nitrogen gas hydrate system, there is a debate over hydrate structure transitions of nitrogen based hydrate mixtures at different temperature ranges. In this work, we use the stability analysis based on Gibb's free energy minimum criteria to determine the hydrate structure type.

The first nitrogen based hydrate mixture considered is that of Methane-N_2. The gas feed mixture contains 89.26% methane and 10.74% nitrogen. Figures 6.18 (a) & (b) demonstrate the prediction of dissociation pressure using both structure I and II at temperatures 273.7-285.3 K. The AADP (%) values for structures I and II are 2.9105% and 3.2924%; respectively. These AADP (%) values show excellent experimental

prediction for both structures. Amadieu et al. (1997) reported that either structure I or II might form for this mixture depending upon gas composition, pressure and temperature of the system. Therefore, stability analysis is carried out for this mixture to find which structure is more stable at the above indicated temperature range. Figure 6.19 illustrates the trend of the Gibbs free energy as a function of temperature. The Gibbs free energy of structure I has lower values as compared to that of structure II. As a result, structure I hydrate will be more thermodynamically stable for methane-N_2 mixture at above indicated temperature range.

(a)

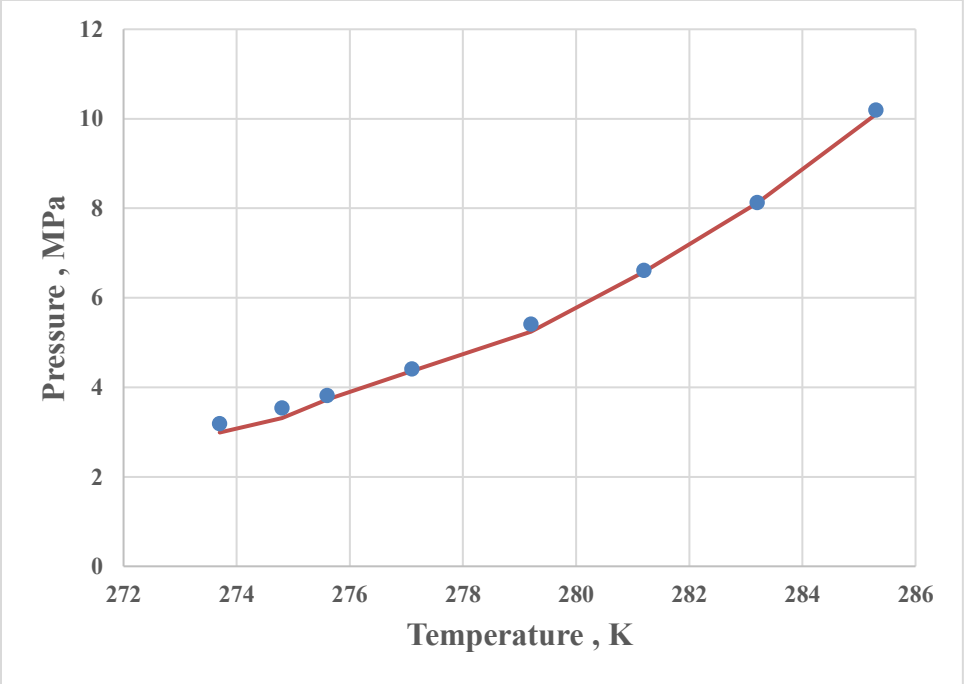

(b)

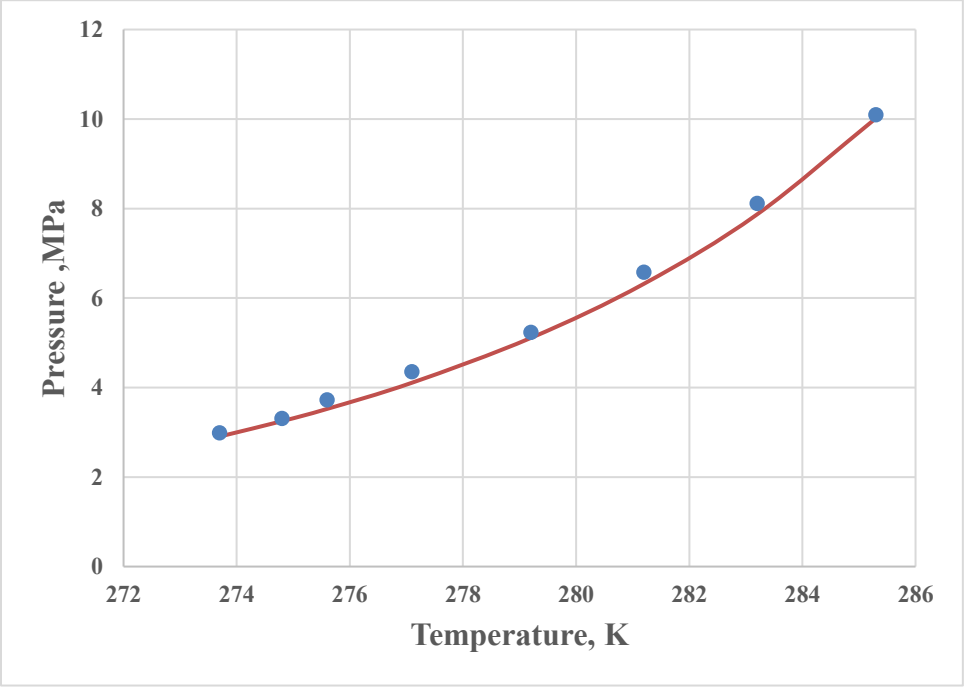

Figure 6.18: Incipient conditions prediction of Methane (89.26%) – N_2 (10.74%) mixed hydrate at temperatures 273.7-285.3 K for (a) Structure I (b) Structure II. The solid line is the correlation of the vdWP model. The points represent experimental gas hydrate equilibrium data (Mei et al., 1996).

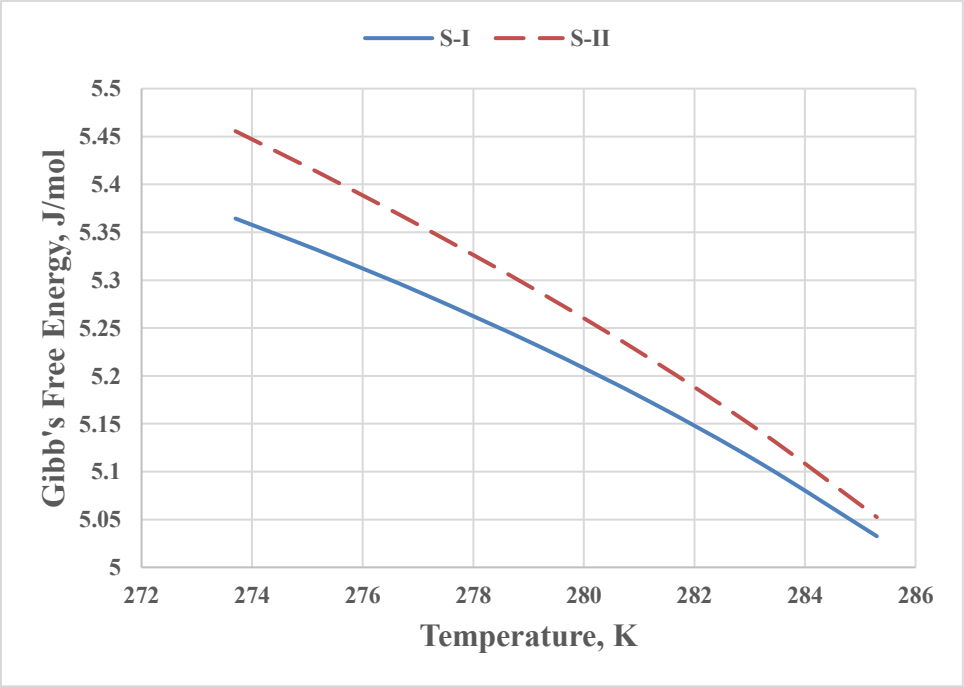

Figure 6.19: Stability assessment for Methane-N_2 hydrate structures.

Propane-N_2 is another mixture studied by the SAFT VR Mie-Novel LJ EOS and vdWP model. The gas composition has 75% propane. Small nitrogen can enter in any of the gas hydrate structures, whereas propane only enters large cavities of structure II. This higher propane content gas hydrate mixture forms structure II (Ng et al., 1977). The gas hydrate calculations using the SAFT VR Mie-Novel LJ EOS and vdWP model is illustrated in Figure 6.20 at temperature range of 274.5-278.7 K. The AADP (%) for propane-N_2 mixture is 4.31% as provided in Table 6-8.

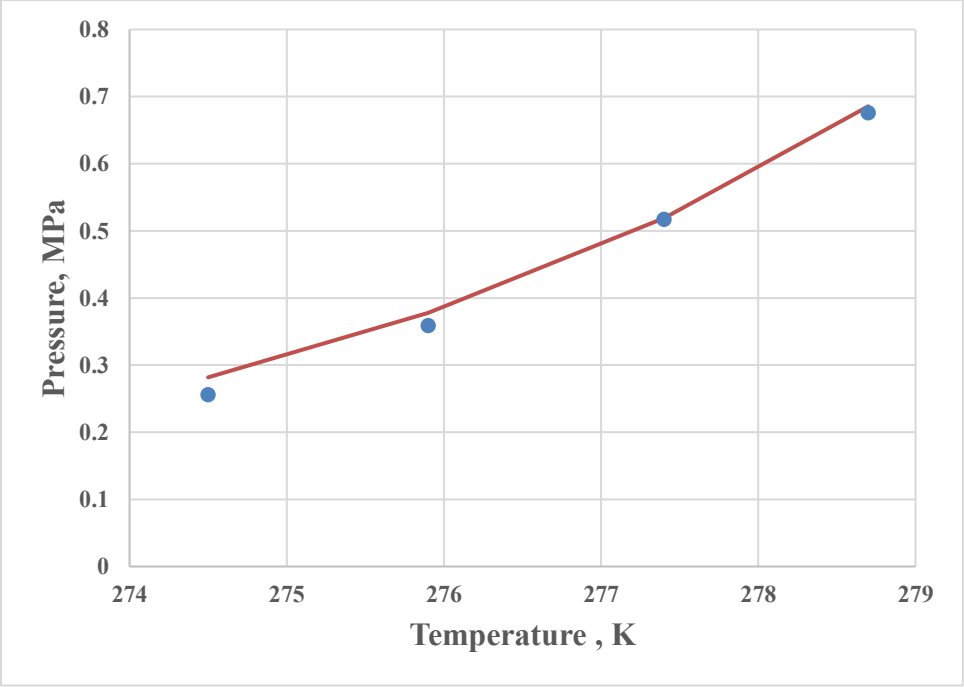

Figure 6.20: Incipient conditions prediction of Propane (75%) – N_2(25%) mixed hydrate for temperatures 274.5-278.7 K. The solid line is the correlation of the vdWP model. The points represent experimental gas hydrate equilibrium data (Ng et al., 1977).

Hydrate technology has also find its importance in carbon capture research field as well (Castellani et al., 2013; Seo, Moudrakovski, Ripmeester, Lee, & Lee, 2005). Carbon dioxide and nitrogen are the main constituents of flue gas from power plants. Hydrate technology have been considered to sequestrate these components and studied process for CO_2 recovery (Seo et al., 2005). The nitrogen-carbon dioxide mixed hydrate mixture is studied by the SAFT VR Mie-Novel LJ EOS and vdWP model. The studied gas mixture has 96.59% CO_2. The presence of nitrogen once again points towards the consideration of both the structures for this hydrate mixture. However, Seo et al. (2005) crystallographic study suggests formation of structure I for a CO_2-N_2 gas mixture with more than 10% CO_2. Therefore, incipient conditions for this mixture were predicted using both the structures. Structure I parameters gave excellent prediction as shown in Figure 6.21, whereas lack of convergence was achieved using structure II parameters. The AADP (%) of 2.3883% shows the remarkable prediction capability of the SAFT VR Mie-Novel LJ EOS and vdWP model for predicting the dissociation pressure for this system. The temperature range for CO_2-N_2 mixture varies from 274.95-283.55 K as specified in Table 6-8.

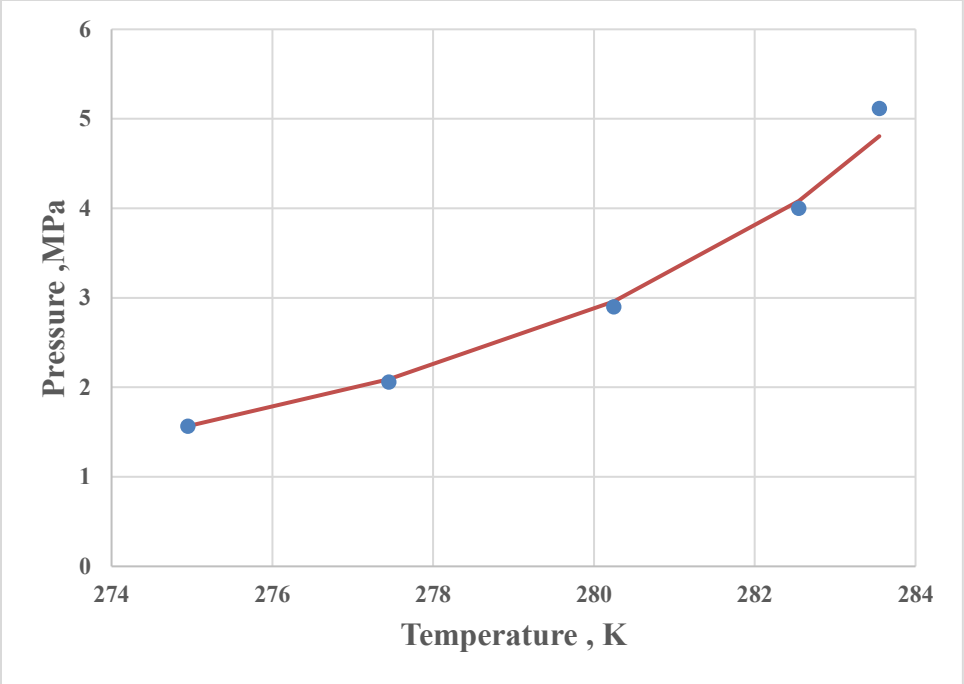

Figure 6.21: Incipient conditions prediction of CO_2 (96.59%) – N_2(3.51%) mixed hydrate for temperatures 274.95-283.55 K. The solid line is the correlation of the vdWP model. The points represent experimental gas hydrate equilibrium data (Kang et al., 2001).

Air gas hydrates is another interesting research topic that can help in determining the historic atmospheric conditions in Arctic and Antarctic regions (Mohammadi et al., 2003). Moreover, separation of nitrogen, oxygen components from air for further industrial applications can be achieved using the hydrate technology. Typical air composition with 21% oxygen and 79% nitrogen is used to predict dissociation pressures of air hydrates. Nitrogen, as a small molecule, is capable to enter any of the gas hydrate structures. Both the structures (I and II) parameters have been used to predict the air hydrate experimental data. As compared to structure II, Structure I parameters gave much better accurate prediction of the dissociation pressures of air gas hydrate system for temperatures 274.05-283.5 K, as depicted in Figure 6.22. The accuracy of prediction can be judged by the AADP (%) value provided in Table 6-8, which is 1.2318%. One

limitation while predicting air gas hydrates is the absence of phase equilibrium calculations for nitrogen-oxygen and water-oxygen systems due to the lack of availability data. This precise air hydrate equilibrium prediction in our work is due to the optimized Langmuir constant parameters of oxygen and nitrogen.

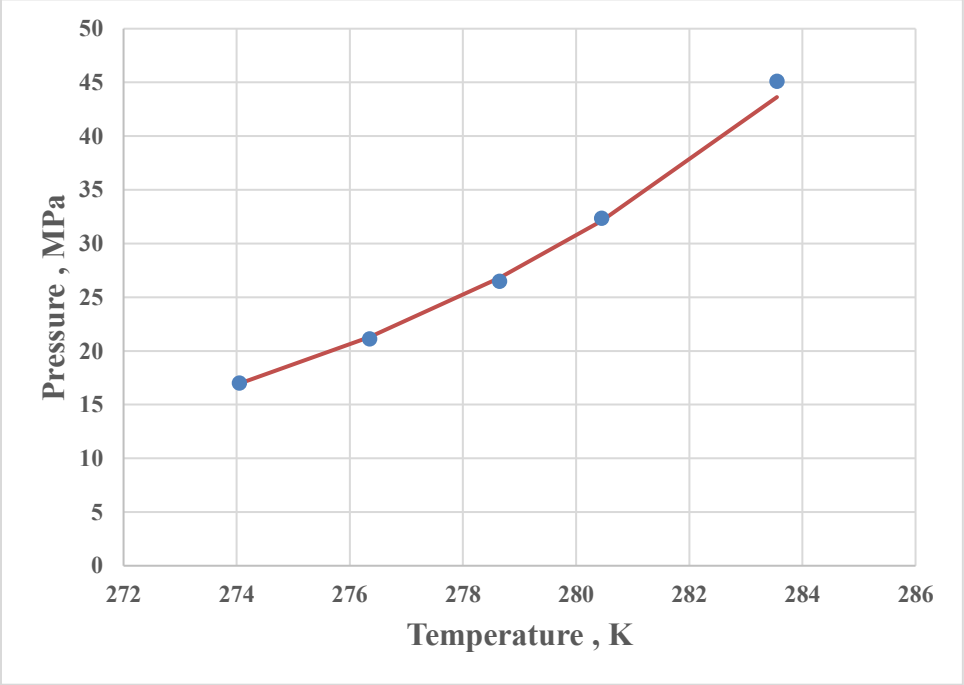

Figure 6.22: Incipient conditions prediction of O_2 (21%) – N_2 (79%) mixed hydrate for temperatures 274.05-283.55 K. The solid line is the correlation of the vdWP model.The points represent experimental gas hydrate equilibrium data (Mohammadi et al., 2003).

Another mixed gas hydrate mixture studied is methane-ethene system. The hydrate technology finds its application in petroleum refining and petrochemical industries as well for the separation of methane and ethene components (Ma et al., 2001). The studied gas mixture contains 5.6% methane. Both methane and ethene form structure I individually, giving a presumption that their mixture will also form structure I (Ma et al., 2001). In this thesis, both structures were used to predict the incipient pressures of methane-ethene mixture. It was found that structure I parameters gave an excellent

prediction for temperatures 273.7-286.2 K, as illustrated in Figure 6.23. The AADP for methane-ethene mixture is 3.2407% which further validates the accuracy of our proposed model.

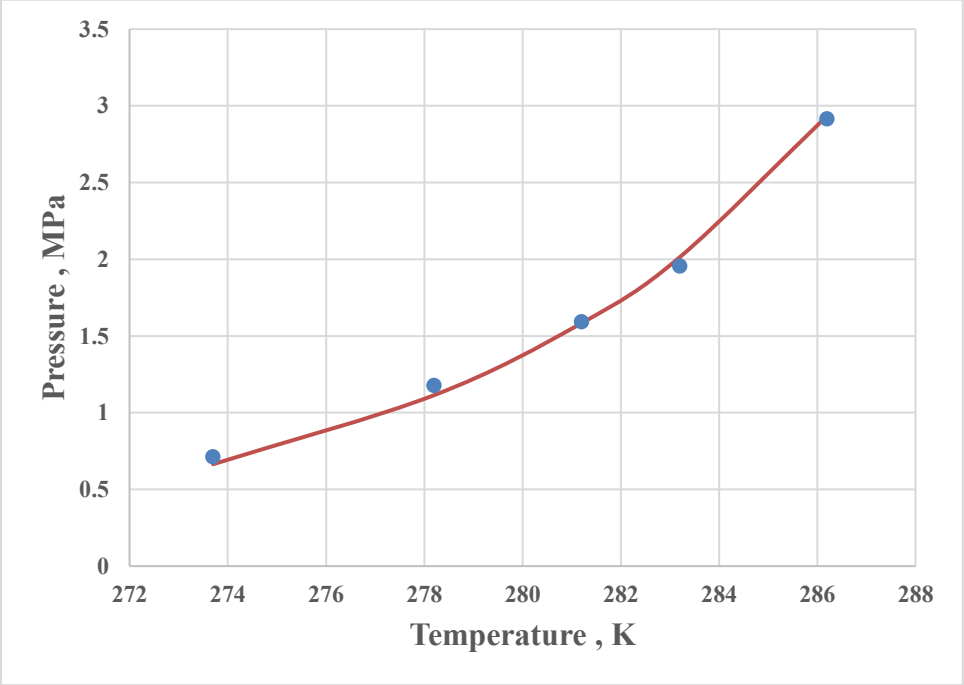

Figure 6.23: Incipient conditions prediction of Methane (5.6%) – Ethene (94.4%) mixed hydrate for temperatures 273.7-286.2 K. The solid line is the correlation of the vdWP model.The points represent experimental gas hydrate equilibrium data (Ma et al., 2001).

A comprehensive review of binary gas hydrate results is given in Table 6-8. From AADP (%) values of each studied binary gas hydrate system, it is apparent the deviations compared to the experimental data are always less than 5 %. Overall deviation value of all studied binary gas hydrate systems is 2.390% that points towards the excellent prediction of binary gas hydrate systems.

Table 6-8: Gas hydrate equilibrium results summary for binary gas hydrate systems

Gas hydrate	Temperature Range	Exp. Points	Structure	AADP%	Data Reference
Methane (94.6%)-Ethane (5.4%)	284.9-299.1	6	I	2.4501	(McLeod Jr. & Campbell, 1961)
Methane (71.2%)-Propane (28.8%)	274.8-283.2	4	II	0.9856	(Deaton & Frost, 1946)
Methane (36.4%) -Isobutane (63.6%)	273.8-276.9	3	II	1.6503	(Wu et al., 1976)
Ethane (28%)-Propane (72%)	276.5-277.9	3	II	1.7387	(Holder & Hand, 1982)
Methane (92%)-Carbon Dioxide (8%)	277.8-285.1	4	I	2.172	(Adisasmito et al., 1991)
Methane (89.26%)-Nitrogen (10.74%)	273.7-285.3	8	I	2.9105	(Mei et al., 1996)
Propane (75%)-Nitrogen (25%)	274.5-278.7	4	II	4.3148	(Ng et al., 1977)
Nitrogen (3.41%) - Carbon dioxide (96.59%)	274.95-283.55	5	I	2.3883	(Kang et al., 2001)
Oxygen (21%)-Nitrogen (79%)	274.05-283.55	5	I	1.2318	(Mohammadi et al., 2003)
Methane (94.4%) - Ethene (5.6%)	273.7-286.2	5	I	3.2407	(Ma et al., 2001)
Overall	**-**	**47**	**-**	**2.390**	**-**

6.5.2 Multicomponent Gas Hydrate Systems

In order to test the accuracy for multicomponent systems, the gas hydrate model is further extended for ternary, quaternary and natural gas systems There are seven multicomponent systems studied in this work. Table 6-9 gives AADP (%) and gas hydrate structures for these system. Figures 6.24, 6.25 & 6.26 show the examples of gas hydrate equilibrium results for a ternary (Methane-CO_2-N_2), a quaternary (Methane-Ethane-CO_2-N_2) and a natural gas (Methane-Ethane-Propane-CO_2-N_2) system.

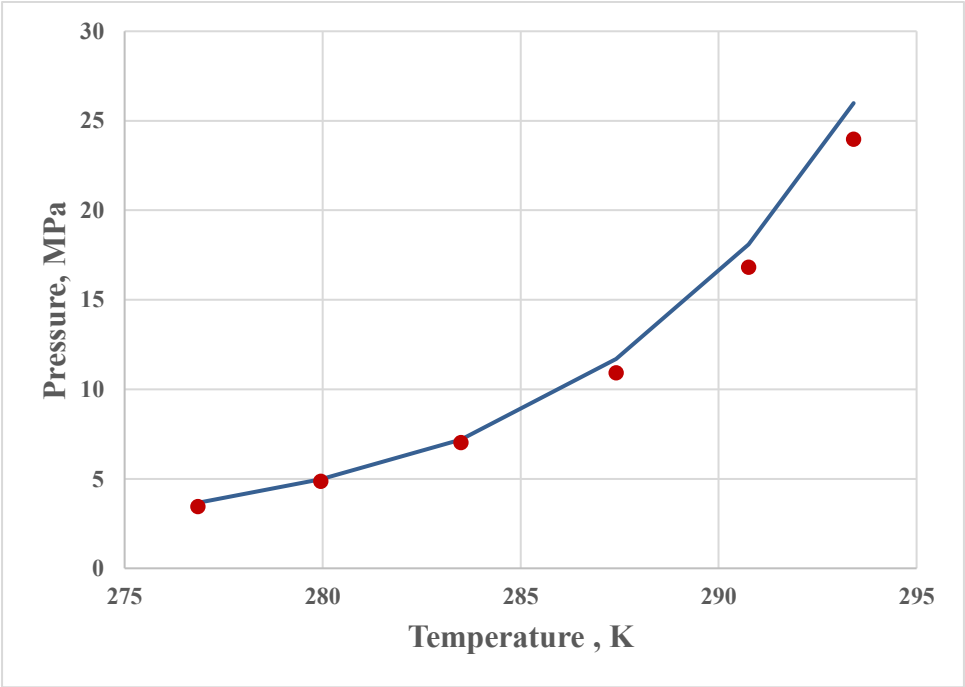

Figure 6.24: Incipient conditions prediction of Methane (89.40%) – CO_2 (8.09%) – Nitrogen (0.02%) mixed hydrate for temperatures 276.85-293.41 K. The solid line is the correlation of the vdWP model.The points represent experimental gas hydrate equilibrium data (Nixdorf & Oellrich, 1997).

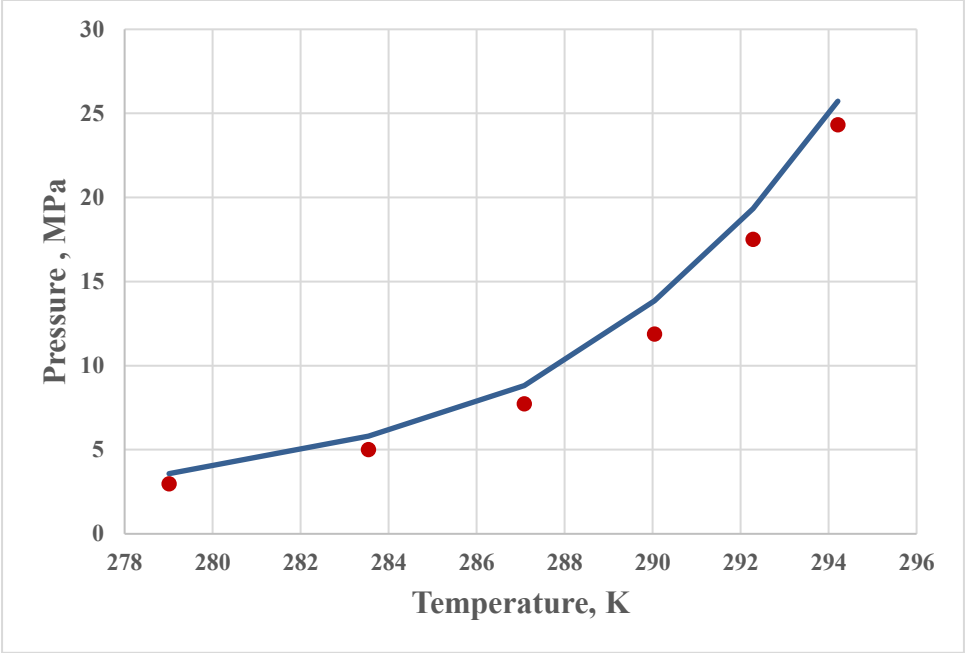

Figure 6.25: Incipient conditions prediction of Methane (89.60%) –Ethane (5.13%)- CO_2 (5.25%) – Nitrogen (0.02%) mixed hydrate for temperatures 279.01-294.21 K. The solid line is the correlation of the vdWP model.The points represent experimental gas hydrate equilibrium data (Nixdorf & Oellrich, 1997).

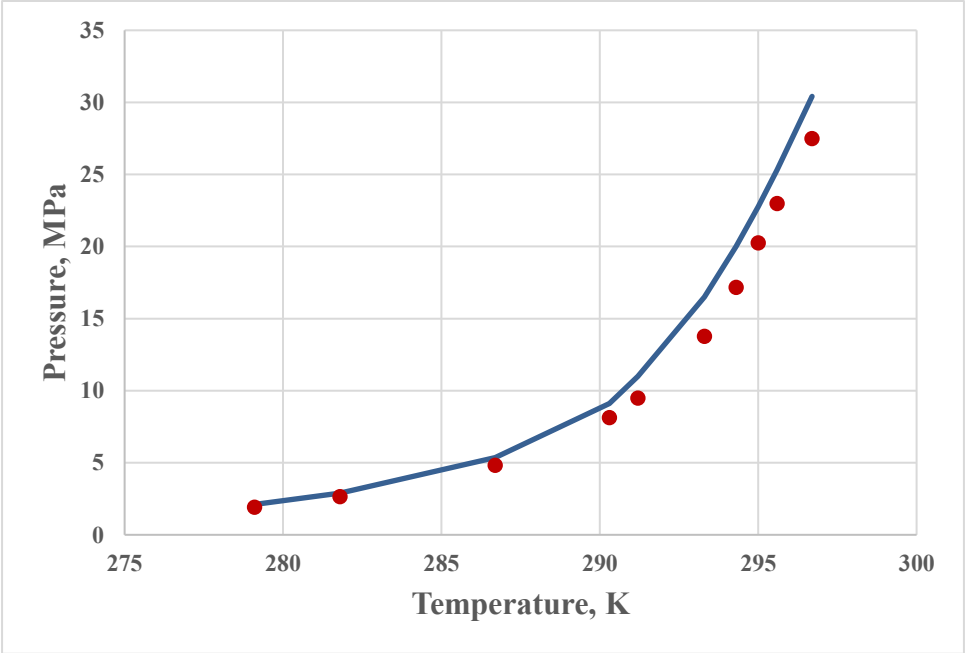

Figure 6.26: Incipient conditions prediction of natural gas mixture with Methane (93.20%) –Ethane (4.25%)- Propane (1.61%) - CO_2 (0.51%) – Nitrogen (0.43%) mixed hydrate for temperatures 279.1-296.7 K. The solid line is the correlation of theVdwP model. The points represent experimental gas hydrate equilibrium data (W. Wilcox, Carson, & Katz, 1941).

While analyzing the results of multicomponent hydrate systems provided in Figures 6.24, 6.25, 6.26 and Table 6-9, an increase in AADP (%) is observed as compared to single and binary hydrate systems. This is because EOS models approximate multibody interactions with pair-wise additive potentials while predicting VLE behavior (Hasse, 2010). Pair-wise additivity works well with the lighter molecules. However, the multicomponent gas hydrate mixtures contain heavy molecules like propane, isobutane that certainly enhances the need of consideration of multibody interactions (Sadus, 2002). Significant research (Hasse, 2010; Marcelli, Todd, & Sadus, 2002; Sadus, 2002) is going on to incorporate multibody interactions for the improved prediction of the thermodynamic properties and VLE in future.

6.6 Gas hydrate Results Comparison with other EOS models

As indicated in Chapter 3, adequate EOS is required for accurate flash calculations, which helps in precise prediction of gas hydrate incipient conditions. This work selected SAFT-VR Mie-Novel LJ EOS, for its recent success in predicting accurate thermodynamic properties and VLE (Dufal, Lafitte, Haslam, et al., 2015; Lafitte et al., 2013). Single and mixed gas hydrate results achieved in this thesis, using SAFT-VR Mie-Novel LJ EOS, have shown promise in accurate prediction of gas hydrate equilibrium.

A recent study by Meragawi et al. (2016) has reported the gas hydrate results using Peng Robinson (PR) and PC-SAFT EOS, in combination with Parish and Prausnitz extension. This gives an excellent opportunity to vet the accuracy of gas hydrate results obtained through SAFT-VR Mie-Novel LJ EOS in comparison with other well-known EOSs.

Table 6-9: Gas hydrate equilibrium results summary for multicomponent gas hydrate systems

Components	Exp. Points	Temperature Range, K	AADP (%)	Structure Type	Data Reference
Ternary Systems					
Methane (94.97%)- CO_2 (5.00 %) - N_2 (0.03%)	6	276.85-293.41	5.53	I	(Nixdorf & Oellrich, 1997)
Methane (90.93%) - Ethane (4.89%) - N_2 (4.18%)	7	277.36-294.23	18.96	I	(Nixdorf & Oellrich, 1997)
Methane (95.02%)-Ethane (3.98%)-Propane (1.00%)	6	279.1-295.76	20.04	II	(Nixdorf & Oellrich, 1997)
Quaternary Systems					
Methane (89.60%) -Ethane (5.13%) -CO_2 (5.25%) -N_2 (0.02%)	6	279.01-294.21	13.94	I	(Nixdorf & Oellrich, 1997)
Methane (89.40%)-Propane (2.49%)-CO_2 (8.09%)- N_2 (0.02%)	6	279.19-296.07	16.61	II	(Nixdorf & Oellrich, 1997)
Natural Gas Mixtures					
Methane (93.20%)- Ethane (4.25%)- Propane (1.61%)-N_2 (0.43%)-CO_2 (0.51%)	10	279.1-296.7	12.76	II	(W. Wilcox et al., 1941)
Methane (96.5%)- Ethane (0.9%)- Propane (1.8%)-N_2 (0.6%)-CO_2 (0.2%)	9	273.7-289.8	19.03	II	(Deaton & Frost, 1946)
Overall	**50**	**-**	**15.37**		**-**

Table 6-10: AADP (%) values comparison for gas hydrate results using PC-SAFT, PR and SAFT-VR Mie-Novel LJ EOS

Components	Exp. Points	Temperature Range, K	%AADP			Data Reference
			PC-SAFT[a]	PR[a]	SAFT-VR Mie-Novel LJ	
Single Systems						
Methane	33	273.7-320.10	11.12	6.86	7.66	(Deaton & Frost, 1946; D. R. Marshall et al., 1964)
Ethane	24	273.15-284.65	19.97	20.05	2.94	(Holder, Zetts, & Pradhan, 1988)
Propane	21	273.15-278.15	4.97	4.90	1.58	(Holder et al., 1988)
Isobutane	21	273.15-274.8	1.04	1.17	2.21	(Holder et al., 1988)
Nitrogen	25	273.15-298.15	2.24	6.61	3.95	(Holder et al., 1988)
Binary Systems						
Methane-H_2S	20	276.5-295.4	8.31	8.03	6.80	(Noaker & Katz, 1954)
Methane-Ethane	24	274.8-283.2	20.37	17.02	16.08	(Deaton & Frost, 1946)
Methane-Propane	25	274.8-283.2	4.54	3.46	3.81	(Deaton & Frost, 1946)
Propane-Nitrogen	29	274.2-289.2	42.09	34.41	24.75	(Ng et al., 1977)
Ternary Systems						
Methane-CO_2-N_2	6	276.85-293.41	0.83	13.20	5.53	(Nixdorf & Oellrich, 1997)

Methane-Ethane-N_2	7	277.36-294.23	20.34	20.77	18.96	(Nixdorf & Oellrich, 1997)
Methane-Ethane-Propane	13	277.1-298.14	42.96	26.16	27.00	(Nixdorf & Oellrich, 1997)
Quaternary Systems						
Methane-Ethane-CO_2-N_2	6	279.01-294.21	17.38	8.28	13.94	(Nixdorf & Oellrich, 1997)
Methane-Propane-CO_2-N_2	6	279.19-296.07	22.17	27.02	16.61	(Nixdorf & Oellrich, 1997)
Overall	**260**	**-**	**15.23**	**13.19**	**9.76**	**-**

[a](El Meragawi, Diamantonis, Tsimpanogiannis, & Economou, 2016)

Table 6-10 shows the comparison of AADP (%) values of gas hydrate results for PC-SAFT, PR and SAFT-VR Mie-Novel LJ EOS. While analyzing the AADP (%) values, it is observed that SAFT-VR Mie-Novel LJ EOS have lower AADP (%) values for most of gas hydrate systems. The AADP (%) values for SAFT-VR Mie-Novel LJ EOS are of moderate and practical nature. On the other hand, PC-SAFT and PR EOS AADP (%) are either very high or very low. The overall AADP (%) value of all compared gas hydrate systems for SAFT-VR Mie-Novel LJ EOS is 9.76% that is lowest among PC-SAFT and PR EOS models.

In a nutshell, the gas hydrate model based on SAFT-VR Mie-Novel LJ EOS with Parish and Prausnitz extension, has predicted excellent gas hydrate incipient conditions. AADP (%) values of studied single hydrate systems are found to be less than 4 %. Similarly, for considered binary hydrate systems, AADP (%) values were found to be less than 5%. Looking at single and binary hydrate results, the gas hydrate model was extended to seven multicomponent systems and was analyzed accordingly. Finally, a gas hydrate equilibrium results achieved in this thesis were compared with other studies (El Meragawi et al., 2016). It was found out that the model used in this thesis provided better prediction with an overall AADP (%) of 9.76%.

CHAPTER 7

CONCLUSIONS & RECOMMENDATIONS

7.1 Conclusion

This thesis work was carried out to assess the applicability of SAFT-VR Mie EOS in combination with vdWP (Parish & Prausnitz extension) model, in predicting the incipient conditions of single and mixed gas hydrate systems. The work was successfully completed and produced more accurate results as compared to other well-known EOS models. The research work completion approach can be broadly classified into two parts. First part addressed the VLE calculations of gas hydrate mixtures including non-polar and water-nonpolar mixtures. The other part includes the calculations of gas hydrate incipient conditions for single and mixed gas hydrate systems.

VLE calculations of non-polar (hydrate formers) systems gave excellent prediction of the experimental VLE data, as reported in Chapter 4. The quantitative prediction of VLE behavior of non-polar systems was achieved by adjustment of binary interaction parameters. The binary interaction parameter values were very small and almost close to zero. These remarkable VLE results using SAFT-VR Mie allowed to extend the VLE calculations to more complex systems.

VLE behavior prediction of water-nonpolar mixtures is considered as complex and a challenging task. Before carrying out the VLE calculations of water-nonpolar mixtures, three association schemes were evaluated and finalized for water. Novel LJ

association scheme was selected among these three association schemes, based on VLE prediction of water-nonpolar mixtures with smaller phase-wise k_{ij} values. SAFT VR-Mie with Novel LJ association scheme predicted the VLE behavior of water-nonpolar mixtures with considerable accuracy, as can be seen in Chapter 5. These accurate VLE results were further applied in gas hydrate equilibrium calculations (see Chapter 6).

For accurate L_w-H-V gas hydrate equilibrium calculations, literature based Langmuir constant adjustable parameters were tested. The components whose parameters gave accurate results were selected, while others were optimized in this work. Similarly, reference energy parameters that provided excellent single hydrate results were selected. Accuracy of prediction of gas hydrate incipient conditions and stability of gas hydrate helped in selection of gas hydrate structures. Incipient conditions of eleven single gas hydrate systems were predicted with an AADP (%) of less than 4%.

Excellent results of single gas hydrate systems allowed to extend the model to mixed hydrate systems. About ten binary mixed hydrate systems were studied in this work. Different types of binary hydrate systems have studied to check the applicability of selected gas hydrate model. The AADP (%) of all the studied binary hydrate systems were found less than 5%. The accuracy of binary hydrate systems is slightly less as compared to single hydrate systems, but still the prediction of incipient conditions is reasonably good.

Moreover, the selected gas hydrate model is further extended to seven multicomponent gas hydrate systems. These multicomponent gas hydrate systems include ternary, quaternary and natural gas mixtures. The overall AADP (%) of multicomponent

hydrate systems is about 16%. As compared to single and binary hydrate systems, the reduction in accuracy for multicomponent systems is due to the approximation of high multibody interactions through pair wise additive potentials.

In order to ascertain the accuracy of prediction of incipient conditions of SAFT-VR Mie-Novel LJ based gas hydrate model, a comparison with well-known PR and PC-SAFT based gas hydrate models was carried out in this work. It was found that our selected model gives the lowest overall AADP (%) of various compared gas hydrate systems including both single and mixed gas hydrate systems. Although certain gas hydrate systems have lower AADP (%) for either PR or PC-SAFT based gas hydrate models, SAFT-VR Mie-Novel LJ based gas hydrate model predicts with higher accuracy for majority of gas hydrate systems.

Another important point to mention is the time taken to predict a certain incipient condition of gas hydrates. Although SAFT-VR Mie is a lengthy and complex analytical equation, it took approximately thirty seconds to predict a single data point in gas hydrate equilibrium curve.

To sum up, SAFT VR-Mie EOS with novel LJ association scheme has predicted quite accurate VLE behavior for both nonpolar-water-nonpolar mixtures. This accurate VLE behavior prediction of gas hydrate mixtures were translated in to the excellent prediction of gas hydrate incipient conditions. The accuracy achieved by SAFT-VR Mie-Novel LJ based gas hydrate model was found to be better as compared to well-known PR and PC-SAFT based gas hydrate models.

7.2 Recommendations for Future Work

Gas hydrate is a vast research area and has gained importance since last decade. On the other hand, SAFT-VR Mie EOS has recently gained reputation in accurate prediction of thermodynamic properties and VLE calculation. However, its applicability in gas hydrate research is rare. This work has assessed SAFT-VR Mie EOS's applicability in prediction of L_w-H-V single and mixed gas hydrate equilibrium. There can be many recommendations for using SAFT-VR Mie EOS in gas hydrate research area in future. Some of them are as follows:

1. Applicability of SAFT-VR Mie EOS can be extended to other types of multiphase hydrate equilibrium calculations such as Ice-Hydrate-Vapor, Liquid Water-Hydrate-Hydrocarbon Liquid, Ice-Liquid Water-Hydrate-Vapor, Liquid Water-Hydrate-Vapor-Hydrocarbon liquid.
2. This work can be further extended by assessing the effect of various thermodynamic inhibitors and electrolyte solutions on the L_w-H-V gas hydrate equilibrium conditions. The association effects and coulomb effects will add a new dimension to this work.
3. Industrial natural gas mixtures composition includes contents of heavy hydrocarbons such as n-butane, n-pentane, isopentane, n-hexane, n-heptane. These heavy hydrocarbons are usually considered as non-gas hydrate formers (Carroll, 2009). This work can be extended to study the effect of these heavier components on the prediction of gas hydrate incipient conditions.

APPENDIX - A

ASSOCIATION THEORIES

Table A-1: Description and Limitations of Association Theories (Müller & Gubbins, 2001)

Associating theory	Brief Description	Limitations
Dolazalek's Chemical Theory (Dolezalek, 1908)	1) Association is represented by chemical reaction of monomers to form dimers. 2) Equilibrium constants 'K' of reaction helps in determining the thermodynamic properties. 3) In case of chain-like formation of associate complexes, equilibrium constants of all chemical reactions have to be calculated. 4) This theory is based on principle that monomers and	1) The success of this theory depends upon an intelligent guess of number of reactions and type of associate complexes being formed. 2) This theory does not address non ideal associate systems. 3) As equilibrium constants of associate complexes cannot be measured experimentally, hence they are treated as adjustable

	formed associates will be in ideal gas or solution phase.	parameters. The more the reactions, the more the number of equilibrium constants that need to be adjusted. This makes the computation complicated.
Hiedman and Prausnitz Approach (Heidemann & Prausnitz, 1976)	1) In order to address the non-ideal systems, fugacity coefficients were added to the chemical theory. 2) This approach has two parts, the physical part addressed by a suitable equation of state and the chemical part that addresses association thru chemical theory. 3) The equilibrium constant for all chain reactions is equivalent.	1) Performance is based on intelligent guess for number and types of reactions and appropriate combining rules. 2) Thermodynamic inconsistency can exist due to consideration of separate physical and chemical interactions. (Anderko, Economou, & Donohue, 1993)
Guggenheim Quasi-Chemical Theory	1) Association effect on fluid behavior is pointed towards the existence of nonrandom mixing in associating molecules.	1) This theory does not predict well near or above critical region for association and polar molecules. Hence, its inapplicable the whole

(Guggenheim, 1948)	2) The effect of strong association interactions is addressed by large energy parameters in the models. 3) It serves as a basis for all activity coefficient models such as NRTL, UNIFAC, UNIQUAC etc. that predict liquid thermodynamic properties quite well.	fluid range. 2) Parameters found from VLE data do not work well with LLE calculations.
Lattice Fluid Theory (Economou, 2000; Panayiotou, 1987)	1) This theory treats liquid structure as a solid-like lattice structure. 2) It predicts excess properties of liquid mixtures quite well. 3) Due to its random mixing basis, a quasi-chemical approximation is considered to cater the effects of non-random mixing usually found in associating molecules.	1) This theory predicts quite well the qualitative thermodynamic properties of liquid (Economou, 2000) but prediction of quantitative thermodynamic properties require improvement (Panayiotou, 1987).

Andersen's Theory (Andersen & C., 1973, 1974; Dahl & Andersen, 1983)	1) This is a physical theory based on statistical mechanics principles. 2) The geometry of interaction of hydrogen bonding fluids considered is a short-ranged, highly directional attraction site attached to repulsive core. 3) A cluster expansion series in terms of total number density was carried out, which was simplified using the assumption of one bond per attraction site by the cancellation of graphs.	1) Graph cancellation due to steric effects is cumbersome and ineffective in single density formalism, which is the initial step in determination of association effects in fluids (K. Jog, W. G. Chapman, 1999).

APPENDIX - B

CALCULATION PROCEDURES

This appendix deals with the procedure to calculate PVT properties of pure components and VLE behavior of thermodynamic mixtures. Both PVT and VLE calculations are performed by simultaneous solution of nonlinear equations. These nonlinear equations are based on thermodynamic equilibrium principle, which states:

"At equilibrium, chemical potentials or fugacities of each component (i) between the phases are equal at constant temperature and pressure"

Mathematically, thermodynamic equilibrium principle translates into following equations:

1. Thermal equilibrium $$T^{\alpha} = T^{\beta} \quad \text{(B.1)}$$
2. Mechanical equilibrium $$P^{\alpha} = P^{\beta} \quad \text{(B.2)}$$
3. Chemical equilibrium $$\mu_i^{\alpha} = \mu_i^{\beta} \text{ or } f_i^{\alpha} = f_i^{\beta} \quad \text{(B.3)}$$

(i = no. of components)

The nonlinear equations for PVT and VLE calculations are established by following pressure and fugacity equations. Fugacity for pure component 'i' is given by:

$$RT \ln \phi_i = RT \ln \frac{f_i}{P} = A^R + RT \ln Z \quad \text{(B.4)}$$

Similarly, fugacity of a component ‘k’ in the mixture is represented by:

$$\ln \phi_k = \ln \frac{f_k}{y_k P} = \frac{\mu_k^{res}(T,v)}{kT} - \ln Z \tag{B.5}$$

$$\frac{\mu_k^{res}(T,v)}{kT} = a^{res} + (Z-1) + \left(\frac{\partial a^{res}}{\partial x_k}\right)_{T,v,x_{i\neq k}} - \sum_{j=1}^{N}\left[x_j \left(\frac{\partial a^{res}}{\partial x_j}\right)_{T,v,x_{i\neq j}}\right] \tag{B.6}$$

where,

$$a^{res} = \frac{A^{res}}{NkT} \tag{B.7}$$

$$Z = \frac{PV}{nRT} \tag{B.8}$$

$$P = \frac{nRT}{V} - \left(\frac{\partial A^{RES}}{\partial V}\right)_{T,n} \tag{B.9}$$

In this thesis, the PVT calculations are carried out for the optimization of SAFT-VR Mie pure component parameters. On the other hand, multicomponent VLE calculations for nonpolar mixtures and water-nonpolar mixtures are performed using above mentioned nonlinear equations. Both PVT and VLE models are coded in MATLAB®. These codes are user friendly, easily extensible and could be used for calculating various other thermodynamic properties.

References

Adisasmito, S., Frank, R. J., & Sloan, E. D. (1991). Hydrates of Carbon-Dioxide and Methane Mixtures. *Journal of Chemical and Engineering Data*, *36*(1), 68–71. https://doi.org/10.1021/je00001a020

Anderko, A., Economou, I. G., & Donohue, M. D. (1993). Comments on "Thermodynamic Inconsistencies in and Accuracy of Chemical Equations, (4), 245–246.

Andersen, H. C., & C., H. (1973). Cluster expansions for hydrogen-bonded fluids. I. Molecular association in dilute gases. *The Journal of Chemical Physics*, *59*(9), 4714–4725. https://doi.org/10.1063/1.1680684

Andersen, H. C., & C., H. (1974). Cluster expansions for hydrogen bonded fluids. II. Dense liquids. *The Journal of Chemical Physics*, *61*(12), 4985–4992. https://doi.org/10.1063/1.1681838

Anderson, F. E., & Prausnitz, J. M. (1986). Inhibition of gas hydrates by methanol. *AIChE Journal*, *32*(8), 1321–1333. https://doi.org/10.1002/aic.690320810

Anthony, R. G., & McKetta, J. J. (1967). Phase equilibrium in the ethylene-water system. *Journal of Chemical & Engineering Data*, *12*(1), 17–20. https://doi.org/10.1021/je60032a006

Avlonitis, D. (1988). *Multiphase Equilibria in Oil-Water Hydrate Forming Systems*. Heriot-Watt University, Edinburgh, Scotland.

Avlonitis, D. (1994). The determination of kihara potential parameters from gas hydrate data. *Chemical Engineering Science*, *49*(8), 1161–1173. https://doi.org/10.1016/0009-2509(94)85087-9

B. H. Patel, †, P. Paricaud, †, A. Galindo, *,† and, & Maitland‡, G. C. (2003). Prediction of the Salting-Out Effect of Strong Electrolytes on Water + Alkane Solutions. https://doi.org/10.1021/IE020918U

Baillie, C., & Wichert, E. (1987). Chart Gives Hydrate Formation Temperature for Natural Gas. *Oil & Gas Journal*, *85*(4), 37–39.

Bakker, R. J. (1998). Improvements in clathrate modelling II: the H2O-CO2-CH4-N2-C2H6 fluid system. *Geological Society, London, Special Publications*, *137*(1), 75–105.

Ballard, A. L., & Sloan, E. D. (2002). The Next Generation of Hydrate Prediction: An Overview. *Journal of Supramolecular Chemistry*, *2*(4–5), 385–392. https://doi.org/10.1016/S1472-7862(03)00063-7

Barkan, E. S., & Sheinin, D. a. (1993). A general technique for the calculation of formation conditions of natural gas hydrates. *Fluid Phase Equilibria*, *86*, 111–136. https://doi.org/10.1016/0378-3812(93)87171-V

Behzadi, B., Patel, B. H., Galindo, A., & Ghotbi, C. (2005). Modeling electrolyte solutions with the SAFT-VR equation using Yukawa potentials and the mean-spherical approximation. *Fluid Phase Equilibria*, *236*(1), 241–255. https://doi.org/10.1016/j.fluid.2005.07.019

Besserer, G. J., & Robinson, D. B. (1973a). Equilibrium-phase properties of isobutane-carbon dioxide system. *Journal of Chemical & Engineering Data*, *18*(3), 298–301. https://doi.org/10.1021/je60058a010

Besserer, G. J., & Robinson, D. B. (1973b). Equilibrium-phase properties of isobutane-ethane system. *Journal of Chemical and Engineering Data*, *18*(3), 301–304.

Blanc, C. J., & Setier, J. C. B. (1988). Vapor-liquid equilibria for the ethane-propane system at low temperature. *Journal of Chemical & Engineering Data*, *33*(2), 111–115. https://doi.org/10.1021/je00052a015

Blas, F. J., & Vega, L. F. (1998). Prediction of Binary and Ternary Diagrams Using the Statistical Associating Fluid Theory (SAFT) Equation of State. *Industrial & Engineering Chemistry Research*, *37*(2), 660–674. https://doi.org/10.1021/ie970449+

Boublík, T. (1986). Background correlation functions in the hard sphere systems. *Molecular Physics*, *59*(4), 775–793. https://doi.org/10.1080/00268978600102391

Breland, E., & Englezos, P. (1996). Equilibrium hydrate formation data for carbon dioxide in aqueous glycerol solutions. *Journal of Chemical and Engineering Data*, *41*, 11–13. https://doi.org/10.1021/je950181y

Brown, T. S., Sloan, E. D., & Kidnay, A. J. (1989). Vapor-liquid equilibria in the nitrogen + carbon dioxide + ethane system. *Fluid Phase Equilibria*, *51*, 299–313. https://doi.org/10.1016/0378-3812(89)80372-3

Carroll, J. J. (2009). *Natural gas hydrates : a guide for engineers*. Gulf Professional Pub./Elsevier.

Carroll, J. J., & Duan, J. (2002). Relational expression of the conditions forming hydrates of various components in natural Gas. *Natural Gas Industry*, *22*(2), 66–71.

Carson, D. B., & Katz, D. . (1942). Natural Gas hydrates:Petroleum Transactions of the American Institute of Mining Engineers, *146*, 150–158.

Castellani, B., Filipponi, M., Nicolini, A., Cotana, F., & Rossi, F. (2013). Carbon Dioxide Capture Using Gas Hydrate Technology. *Journal of Energy and Power Engineering*, *7*, 883–890.

Chaplin, M. (2000). Hydrogen bonding in water. Retrieved February 28, 2017, from http://www1.lsbu.ac.uk/water/water_hydrogen_bonding.html

Chapman, W. G. (1988). *Theory and Simulation of Associating Liquid Mixtures.* Cornel1 University, Ithaca, NY.

Chapman, W. G., Gubbins, K. E., Jackson, G., & Radosz, M. (1989). SAFT : Equation - of - State Solution Model for Associating Fluids. *Fluid Phase Equilibria Elsevier Science Publishers B . V*, *52*(3). https://doi.org/10.1016/0378-3812(89)80308-5

Chapman, W. G., Gubbins, K. E., Jackson, G., & Radosz, M. (1990). New reference equation of state for associating liquids. *Industrial & Engineering Chemistry Research*, *29*(8), 1709–1721. https://doi.org/10.1021/ie00104a021

Chapoy, A., Coquelet, C., & Richon, D. (2003). Measurement of the water solubility in the gas phase of the ethane + water binary system near hydrate forming conditions. *Journal of Chemical and Engineering Data*, *48*(4), 957–966. https://doi.org/10.1021/je0202230

Chapoy, A., Coquelet, C., & Richon, D. (2005). Erratum: Revised solubility data and modeling of water in the gas phase of the methane/water binary system at temperatures from 283.08 to 318.12 K and pressures up to 34.5 MPa (Fluid Phase Equilibria (2003) 214 (101-117)). *Fluid Phase Equilibria*, *230*(1–2), 210–214. https://doi.org/10.1016/j.fluid.2004.07.005

Chapoy, A., Mohammadi, A. H., Chareton, A., Tohidi, B., & Richon, D. (2004). Measurement and Modeling of Gas Solubility and Literature Review of the Properties for the Carbon Dioxide−Water System. *Industrial & Engineering Chemistry Research*, *43*, 1794–1802. https://doi.org/10.1021/ie034232t

Chapoy, A., Mohammadi, A. H., Tohidi, B., & Richon, D. (2004). Gas Solubility Measurement and Modeling for the Nitrogen + Water System from 274 . 18 K to 363 . 02 K. *Engineering*, *49*(Figure 1), 1110–1115. https://doi.org/10.1021/je049869d

Chapoy, A., Mohammadi, A. H., Tohidi, B., Valtz, A., & Richon, D. (2005). Experimental Measurement and Phase Behavior Modeling of Hydrogen Sulfide−Water Binary System. *Industrial & Engineering Chemistry Research*, *44*, 7567–7574. https://doi.org/10.1021/ie050201h

Chapoy, A., Mokraoui, S., Valtz, A., Richon, D., Mohammadi, A. H., & Tohidi, B. (2004). Solubility measurement and modeling for the system propane-water from 277.62 to 368.16 K. *Fluid Phase Equilibria*, *226*(1–2), 213–220. https://doi.org/10.1016/j.fluid.2004.08.040

Chen, S., Banaszak, M., & Radosz, M. (1995). Phase Behavior of Poly(ethylene-1-butene) in Subcritical and Supercritical Propane: Ethyl Branches Reduce Segment Energy and Enhance Miscibility. *Macromolecules*, *28*(6), 1812–1817.

https://doi.org/10.1021/ma00110a014

Clark, G. N. I., Haslam, A. J., Galindo, A., & Jackson, G. (2006). Developing optimal Wertheim-like models of water for use in Statistical Associating Fluid Theory (SAFT) and related approaches. *Molecular Physics*, *104*(December 2013), 3561–3581. https://doi.org/10.1080/00268970601081475

Coquelet, C., Valtz, A., Stringari, P., Popovic, M., Richon, D., & Mougin, P. (2014). Phase equilibrium data for the hydrogen sulphide+methane system at temperatures from 186 to 313K and pressures up to about 14MPa. *Fluid Phase Equilibria*, *383*, 94–99. https://doi.org/10.1016/j.fluid.2014.09.025

Dadmohammadi, Y., Gebreyohannes, S., Abudour, A. M., Neely, B. J., & Gasem, K. A. M. (2016). Representation and Prediction of Vapor–Liquid Equilibrium Using the Peng–Robinson Equation of State and UNIQUAC Activity Coefficient Model. *Industrial & Engineering Chemistry Research*, *55*(4), 1088–1101. https://doi.org/10.1021/acs.iecr.5b03475

Dahl, L. W., & Andersen, H. C. (1983). Cluster expansions for hydrogen-bonded fluids. III. Water. *The Journal of Chemical Physics*, *78*(4), 1962–1979. https://doi.org/10.1063/1.444943

Davidson, D. W., Gough, S. R., Ripmeester, J. A., & Nakayama, I. H. (1981). The effect of methanol on the stability of clathrate hydrates1. *Canadian Journal of Chemistry*, *59*(2), 2587–2590.

Deaton, W. M., & Frost, E. M. J. (1946). *Gas Hydrates and Their Relation to the Operation of Natural-Gas Pipe Lines*.

Dharmawardhana, P. B., Parrish, W. R., & Sloan, E. D. (1980). Experimental Thermodynamic Parameters for the Prediction of Natural Gas Hydrate Dissociation Conditions. *Industrial & Engineering Chemistry Fundamentals*, *19*(4), 410–414. https://doi.org/10.1021/i160076a015

Dias, A. M. A., Llovell, F., Coutinho, J. A. P., Marrucho, I. M., & Vega, L. F. (2009). Thermodynamic characterization of pure perfluoroalkanes, including interfacial and second order derivative properties, using the crossover soft-SAFT EoS. *Fluid Phase Equilibria*, *286*, 134–143. https://doi.org/10.1016/j.fluid.2009.08.018

Dolezalek, F. (1908). Theory of binary mixtures and concentrated solutions. *Z. Phys. Chem.*, *64*, 727.

Dufal, S., Lafitte, T., Galindo, A., Jackson, G., & Haslam, A. J. (2015). Developing intermolecular-potential models for use with the SAFT-VRMie equation of state. *AIChE Journal*, *61*(9), 2891–2912. https://doi.org/10.1002/aic.14808

Dufal, S., Lafitte, T., Haslam, A. J., Galindo, A., Clark, G. N. I., Vega, C., & Jackson, G. (2015). The A in SAFT: developing the contribution of association to the Helmholtz

free energy within a Wertheim TPT1 treatment of generic Mie fluids. *Molecular Physics*, *113*(9–10), 948–984. https://doi.org/10.1080/00268976.2015.1029027

Economou, I. G. (2000). Lattice-fluid theory prediction of high-density polyethylene-branched polyolefin blend miscibility. *Macromolecules*, *33*(13), 4954–4960. https://doi.org/10.1021/ma991656j

El Meragawi, S., Diamantonis, N. I., Tsimpanogiannis, I. N., & Economou, I. G. (2016). Hydrate - fluid phase equilibria modeling using PC-SAFT and Peng-Robinson equations of state. *Fluid Phase Equilibria*, *413*, 209–219. https://doi.org/10.1016/j.fluid.2015.12.003

Englezos, P. (1993). Clathrates hydrates. *Industrial and Engineering Chemical Research*, *32*(7), 1251–1274. https://doi.org/10.1021/ie00019a001

Englezos, P., Huang, Z., & Bishnoi, P. R. (1991). Prediction of natural gas hydrate formation conditions in the presence of methanol using the Trebble-Bishnoi equation of state. *The Journal of Canadian Petroleum Technology*, *30*(2), 148–155.

Fateen, S. E. K., Khalil, M. M., & Elnabawy, A. O. (2013). Semi-empirical correlation for binary interaction parameters of the Peng-Robinson equation of state with the van der Waals mixing rules for the prediction of high-pressure vapor-liquid equilibrium. *Journal of Advanced Research*, *4*(2), 137–145. https://doi.org/10.1016/j.jare.2012.03.004

Fu, Y.-H., & Sandler, S. I. (1995). A Simplified SAFT Equation of State for Associating Compounds and Mixtures. *Industrial & Engineering Chemistry Research*, *34*(5), 1897–1909. https://doi.org/10.1021/ie00044a042

Fuchs, D., Fischer, J., Tumakaka, F., & Sadowski, G. (2006). Solubility of Amino Acids: Influence of the pH value and the Addition of Alcoholic Cosolvents on Aqueous Solubility. *Industrial & Engineering Chemistry Research*, *45*(19), 6578–6584. https://doi.org/10.1021/ie0602097

Galindo, A., Whitehead, P. J., & Jackson, G. (1996). Predicting the High-Pressure Phase Equilibria of Water + n-Alkanes Using a Simplified SAFT Theory with Transferable Intermolecular Interaction Parameters. *The Journal of Physical Chemistry*, *100*(16), 6781–6792. https://doi.org/10.1021/jp952969t

GilVillegas, A., Galindo, A., Whitehead, P. J., Mills, S. J., Jackson, G., & Burgess, A. N. (1997). Statistical associating fluid theory for chain molecules with attractive potentials of variable range. *Journal of Chemical Physics*, *106*(10), 4168–4186. https://doi.org/10.1063/1.473101

Gonzalez, A., Pereira, L., Paricaud, P., Coquelet, C., & Chapoy, A. (2015). Modeling of Transport Properties Using the SAFT-VR Mie Equation of State. *SPE Annual Technical Conference and Exhibition*. https://doi.org/10.2118/175051-MS

Gross, J., & Sadowski, G. (2002). Application of the Perturbed-Chain SAFT Equation of State to Associating Systems. *Industrial & Engineering Chemistry Research*, *41*(22), 5510–5515. https://doi.org/10.1021/ie010954d

Guggenheim, E. A. (1948). Statistical thermodynamics of co-operative systems (a generalization of the quasi-chemical method). *Transactions of the Faraday Society*, *44*(0), 1007. https://doi.org/10.1039/tf9484401007

Haghighi, H., Chapoy, A., Burgess, R., & Tohidi, B. (2009). Experimental and thermodynamic modelling of systems containing water and ethylene glycol: Application to flow assurance and gas processing. *Fluid Phase Equilibria*, *276*(1), 24–30. https://doi.org/10.1016/j.fluid.2008.10.006

Handa, Y. P., & Tse, J. S. (1986). Thermodynamic properties of empty lattices of structure I and structure II clathrate hydrates. *The Journal of Physical Chemistry*, *90*(22), 5917–5921.

Hasse, H. (2010). *Molecular Modeling and Simulation of Real Fluids for Applications in Process Engineering*. Retrieved from http://d-nb.info/1033765546/34

Heidemann, R. A., & Prausnitz, J. M. (1976). A van der Waals-type equation of state for fluids with associating molecules. *Proceedings of the National Academy of Sciences of the United States of America*, *73*(6), 1773–6. Retrieved from http://www.ncbi.nlm.nih.gov/pubmed/16592320

Henley, H., Thomas, E., & Lucia, A. (2014). Density and phase equilibrium for ice and structure I hydrates using the Gibbs-Helmholtz constrained equation of state. *Chemical Engineering Research and Design*, *92*(12), 1977–1991. https://doi.org/10.1016/j.cherd.2014.06.011

Herzog, H. J. (1998). OCEAN SEQUESTRATION OF CO 2 — AN OVERVIEW. In *Fourth International Conference on Greenhouse Gas Control Technologies* (p. 7). Interlaken, Switzerland.

Holder, G. D., Corbin, G., & Papadopoulos, K. D. (1980). Thermodynamic and Molecular Properties of Gas Hydrates from Mixtures Containing Methane, Argon, and Krypton. *Industrial & Engineering Chemistry Fundamentals*, *19*(3), 282–286. https://doi.org/10.1021/i160075a008

Holder, G. D., & Hand, J. H. (1982). Multiple-phase equilibria in hydrates from methane, ethane, propane and water mixtures. *AIChE Journal*, *28*(12), 440–447. https://doi.org/10.1002/aic.690280312

Holder, G. D., Malekar, S. . T., & Sloan, E. D. (1984). Determination of hydrate thermodynamic reference properties from experimental hydrate composition data. *Industrial & Engineering Chemistry Fundamentals*, *23*(1), 123–126.

Holder, G. D., Zetts, S. P., & Pradhan, N. (1988). Phase Behavior in Systems Containing

Clathrate Hydrates. *Reviews in Chemical Engineering*, *5*, 1–70.

Hou, S.-X., Maitland, G. C., & Trusler, J. P. M. (2013). Measurement and modeling of the phase behavior of the (carbon dioxide+water) mixture at temperatures from 298.15K to 448.15K. *The Journal of Supercritical Fluids*, *73*, 87–96. https://doi.org/10.1016/j.supflu.2012.11.011

HØye, J. S., & Olaussen, K. (1980). Statistical mechanical model with chemical reaction. *Physica A: Statistical Mechanics and Its Applications*, *104*(3), 435–446. https://doi.org/10.1016/0378-4371(80)90006-0

Huang, S. H., & Radosz, M. (1990). Equation of state for small, large, polydisperse and associating molecules. *Ind. Eng. Chem. Res.*, *29*, 2284–2294. https://doi.org/10.1021/ie00107a014

Huang, S. H., & Radosz, M. (1991). Equation of state for small, large, polydisperse, and associating molecules: extension to fluid mixtures. *Industrial & Engineering Chemistry Research*, *30*(8), 1994–2005. https://doi.org/10.1021/ie00056a050

Hunt, A. (1996). Fluid properties determine flow line blockage potential - Oil & Gas Journal. Retrieved from http://www.ogj.com/articles/print/volume-94/issue-29/in-this-issue/drilling/fluid-properties-determine-flow-line-blockage-potential.html

J.S. Tse C.I. Ratcliffe, Y. P. H., & Powell, B. M. (1986). Structure of Oxygen Clathrate Hydrate by Neutron Powder Diffraction. *Journal of Inclusion Phenomena*, *4*, 235–240. https://doi.org/10.1007/BF00657996

Jackson, G., Chapman, W. G., & Gubbins, K. E. (1988). Phase equilibria of associating fluids of spherical and chain molecules. *International Journal of Thermophysics*, *9*(5), 769–779. https://doi.org/10.1007/BF00503243

Jin, Z., Liu, K., & Sheng, W. (1993). Vapor-liquid equilibrium in binary and ternary mixtures of nitrogen, argon, and methane. *Journal of Chemical & Engineering Data*, *38*(3), 353–355. https://doi.org/10.1021/je00011a004

Jog, P. K., Garcia-Cuellar, A., & Chapman, W. G. (1999). Extensions and applications of the SAFT equation of state to solvents, monomers, and polymers. *Fluid Phase Equilibria*, *158*, 321–326. https://doi.org/10.1016/S0378-3812(99)00069-2

John, V., & Holder, G. (1982). Contribution of second and subsequent water shells to the potential energy of guest-host interactions in clathrate hydrates. *The Journal of Physical Chemistry*, *86*(1), 455–459. Retrieved from http://pubs.acs.org/doi/abs/10.1021/j100393a008

John, V. T., Papadopoulos, K. D., & Holder, G. D. (1985). A generalized model for predicting equilibrium conditions for gas hydrates. *AIChE Journal*, *31*(2), 252–259. https://doi.org/10.1002/aic.690310212

Jusoh, N.W., K. K. L. and A. M. S. (2012). Purification of Natural Gas with Impurities using Membrane Processes : Parameter Estimation. *American J. of Engineering and Applied Sciences*, *5*(1), 78–83.

K. Jog, W. G. Chapman, P. (1999). Application of Wertheim's thermodynamic perturbation theory to dipolar hard sphere chains. *Molecular Physics*, *97*(3), 307–319. https://doi.org/10.1080/002689799163703

Kang, S.-P., Lee, H., & Ryu, B.-J. (2001). Enthalpies of dissociation of clathrate hydrates of carbon dioxide, nitrogen, (carbon dioxide+ nitrogen), and (carbon dioxide + nitrogen+ tetrahydrofuran). *The Journal of Chemical Thermodynamics*, *33*(5), 513–521. https://doi.org/10.1006/jcht.2000.0765

Kennan, R. P., & Pollack, G. L. (1990). Pressure dependence of the solubility of nitrogen, argon, krypton, and xenon in water. *The Journal of Chemical Physics*, *93*(4), 2724–2735. https://doi.org/10.1063/1.458911

Klauda, J. B., & Sandler, S. I. (2000). A Fugacity Model for Gas Hydrate Phase Equilibria. *Industrial & Engineering Chemistry Research*, *39*, 3377–3386. https://doi.org/10.1021/ie000322b

Klauda, J. B., & Sandler, S. I. (2003). Phase behavior of clathrate hydrates: A model for single and multiple gas component hydrates. *Chemical Engineering Science*, *58*, 27–41. https://doi.org/10.1016/S0009-2509(02)00435-9

Kleiner, M., Tumakaka, F., Sadowski, G., Latz, H., & Buback, M. (2006). Phase equilibria in polydisperse and associating copolymer solutions: Poly(ethene-co-(meth)acrylic acid)–monomer mixtures. *Fluid Phase Equilibria*, *241*(1), 113–123. https://doi.org/10.1016/j.fluid.2005.12.027

Kobayashi, R., & Katz, D. (1953). Vapor-liquid equilibria for binary hydrocarbon-water systems. *Industrial & Engineering Chemistry*, *45*(2), 446–451. https://doi.org/10.1021/ie50518a051

Kontogeorgis, G. M., & Folas, G. K. (2010). *Thermodynamic Models for Industrial Applications*. Chichester, UK: John Wiley & Sons, Ltd. https://doi.org/10.1002/9780470747537

Konynenburg, P. H. Van, & Scott, R. L. (1980). Critical Lines and Phase Equilibria in Binary Van Der Waals Mixtures. *Philosophical Transactions of the Royal Society of London. Series A, Mathematical and Physical Sciences*, *298*(1442), 495 LP-540. Retrieved from http://rsta.royalsocietypublishing.org/content/298/1442/495.abstract

Kraska, T., & Gubbins, K. (1996). Phase equilibria calculations with a modified SAFT equation of state. 2. Binary mixtures of n-alkanes, 1-alkanols, and water. *Ind. Eng. Chem. Res.*, *35*(2), 4738–4746. https://doi.org/10.1021/ie960233s

Kvenvolden, K. A., & Claypool, G. E. (1988). *Gas hydrates in oceanic sediment*. *Open-*

File Report. Retrieved from http://pubs.er.usgs.gov/publication/ofr88216

Kvenvolden, K. A., & Lorenson, T. D. (2001). Global occurrences of gas hydrate. In *Proceedings of the International Offshore and Polar Engineering Conference* (pp. 462–467). Stavanger. Retrieved from http://pubs.er.usgs.gov/publication/70023750

Lafitte, T., Apostolakou, A., Avenda??o, C., Galindo, A., Adjiman, C. S., M??ller, E. A., & Jackson, G. (2013). Accurate statistical associating fluid theory for chain molecules formed from Mie segments. *Journal of Chemical Physics*, *139*(15). https://doi.org/10.1063/1.4819786

Lafitte, T., Bessieres, D., Piñeiro, M. M., & Daridon, J.-L. (2006). Simultaneous estimation of phase behavior and second-derivative properties using the statistical associating fluid theory with variable range approach. *The Journal of Chemical Physics*, *124*(2), 24509. https://doi.org/10.1063/1.2140276

Le Quang, D., Le Quang, D., Bouillot, B., Herri, J.-M., Glenat, P., & Duchet-Suchaux, P. (2016). Experimental procedure and results to measure the composition of gas hydrate, during crystallization and at equilibrium, from N2–CO2–CH4–C2H6–C3H8–C4H10 gas mixtures. *Fluid Phase Equilibria*, *413*, 10–21. https://doi.org/10.1016/j.fluid.2015.10.022

Lennard-Jones, J. E., & Devonshire, A. F. (1937). Critical Phenomena in Gases. I. *Proceedings of the Royal Society of London. Series A, Mathematical and Physical Sciences*, *163*(912), 53–70. Retrieved from http://www.jstor.org/stable/97067

Lennard-Jones, J. E., & Devonshire, A. F. (1938). Critical Phenomena in Gases. II. Vapour Pressures and Boiling Points. *Proceedings of the Royal Society of London. Series A, Mathematical and Physical Sciences*, *165*(920), 1–11. Retrieved from http://www.jstor.org/stable/96981

Li, X. Sen, Wu, H. J., & Englezos, P. (2006). Prediction of gas hydrate formation conditions in the presence of methanol, glycerol, ethylene glycol, and triethylene glycol with the statistical associating fluid theory equation of state. *Industrial and Engineering Chemistry Research*, *45*, 2131–2137. https://doi.org/10.1021/ie051204x

Lim, J. S., Ho, Q. N., Park, J.-Y., & Lee, B. G. (2004). Measurement of Vapor−Liquid Equilibria for the Binary Mixture of Propane (R-290) + Isobutane (R-600a). *Journal of Chemical & Engineering Data*, *49*(2), 192–198. https://doi.org/10.1021/je030106k

Luongo-Ortiz, J. F., & Starling, K. E. (1997). A new combining rule for mixture equations of state: higher order composition dependencies reduce to quadratic composition dependence. *Fluid Phase Equilibria*, *132*(1–2), 159–167. https://doi.org/10.1016/S0378-3812(96)03116-0

Ma, C. F., Chen, G. J., Wang, F., Sun, C. Y., & Guo, T. M. (2001). Hydrate formation of (CH4 + C2H4) and (CH4 + C3H6) gas mixtures. *Fluid Phase Equilibria*, *191*(1–2),

41–47. https://doi.org/10.1016/S0378-3812(01)00610-0

Mansoori, G. A., Carnahan, N. F., Starling, K. E., & Leland, T. W. (1971). Equilibrium Thermodynamic Properties of the Mixture of Hard Spheres. *The Journal of Chemical Physics*, *54*(4), 1523–1525. https://doi.org/10.1063/1.1675048

Marcelli, G., Todd, B. D., & Sadus, R. J. (2002). Beyond Traditional Effective Intermolecular Potentials and Pairwise Interactions in Molecular Simulation (pp. 932–941). Springer, Berlin, Heidelberg. https://doi.org/10.1007/3-540-47789-6_98

Marshall, B. D. (2014). *Thermodynamic perturbation theory for associating fluids: Beyond first order*. Retrieved from http://arxiv.org/abs/1405.1775

Marshall, D. R., Saito, S., & Kobayashi, R. (1964). High pressures : Part I. methane-water, argon-water, and nitrogen-water systems. *AIChE Journal*, *10*(2), 202–205.

McCabe, C., & Jackson, G. (1999). SAFT-VR modelling of the phase equilibrium of long-chain n-alkanes. *Physical Chemistry Chemical Physics*, *1*(9), 2057–2064. https://doi.org/10.1039/a808085b

McKoy, V., & Sinanoğlu, O. (1963). Theory of Dissociation Pressures of Some Gas Hydrates. *The Journal of Chemical Physics*, *38*(12), 2946. https://doi.org/10.1063/1.1733625

McLeod Jr., H. O., & Campbell, J. M. (1961). Natural Gas Hydrates at Pressures to 10,000 psia. *Journal of Petroleum Technology*, *13*(6), 590–594. https://doi.org/10.2118/1566-G-PA

Mei, D.-H., Liao, J., Yang, J.-T., & Guo, T.-M. (1996). Experimental and Modeling Studies on the Hydrate Formation of a Methane + Nitrogen Gas Mixture in the Presence of Aqueous Electrolyte Solutions. *Industrial & Engineering Chemistry Research*, *35*(11), 4342–4347. https://doi.org/10.1021/ie9601662

Miller, B., & Strong, E. R. (1946). No Title. *Am. Gas Assoc. Monthly*, *28*, 63.

Miller, R. C., Kidnay, A. J., & Hiza, M. J. (1977). Liquid + vapor equilibria in methane + ethene and in methane + ethane from 150.00 to 190.00 K. *The Journal of Chemical Thermodynamics*, *9*(2), 167–178. https://doi.org/10.1016/0021-9614(77)90082-9

Mohammadi, A. H., Chapoy, A., Tohidi, B., & Richon, D. (2004). Measurements and Thermodynamic Modeling of Vapor−Liquid Equilibria in Ethane−Water Systems from 274.26 to 343.08 K. *Industrial & Engineering Chemistry Research*, *43*(17), 5418–5424. https://doi.org/10.1021/ie049747e

Mohammadi, A. H., Tohidi, B., & Burgass, R. W. (2003). Equilibrium data and thermodynamic modeling of nitrogen, oxygen, and air clathrate hydrates. *Journal of Chemical and Engineering Data*, *48*(3), 612–616. https://doi.org/10.1021/je025608x

Mraw, S. C., Hwang, S.-C., & Kobayashi, R. (1978). Vapor-liquid equilibrium of the methane-carbon dioxide system at low temperatures. *Journal of Chemical & Engineering Data*, *23*(2), 135–139. https://doi.org/10.1021/je60077a014

Müller, E. A., & Gubbins, K. E. (1995). An Equation of State for Water from a Simplified Intermolecular Potential. *Industrial & Engineering Chemistry Research*, *34*(10), 3662–3673. https://doi.org/10.1021/ie00037a055

Müller, E. A., & Gubbins, K. E. (2001). Molecular-based equations of state for associating fluids: A review of SAFT and related approaches. *Industrial & Engineering Chemistry Research*, *40*, 2193–2211. https://doi.org/10.1021/ie000773w

Nagahama, K., Konishi, H., Hoshino, D., & Hirata, M. (1974). Binary Vapor-Liquid Equilibria of Carbon Dioxide-Light Hydrocarbons At Low Temperature. *Journal of Chemical Engineering of Japan*, *7*(5), 323–328. https://doi.org/10.1252/jcej.7.323

Nakamura, T., Makino, T., Sugahara, T., & Ohgaki, K. (2003). Stability boundaries of gas hydrates helped by methane - Structure-H hydrates of methylcyclohexane and cis-1,2-dimethylcyclohexane. *Chemical Engineering Science*, *58*, 269–273. https://doi.org/10.1016/S0009-2509(02)00518-3

Nezbeda, I., Kolafa, J., & Kalyuzhnyi, Y. (1989). Primitive model of water. *Molecular Physics*, *68*(1), 143–160. https://doi.org/10.1080/00268978900102021

Nezbeda, I., & Pavlíček, J. (1996). Application of primitive models of association: A simple theoretical equation of state of water. *Fluid Phase Equilibria*, *116*(1–2), 530–536. https://doi.org/10.1016/0378-3812(95)02927-3

Ng, H.-J., Petrunia, J. P., & Robinson, D. B. (1977). Experimental measurement and prediction of hydrate forming conditions in the nitrogen-propane-water system. *Fluid Phase Equilibria*, *1*(4), 283–291. https://doi.org/10.1016/0378-3812(77)80011-3

Ng, H.-J., & Robinson, D. B. (1985). Hydrate formation in systems containing methane, ethane, propane, carbon dioxide or hydrogen sulfide in the presence of methanol. *Fluid Phase Equilibria*, *21*(1–2), 145–155. https://doi.org/10.1016/0378-3812(85)90065-2

Nguyen-Huynh, D., Passarello, J.-P., Tobaly, P., & de Hemptinne, J.-C. (2008). Modeling Phase Equilibria of Asymmetric Mixtures Using a Group-Contribution SAFT (GC-SAFT) with a k ij Correlation Method Based on London's Theory. 1. Application to CO 2 + n -Alkane, Methane + n -Alkane, and Ethane + n -Alkane Systems. *Industrial & Engineering Chemistry Research*, *47*(22), 8847–8858. https://doi.org/10.1021/ie071643r

Nixdorf, J., & Oellrich, L. R. (1997). Experimental determination of hydrate equilibrium conditions for pure gases, binary and ternary mixtures and natural gases. *Fluid*

Phase Equilibria, *139*, 325–333.

Noaker, L. J., & Katz, D. L. (1954). Gas Hydrates of Hydrogen Sulfide-Methane Mixtures. *Journal of Petroleum Technology*, *6*(9), 135–137. https://doi.org/10.2118/367-G

Olds, R. H., Sage, B. H., & Lacey, W. N. (1942). Methane-isobutane system. *Industrial and Engineering Chemistry*, *34*, 1008–1013. https://doi.org/10.1021/ie50392a027

Pan, D., & Galli, G. (2016). The fate of carbon dioxide in water-rich fluids under extreme conditions. *Science Advances*, *2*(10). Retrieved from http://advances.sciencemag.org/content/2/10/e1601278.full

Panayiotou, C. (1987). Lattice-fluid theory of polymer solutions. *Macromolecules*, *20*, 861–871. https://doi.org/10.1021/ma00170a026

Papaioannou, V., Lafitte, T., Avendaño, C., Adjiman, C. S., Jackson, G., Müller, E. A., & Galindo, A. (2014). Group contribution methodology based on the statistical associating fluid theory for heteronuclear molecules formed from Mie segments. *The Journal of Chemical Physics*, *140*(5), 54107. https://doi.org/10.1063/1.4851455

Parrish, W. R., & Prausnitz, J. M. (1972). Dissociation Pressures of Gas Hydrates Formed by Gas Mixtures. *Industrial & Engineering Chemistry Process Design and Development*, *11*(1), 26–35. https://doi.org/10.1021/i260041a006

Pauling, L., & Marsh, R. E. (1952). The Structure of Chlorine Hydrate. *Proceedings of the National Academy of Sciences of the United States of America*, *38*(2), 112–8. Retrieved from http://www.ncbi.nlm.nih.gov/pubmed/16589062

Pedrosa, N., Pàmies, J. C., Coutinho, J. A. P., Marrucho, I. M., & Vega, L. F. (2005). Phase Equilibria of Ethylene Glycol Oligomers and Their Mixtures. *Industrial & Engineering Chemistry Research*, *44*(17), 7027–7037. https://doi.org/10.1021/ie050361t

Perez, A. G., Valtz, A., Coquelet, C., Paricaud, P., & Chapoy, A. (2016). Experimental and modelling study of the densities of the hydrogen sulphide??+ methane mixtures at 253, 273 and 293??K and pressures up to 30??MPa. *Fluid Phase Equilibria*, *427*, 371–383. https://doi.org/10.1016/j.fluid.2016.08.002

Rigby, M., & Prausnitz, J. M. (1968). Solubility of water in compressed nitrogen, argon, and methane. *The Journal of Physical Chemistry*, *72*, 330–334. https://doi.org/10.1021/j100847a064

Rouher, O. S., & Barduhn, A. J. (1969). Hydrates of iso- and normal butane and their mixtures. *Desalination*, *6*(1), 57–73. https://doi.org/10.1016/S0011-9164(00)80011-9

Sadus, R. J. (2002). *Molecular simulation of fluids : theory, algorithms, and object-*

orientation. Elsevier. Retrieved from https://books.google.com.sa/books?id=kVeg20PS-7kC&pg=PA127&lpg=PA127&dq=Sadus+R.+J.+and+Prausnitz+J.+M#v=onepage&q=multibody&f=false

Saito, S., Marshall, D. R., & Kobayashi, R. (1964). Hydrates at high pressure: Part II. Application of statistical mechanics to the study of hydrates of methane, argon, and nitrogen. *AlChE J.*, *10*, 734–740. https://doi.org/10.1002/aic.690100530

Sapate, A. (2015). *Methane Hydrate Production Using Mixture Of CO2 and N2*.

Schneider, G. R., & Farrar, J. (1968). *Res. Dev. Report No 292*.

Selleck, F. T., Carmichael, L. T., & Sage, B. H. (1952). Phase Behavior in the Hydrogen Sulfide-Water System. *Industrial and Engineering Chemistry*, *44*(9), 2219–2226. https://doi.org/10.1021/ie50513a064

Sengers, J. V, & Sengers, J. M. H. L. (1986). Thermodynamic Behavior of Fluids Near the Critical Point. *Annual Review of Physical Chemistry*, *37*(1), 189–222. https://doi.org/10.1146/annurev.pc.37.100186.001201

Seo, Y.-T., Moudrakovski, I. L., Ripmeester, J. A., Lee, J.-W., & Lee, H. (2005). Efficient Recovery of CO_2 from Flue Gas by Clathrate Hydrate Formation in Porous Silica Gels. *Environmental Science & Technology*, *39*(7), 2315–2319. https://doi.org/10.1021/es049269z

Servio, P., & Englezos, P. (2001). Effect of temperature and pressure on the solubility of carbon dioxide in water in the presence of gas hydrate. *Fluid Phase Equilibria*, *190*(1), 127–134. https://doi.org/10.1016/S0378-3812(01)00598-2

Servio, P., Lagers, F., Peters, C., & Englezos, P. (1999). Gas hydrate phase equilibrium in the system methane–carbon dioxide–neohexane and water. *Fluid Phase Equilibria*, *158–160*, 795–800. https://doi.org/10.1016/S0378-3812(99)00084-9

Shimekit, B., & Mukhtar, H. (2012). Natural Gas Purification Technologies–Major Advances for CO2 Separation and Future Directions. *Advances in Natural Gas Technology*, 235–270. https://doi.org/10.5772/38656

Sivaraman, R. (2002). Flow Assurance: Understanding and Controlling Natural Gas Hydrate. *Gas TIPS*, 18–23.

Sloan, E. D. (1994). Conference Overview. *Annals of the New York Academy of Sciences*, *715*(1 Natural Gas H), 1–23. https://doi.org/10.1111/j.1749-6632.1994.tb38819.x

Sloan, E. D. (2000). Clathrate Hydrates: The Other Common Solid Water Phase. *Industrial & Engineering Chemistry Research*, *39*(9), 3123–3129. https://doi.org/10.1021/ie000574c

Sloan, E. D. (2004). Introductory overview: Hydrate knowledge development. *American Mineralogist*, *89*(8–9), 1155–1161. https://doi.org/10.2138/am-2004-8-901

Sloan, E. D., & Koh, C. A. (2008). *E Dendy Sloan-Clathrate hydrates of natural gases-Marcel Dekker (2008).pdf* (3rd ed.). CRC Press.

Stefan Glos, Kleinrahm, R., & Wagner, W. (2004). Measurement of the (p, ρ, T) relation of propane, propylene, n-butane, and isobutane in the temperature range from (95 to 340) K at pressures up to 12 MPa using an accurate two-sinker densimeter. *J. Chem. Thermodynamics*, *36*, 1037–1059.

Stryjek, R., Chappelear, P. S., & Kobayashi, R. (1974). Low-temperature vapor-liquid equilibriums of nitrogen-methane system. *Journal of Chemical & Engineering Data*, *19*(4), 334–339. https://doi.org/10.1021/je60063a023

Suresh, J., & Beckman, E. J. (1994). Prediction of liquid-liquid equilibria in ternary mixtures from binary data. *Fluid Phase Equilibria*, *99*, 219–240. https://doi.org/10.1016/0378-3812(94)80033-2

Sutherland, W. (1887). On the law of molecular force. *Philosophical Magazine Series 5*, *24*(146), 113–134. https://doi.org/10.1080/14786448708628067

Tumakaka, F., Prikhodko, I. V., & Sadowski, G. (2007). Modeling of solid–liquid equilibria for systems with solid-complex phase formation. *Fluid Phase Equilibria*, *260*(1), 98–104. https://doi.org/10.1016/j.fluid.2007.05.028

Tumba, K., Hashemi, H., Naidoo, P., Mohammadi, A. H., & Ramjugernath, D. (2013). Dissociation data and thermodynamic modeling of clathrate hydrates of ethene, ethyne, and propene. *Journal of Chemical and Engineering Data*, *58*(11), 3259–3264. https://doi.org/10.1021/je400727q

Valtz, A., Chapoy, A., Coquelet, C., Paricaud, P., & Richon, D. (2004). Vapour-liquid equilibria in the carbon dioxide-water system, measurement and modelling from 278.2 to 318.2 K. *Fluid Phase Equilibria*, *226*(1–2), 333–344. https://doi.org/10.1016/j.fluid.2004.10.013

van Cleeff, A., & Diepen, G. A. M. (1960). Gas hydrates of nitrogen and oxygen. *Recueil Des Travaux Chimiques Des Pays-Bas*, *79*(6), 582–586. https://doi.org/10.1002/recl.19600790606

van Cleeff, A., & Diepen, G. A. M. (1965). Gas hydrates of nitrogen and oxygen. II. *Recueil Des Travaux Chimiques Des Pays-Bas*, *84*(8), 1085–1093. https://doi.org/10.1002/recl.19650840815

van der Waals, J. H., & Platteeuw, J. C. (1958). Clathrate solutions. *Advances in Chemical Physics*, *2*, 1–57. https://doi.org/10.1002/9780470143483.ch1

van Schilt, M. A., Wering, R. M., van Meerendonk, W. J., Kemmere, M. F., Keurentjes,

J. T. F., Kleiner, M., … de Loos, T. W. (2005). High-Pressure Phase Behavior of the System PCHC−CHO−CO2 for the Development of a Solvent-Free Alternative toward Polycarbonate Production. *Industrial & Engineering Chemistry Research*, *44*(9), 3363–3366. https://doi.org/10.1021/ie048790z

Vasil'ev, V., Makogon, Y., Trebin, F., Trofimuk, A., & Cherskiy, N. (1970). The property of natural gases to occur in the Earth crust in a solid state and to form gas hydrate deposits. *Otkrytiya v SSSR*, 15–17.

Wang, L. K., Chen, G. J., Han, G. H., Guo, X. Q., & Guo, T. M. (2003). Experimental study on the solubility of natural gas components in water with or without hydrate inhibitor. *Fluid Phase Equilibria*, *207*(1–2), 143–154. https://doi.org/10.1016/S0378-3812(03)00009-8

Ward, Z. T., Deering, C. E., Marriott, R. a, Sum, A. K., Sloan, E. D., & Koh, C. a. (2014). Phase Equilibrium Data and Model Comparisons for H2S Hydrates. *Journal of Chemical & Engineering Data*, *60*, 403–408. https://doi.org/10.1021/je500657f

Wertheim, M. S. (1984). Fluids with highly directional attractive forces. I. Statistical thermodynamics. *Journal of Statistical Physics*, *35*(1), 19–34. https://doi.org/10.1007/BF01017362

Wertheim, M. S. (1986). Fluids with highly directional attractive forces. IV. Equilibrium polymerization. *Journal of Statistical Physics*, *42*(3), 477–492. https://doi.org/10.1007/BF01127722

Wertheim, M. S. (1987). Thermodynamic perturbation theory of polymerization. *The Journal of Chemical Physics*, *87*(12), 7323–7331. https://doi.org/10.1063/1.453326

Wichterle, I., & Kobayashi, R. (1972a). Vapor-liquid equilibrium of methane-ethane system at low temperatures and high pressures. *Journal of Chemical & Engineering Data*, *17*(1), 9–12. https://doi.org/10.1021/je60052a022

Wichterle, I., & Kobayashi, R. (1972b). Vapor-liquid equilibrium of methane-propane system at low temperatures and high pressures. *Journal of Chemical & Engineering Data*, *17*(1), 4–9. https://doi.org/10.1021/je60052a019

Wilcox, W., Carson, D. ., & Katz, L. (1941). Natural gas hydrates. *Industrial and Engineering Chemistry*, *33*(8), 662–665.

Wilcox, W. I., Carson, D. B., & Katz, D. L. (1941). Natural gas hydrates. *Industrial & Engineering Chemistry*, *33*(5), 662–665.

Wolbach, J. P., & Sandler, S. I. (1997). Using Molecular Orbital Calculations To Describe the Phase Behavior of Hydrogen-Bonding Fluids. *Industrial & Engineering Chemistry Research*, *36*(10), 4041–4051. https://doi.org/10.1021/ie9607255

Wu, B.-J., Robinson, D. B., & Ng, H.-J. (1976). Three- and four-phase hydrate forming conditions in methane + isobutane + water. *The Journal of Chemical Thermodynamics*, *8*(5), 461–469. https://doi.org/10.1016/0021-9614(76)90067-7

Yaws, C. L. (2015). *The Yaws handbook of physical properties for hydrocarbons and chemicals : physical properties for more than 54,000 organic and inorganic chemical compounds, coverage for C1 to C100 organics and Ac to Zr inorganics*.

Yucelen, B., & Kidnay, A. J. (1999). Vapor−Liquid Equilibria in the Nitrogen + Carbon Dioxide + Propane System from 240 to 330 K at Pressures to 15 MPa. *Journal of Chemical & Engineering Data*, *44*(5), 926–931. https://doi.org/10.1021/je980321e

Zele, S. R., Lee, S.-Y., & Holder, G. D. (1999). A Theory of Lattice Distortion in Gas Hydrates. *The Journal of Physical Chemistry B*, *103*(46), 10250–10257. https://doi.org/10.1021/jp9917704

Zhang, Z.-Y., Yang, J.-C., & Li, Y.-G. (2000). Prediction of phase equilibria for CO2–C2H5OH–H2O system using the SAFT equation of state. *Fluid Phase Equilibria*, *169*(1), 1–18. https://doi.org/10.1016/S0378-3812(99)00341-6

Zhdanov, R. K., Adamova, T. P., Subbotin, O. S., Pomeranskii, A. A., Belosludov, V. R., Dontsov, V. R., & Nakoryakov, V. E. (2010). Modeling the properties of methane + ethane (Propane) binary hydrates, depending on the composition of gas phase state in equilibrium with hydrate. *Journal of Engineering Thermophysics*, *19*(4), 282–288. https://doi.org/10.1134/S1810232810040041

Vitae

Name	: MUHAMMAD SAAD WASEEM
Nationality	: PAKISTANI
Date of Birth	: 01-Mar-1989
Email	: msw3682@gmail.com
Address	: 23-N, Block - 2 P.E.C.H.S, Karachi Sindh - Pakistan
Academic Background	: M.S. Chemical Engineering KFUPM, Saudi Arabia - Mar 2017 B.E. Chemical Engineering NEDUET, Pakistan - Dec 2010
Research Interests	: My research interests are in molecular and statistical thermodynamics.